

**AN INTEGRATED USED FUEL DISPOSITION AND GENERIC REPOSITORY  
MODEL**

by

Kathryn D. Huff

A dissertation submitted in partial fulfillment of  
the requirements for the degree of

Doctor of Philosophy

(Nuclear Engineering and Engineering Physics)

at the

UNIVERSITY OF WISCONSIN–MADISON

2013



## ACKNOWLEDGMENTS

---

I am grateful to a number of extraordinary professors and colleagues at the Universities of Wisconsin and Chicago who have inspired and encouraged me. Among them, I am especially indebted to my advisor, Paul P.H. Wilson, for his invaluable technical and practical guidance. I am also grateful to my laboratory advisor, Mark Nutt, and laboratory collaborator, Ted Bauer. They have been an outstanding resource for the work at hand and I look forward to learning a great deal from them in the upcoming phase of my research.

## CONTENTS

---

Contents	ii
List of Tables	iv
List of Figures	v
Acronyms	vii
Abstract	viii
<b>1 Introduction</b>	<b>1</b>
1.1 <i>Motivation</i> . . . . .	1
1.2 <i>Methodology</i> . . . . .	7
1.3 <i>Outline</i> . . . . .	9
<b>2 Literature Review</b>	<b>11</b>
2.1 <i>Repository Capabilities within Systems Analysis Tools</i> . . . . .	11
2.2 <i>Conceptual Discussion of Disposal Environments</i> . . . . .	14
2.3 <i>Analytical Models of Radionuclide Transport</i> . . . . .	22
2.4 <i>Analytical Models of Heat Transport</i> . . . . .	37
2.5 <i>Detailed Computational Models of Radionuclide Transport</i> . . . . .	44
2.6 <i>Detailed Computational Models of Heat Transport</i> . . . . .	49
<b>3 Modeling Paradigm</b>	<b>53</b>
3.1 <i>CYCLUS Simulator Paradigm</i> . . . . .	53
3.2 <i>Repository Modeling Paradigm</i> . . . . .	56
<b>4 Methodology</b>	<b>63</b>
4.1 <i>Radionuclide Transport In Cyder</i> . . . . .	63
4.2 <i>Thermal Transport Computational Models</i> . . . . .	74
<b>5 Demonstration Cases and Benchmarking</b>	<b>77</b>
5.1 <i>Nuclide Model Base Cases</i> . . . . .	78
5.2 <i>Nuclide Model Benchmarks</i> . . . . .	78
5.3 <i>Thermal Transport Base Cases</i> . . . . .	78
5.4 <i>Thermal Benchmarking</i> . . . . .	78
5.5 <i>System Level Cases</i> . . . . .	78
<b>6 Conclusions and Future Work</b>	<b>79</b>

<b>A</b>	<b>Radionuclide Transport Sensitivity Analysis</b>	<b>80</b>
A.1	<i>Approach</i> . . . . .	80
A.2	<i>Mean of the Peak Annual Dose</i> . . . . .	80
A.3	<i>Sampling Scheme</i> . . . . .	81
A.4	<i>Clay</i> . . . . .	82
<b>B</b>	<b>Thermal Transport Sensitivity Analysis</b>	<b>131</b>
B.1	<i>Isotopic Thermal Sensitivity Study</i> . . . . .	131
B.2	<i>Thermal Conductivity Sensitivity Study</i> . . . . .	131
B.3	<i>Diffusivity Thermal Transport Sensitivity Study</i> . . . . .	131
B.4	<i>Spacing Thermal Transport Sensitivity Studies</i> . . . . .	131
	<b>References</b>	<b>132</b>

## LIST OF TABLES

---

2.1	Clay Repository Features . . . . .	15
2.2	Granite Repository Features . . . . .	17
2.3	Salt Repository Features . . . . .	19
2.4	Borehole Repository Features . . . . .	21
2.5	Models of Source Term for Various Geologies . . . . .	23
2.6	Waste Form Types . . . . .	25
2.7	Current WP Failure Models . . . . .	27
2.8	Yucca Mountain Footprint Expansion Calculations . . . . .	42
2.9	International Repository Concepts . . . . .	44
2.10	Particle Transport Codes Used in ANDRA Assessment . . . . .	48
2.11	Models for Heat Transport for Various Geologies . . . . .	52
A.1	For an individual one group of 100 realizations was run for each discrete value, $P_i$ , within the range considered for $P$ . . . . .	82
A.2	The simulation groups for a dual simulation sample each parameter within the range over which it was considered. . . . .	82
A.3	Vertical advective velocity and diffusion coefficient simulation groupings. . . . .	84
A.4	Diffusion coefficient and mass factor simulation groupings. . . . .	94
A.5	Safety indicators for soluble, non-sorbing nuclides. . . . .	111
A.6	Safety indicators for solubility limited and sorbing nuclides. . . . .	112
A.7	Safety indicators for the actinides and their daughters. . . . .	113

## LIST OF FIGURES

---

2.1	Various conceptual models may be used for the same natural system [7]. . .	35
2.2	The geometry of the thermal model can be adjusted in two dimensions, altering the tunnel spacing and the vertical distance from the aquifer. . . .	50
3.1	The CYCLUS code repository allows for varied accessibility. . . . .	61
3.2	Module Interfaces and Encapsulation . . . . .	62
3.3	The nested components supply thermal flux and concentration information to each other at the boundaries. . . . .	62
4.1	The boundaries between components (in this case, waste form (wf) and waste package (wp) components) are robust interfaces defined by Source Term, Dirichlet, Neumann, and Cauchy boundary conditions. . . . .	64
4.2	Intact Mixed Cell Control Volume . . . . .	67
4.3	Degrading Mixed Cell Control Volume . . . . .	67
4.4	A system of volumes can be modeled as lumped parameter models in series.	72
4.5	A one dimensional, semi-infinite model, unidirectional flow, solution with Cauchy and Neumann boundary conditions . . . . .	74
A.1	$^{129}\text{I}$ reference diffusivity sensitivity. . . . .	85
A.2	$^{129}\text{I}$ vertical advective velocity sensitivity. . . . .	86
A.3	$^{36}\text{Cl}$ reference diffusivity sensitivity. . . . .	87
A.4	$^{36}\text{Cl}$ vertical advective velocity sensitivity. . . . .	88
A.5	$^{99}\text{Tc}$ reference diffusivity sensitivity. . . . .	89
A.6	$^{99}\text{Tc}$ vertical advective velocity sensitivity. . . . .	90
A.7	$^{237}\text{Np}$ reference diffusivity sensitivity. . . . .	90
A.8	$^{237}\text{Np}$ vertical advective velocity sensitivity. . . . .	91
A.9	$^{79}\text{Se}$ reference diffusivity sensitivity. . . . .	91
A.10	$^{79}\text{Se}$ vertical advective velocity sensitivity. . . . .	92
A.11	$^{129}\text{I}$ relative diffusivity sensitivity. . . . .	95
A.12	$^{129}\text{I}$ mass factor sensitivity. . . . .	96
A.13	$^{36}\text{Cl}$ relative diffusivity sensitivity. . . . .	97
A.14	$^{36}\text{Cl}$ mass factor sensitivity. . . . .	98
A.15	$^{99}\text{Tc}$ relative diffusivity sensitivity. . . . .	99
A.16	$^{99}\text{Tc}$ mass factor sensitivity. . . . .	100
A.17	$^{237}\text{Np}$ relative diffusivity sensitivity. . . . .	101
A.18	$^{237}\text{Np}$ mass factor sensitivity. . . . .	102
A.19	Solubility factor sensitivity. The peak annual dose due to an inventory, $N$ , of each isotope. . . . .	105

A.20 Solubility limit sensitivity. The peak annual dose due to an inventory, $N$ , of each isotope. . . . .	106
A.21 $K_d$ factor sensitivity. The peak annual dose due to an inventory, $N$ , of each isotope. . . . .	108
A.22 $K_d$ sensitivity. The peak annual dose due to an inventory, $N$ , of each isotope. . . . .	109
A.23 $^{129}\text{I}$ waste form degradation rate sensitivity. . . . .	114
A.24 $^{129}\text{I}$ inventory multiplier sensitivity. . . . .	115
A.25 $^{36}\text{Cl}$ waste form degradation rate sensitivity. . . . .	116
A.26 $^{36}\text{Cl}$ inventory multiplier sensitivity. . . . .	117
A.27 $^{99}\text{Tc}$ waste form degradation rate sensitivity. . . . .	118
A.28 $^{99}\text{Tc}$ inventory multiplier sensitivity. . . . .	119
A.29 $^{237}\text{Np}$ waste form degradation rate sensitivity. . . . .	120
A.30 $^{237}\text{Np}$ inventory multiplier sensitivity. . . . .	121
A.31 $^{129}\text{I}$ waste package failure time sensitivity. . . . .	123
A.32 $^{129}\text{I}$ waste package failure time sensitivity. . . . .	124
A.33 $^{36}\text{Cl}$ waste package failure time sensitivity. . . . .	125
A.34 $^{36}\text{Cl}$ waste package failure time sensitivity. . . . .	126
A.35 $^{99}\text{Tc}$ waste package failure time sensitivity. . . . .	127
A.36 $^{99}\text{Tc}$ waste package failure time sensitivity. . . . .	128
A.37 $^{237}\text{Np}$ waste package failure time sensitivity. . . . .	129
A.38 $^{237}\text{Np}$ waste package failure time sensitivity. . . . .	130



## ACRONYMS

---

**ANDRA** Agence Nationale pour la gestion des Déchets RAdioactifs, the French National Agency for Radioactive Waste Management. 13, 35

**DOE** Department of Energy. iv, v, 4, 11, 12

**EBS** Engineered Barrier System. 33, 35, 46

**EDZ** Excavation Disturbed Zone. 33

**EPA** Environmental Protection Agency. 8, 9

**FCO** Fuel Cycle Options. iv, v, 10

**FEPs** Features, Events, and Processes. 29

**GDSM** Generic Disposal System Model. 12, 13, 29–31, 33

**HLW** high level waste. 65

**IAEA** International Atomic Energy Agency. 65

**MTHM** Metric Ton of Heavy Metal. 45, 46

**PEI** Peak Environmental Impact. 10

**RD&D** Research Development and Design. 10

**SNF** spent nuclear fuel. 7, 46, 47

**SWF** Separations and Waste Forms. 10

**UFD** Used Fuel Disposition. iv, v, 10–13, 28, 29, 33, 65

**US** United States. 3, 11

**UW** University of Wisconsin. 16, 21

**YMR** Yucca Mountain Repository Site. 4, 5, 9

# **AN INTEGRATED USED FUEL DISPOSITION AND GENERIC REPOSITORY MODEL**

Kathryn D. Huff

Under the supervision of Professor Paul P.H. Wilson  
At the University of Wisconsin-Madison

As the United States Department of Energy (DOE) simultaneously considers alternative fuel cycles and waste disposal options, an integrated fuel cycle and generic disposal system analysis tool is increasingly necessary for informing domestic nuclear spent fuel policy. A generic repository model capable of illuminating the distinct dominant physics of candidate repository geologies, designs, and engineering components will provide an interface between the Used Fuel Disposition (UFD) and Fuel Cycle Options (FCO) Campaign goals. Repository metrics such as necessary repository footprint and peak annual dose are affected by heat and radionuclide release characteristics specific to variable spent fuel compositions associated with alternative fuel cycles. Computational tools capable of simulating the dynamic, heterogeneous spent fuel isotopics resulting from transition scenarios and alternative fuel cycles are, however, lacking in repository modeling options. This work proposes to construct such a generic repository model appropriate for systems analysis. By emphasizing modularity and speed, the work at hand seeks to provide a tool which captures the dominant physics of detailed repository analysis within the UFD Campaign and can be robustly and flexibly integrated within the CYCLUS fuel cycle simulation tool.

Paul P.H. Wilson

## ABSTRACT

---

As the United States Department of Energy (DOE) simultaneously considers alternative fuel cycles and waste disposal options, an integrated fuel cycle and generic disposal system analysis tool is increasingly necessary for informing domestic nuclear spent fuel policy. A generic repository model capable of illuminating the distinct dominant physics of candidate repository geologies, designs, and engineering components will provide an interface between the Used Fuel Disposition (UFD) and Fuel Cycle Options (FCO) Campaign goals. Repository metrics such as necessary repository footprint and peak annual dose are affected by heat and radionuclide release characteristics specific to variable spent fuel compositions associated with alternative fuel cycles. Computational tools capable of simulating the dynamic, heterogeneous spent fuel isotopics resulting from transition scenarios and alternative fuel cycles are, however, lacking in repository modeling options. This work proposes to construct such a generic repository model appropriate for systems analysis. By emphasizing modularity and speed, the work at hand seeks to provide a tool which captures the dominant physics of detailed repository analysis within the UFD Campaign and can be robustly and flexibly integrated within the CYCLUS fuel cycle simulation tool.

## 1 INTRODUCTION

---

The scope of this work includes implementation of a software library of medium fidelity models to comprehensively represent various long-term disposal system concepts for nuclear material. This software library is integrated with a computational fuel cycle systems analysis platform in order to inform repository performance metrics with respect to candidate fuel cycle options. By abstraction of more detailed models, this work captures the dominant physics of radionuclide and heat transport phenomena affecting repository performance in various geologic media and as a function of arbitrary spent fuel composition.

### 1.1 Motivation

The development of sustainable nuclear fuel cycles is a key challenge as the use of nuclear power expands domestically and internationally. While fuel cycle performance may be measured with respect to a variety of metrics, waste management metrics are of particular importance to the goal of sustainability. Since disposal options are influenced by upstream fuel cycle decisions, a relevant analysis of potential geological disposal and engineered barrier solutions requires a system level approach that is both modular and efficient.

As the merits of numerous combinatoric fuel cycle possibilities are investigated, a top-level simulation tool capable of modular substitution of various fuel cycle facility, repository, and engineered barrier components is needed. The modular waste package and repository models resulting from this work will assist in informing current technology choices, identifying important parameters contributing to key waste disposal metrics, and highlighting the most promising waste disposal combinations with respect to metrics chosen by the user. Specifically, such models will support efforts underway in focusing domestic research and development priorities as well as computational tools under development that quantify these metrics and demonstrate the merits of different fuel cycle alternatives.

System level fuel cycle simulation tools must facilitate efficient sensitivity and uncertainty analyses as well as simulation of a wide range of fuel cycle alternatives. Efficiency is achieved with models at a level of detail that successfully captures significant aspects of the underlying physics while achieving a calculation speed in accordance with use cases requiring repeated simulations. Often termed abstraction, the process of simplifying while maintaining the salient features of the underlying physics is the method by which used fuel disposal system models were developed in this work.

Independent fuel cycle parameters of particular interest in fuel cycle systems analysis have been those related to the front end of the fuel cycle. Deployment decisions concerning reactor types, fast to thermal reactor ratios, and burnup rates can all be

independently varied in fuel cycle simulation codes in such a way as to inform domestic policy decisions going forward. Some of these parameters are coupled, however, to aspects of the back end of the fuel cycle. For example, the appropriate fast reactor ratio is significantly altered by the chosen method and magnitude of domestic spent fuel reprocessing or lack thereof.

However, independent variables representing decisions concerning the back end of the fuel cycle are of increasing interest as the United States further investigates repository alternatives to Yucca Mountain. Parameters such as the repository geology, engineered barriers, appropriate loading strategies and schedules are all independent variables up for debate. Due to the feedback implication of repository capacity and performance, these parameters are coupled with decisions about the fuel cycle.

Thus, while independent parameters can be chosen and varied within a fuel cycle simulation, some parameters are coupled in such a way as to require full synthesis with a systems analysis code that appropriately determines the isotopic mass flows into the repository, their appropriate conditioning, densities, and other physical properties.

## **Future Fuel Cycle Options**

Domestically, nuclear power expansion is motivated by the research, development, and demonstration roadmap being pursued by the United States Department of Energy Office of Nuclear Energy (DOE-NE), which seeks to ensure that nuclear energy remain a viable domestic energy option [22].

As the DOE-NE seeks to develop technologies and strategies to support a sustainable future for nuclear energy, various fuel cycle strategies and corresponding disposal system options are being considered. Specifically, the domestic fuel cycle option space under current consideration is described in terms of three distinct fuel cycle categories with the monikers Once Through, Full Recycle, and Modified Open. Each category presents unique disposal system siting and design challenges. Systems analyses for evaluating these options must be undertaken in order to inform a national decision to deploy a comprehensive fuel cycle system by 2050 [22].

The Once-Through Cycle category includes fuel cycles similar to the continuation of the business as usual case in the United States. Such fuel cycles neglect reprocessing and present challenges associated with high volumes of minimally treated spent fuel streams. In a business as usual scenario, conventional power reactors comprise the majority of nuclear energy production and fuel takes a single pass through a reactor before it is classified as waste and disposed of. In the open cycle, no reprocessing is pursued, but research and development of advanced fuels seek to reduce waste volumes. Calculations from the Electric Power Research Institute corroborated by the United States (US) Department of Energy (DOE) in 2008 indicate that without an increase in the statutory capacity limit of the Yucca Mountain Repository Site (YMR), continuation of the current Once Through fuel cycle will generate a volume of spent fuel that will

necessitate the siting of an additional federal geological repository to accommodate spent fuel [34, 21].

A Full Recycle option, on the other hand, requires the research, development, and deployment of partitioning, transmutation, and advanced reactor technology for the reprocessing of used nuclear fuel. In this scheme, conventional once-through reactors will be phased out in favor of fast reactor and so called Generation IV reactor technologies, which demonstrate transmutation capacity and greater fuel efficiency. All fuel in the Full Recycle strategy will be reprocessed. It may be reprocessed using an accelerator driven system or by cycling through an advanced fast reactor. Such fuel may undergo partitioning, the losses from which will require waste treatment and ultimate disposal in a repository. Thus, a repository under the Full Recycle scenario must support a waste stream composition that is highly variable during transition periods as well as myriad waste forms and packaging associated with isolation of differing waste streams.

Finally, the Modified Open Cycle category of options includes a variety of fuel cycle options that fall between once through and fully closed. Advanced fuel cycles such as deep burn and small modular reactors will be considered within the Modified Open set of fuel cycle options as will partial recycle options. Partitioning and reprocessing strategies, however, will be limited to simplified chemical separations and volatilization under this scheme. This scheme presents a dual challenge in which spent fuel volumes and composition will both vary dramatically among various possibilities within this scheme [22].

Clearly, the myriad waste streams resulting from potential fuel cycles present an array of corresponding waste disposition, packaging, and engineered barrier system options. For a comprehensive analysis of the disposal system, dominant physics models must therefore be developed for each of these subcomponents. Differing spent fuel composition, partitioning, transmutation, and chemical processing decisions upstream in the fuel cycle demand differing performance and loading requirements of waste forms and packaging. The capability to model thermal and radionuclide transport phenomena through vitrified glass as well as ceramic waste forms with various loadings of arbitrary isotopic compositions is therefore required. This work has produced a repository model that meets this need.

## **Future Waste Disposal System Options**

In addition to reconsideration of the domestic fuel cycle policy, the uncertain future of the YMR has driven the expansion of the option space of potential repository host geologies to include, at the very least, granite, clay/shale, salt, and deep borehole concepts [44].

In accordance with various fuel cycle options, corresponding waste form, waste package, and other engineered barrier systems are being considered. Specifically, current considerations include ceramic (e.g. Uranium Oxide), glass (e.g. borosilicate glasses), and metallic (e.g. hydride fuels) waste forms. Waste packages may be copper, steel, or other alloys. Similarly, buffer and backfill materials vary from the crushed salt

recommended for a salt repository to bentonite or concrete in other geologies. Therefore, a repository model capable of modular substitution of waste form models and data is necessary to analyze the full option space.

The physical, hydrologic, and geochemical mechanisms that dictate radionuclide and heat transport vary between the geological and engineered containment systems in the domestic disposal system option space. Therefore, in support of the system level simulation effort, models must be developed that capture the salient physics of these geological options and quantify associated disposal metrics and benefits. Furthermore, in the same way that system level modularity facilitates analysis, so too does modular linkage between subcomponent process modules. These subcomponent models and the repository environmental model must achieve a cohesively integrated disposal system model such as is proposed by this work.

### **Thermal Modeling Needs**

The decay heat from nuclear material generates a significant heat source within a repository. In order to arrive at loading strategies that comply with thermal limits in the engineered barrier system and the geological medium, a thermal modeling capability must be included in the repository model. Such a model is also necessary to inform material and hydrologic phenomena that affect radionuclide transport and are thermally coupled.

Partitioning and transmutation of heat generating radionuclides within some fuel cycles will alter the heat evolution of the repository [57]. Thus, to distinguish between the repository heat evolution associated with various fuel cycles involving partitioning and transmutation, a repository analysis model, must at the very least, capture the decay heat behavior of dominant heat contributors. Plutonium, Americium, and their decay daughters dominate decay heat contribution within used nuclear fuels. Other contributing radionuclides include Cesium, Strontium, and Curium [48].

Thermal limits within a used nuclear fuel disposal system are waste form, package, and geology dependent. The heat evolution of the repository constrains waste form loadings and package loadings as heat generated in the waste form is transported through the package. It also places requirements on the size, design, and loading strategy in a potential geological repository as that heat is deposited in the engineered barrier system and host geology.

Thermal limits of various waste forms have their technical basis in the temperature dependence of isolation integrity of the waste form. Waste form alteration, degradation, and dissolution behavior is a function of heat in addition to redox conditions and constrains loading density within the waste form.

Thermal limits of various engineered barrier systems similarly have a technical basis in the temperature dependent alteration, corrosion, degradation, and dissolution rates of the materials from whence they are constructed.

Thermal limits of the geologic environment can be based on the mechanical integrity of the rock as well as mineralogical, hydrologic and geochemical phenomena. The isolating characteristics of a geological environment are most sensitive to hydrologic and geochemical effects of thermal loading. Thus, heat load constraints are typically chosen to control hydrologic and geochemical response to thermal loading. In the United States, current regulations necessitate thermal limits in order to passively steward the repository's hydrologic and geochemical integrity against radionuclide release for the first 10,000 years of the repository.

The two heat load constraints that primarily determined the heat-based spent nuclear fuel (SNF) capacity limit in the Yucca Mountain Repository design, for example, are specific to unsaturated tuff. These are given here as an example of the type of regulatory constraints that this model captures for various geologies.

The first Yucca Mountain heat load constraint is intended to promote constant drainage, thereby preventing episodic flow into waste package tunnels and subsequent contaminated water flow through the repository. It requires that the minimum temperature in the tuff between drifts be no more than the boiling temperature of water, which is  $96^{\circ}\text{C}$  at the altitude in question. For a repository with homogeneous waste composition in parallel drifts, this constraint limits the temperature exactly halfway between adjacent drifts, where the temperature is at a minimum.

The second constraint is intended to prevent high rock temperatures that could induce fractures and alteration of the rock. It stated that no part of the rock reach a temperature above  $200^{\circ}\text{C}$ , and was effectively a limit on the temperature at the drift wall, where the rock temperature is a maximum.

Analogous constraints for a broader set of possible geological environments depend on heat transport properties and geochemical behaviors of the rock matrix as well as its hydrologic state. Such constraints affect the repository drift spacing, waste package spacing, and repository footprint among other parameters.

In addition to development of a concept of heat transport within the repository in order to meet heat load limitations, it is also necessary to model temperature gradients in the repository in order to support modeling of thermally dependent hydrologic and material phenomena. As mentioned above, waste form corrosion processes, waste form dissolution rates, diffusion coefficients, and the mechanical integrity of engineered barriers and geologic environment are coupled with temperature behavior. Only a coarse time resolution is necessary to capture that coupling however, since time evolution of repository heat is such that thermal coupling can typically be treated as quasi static for long time scales. [8].

### Source Term Modeling Needs

Domestically, the Environmental Protection Agency (EPA) has defined a limit on human exposure due to the repository. This regulation places important limitations on capacity, design, and loading techniques for repository concepts under consideration. Repository



concepts developed in this work must therefore quantify radionuclide transport through the geological environment in order to calculate repository capacity and other benefit metrics.

The exposure limit set by the EPA is based on a ‘reasonably maximally exposed individual.’ For the YMR, the limiting case is a person who lives, grows food, drinks water and breathes air 18 km downstream from the repository. The Yucca Mountain Repository EPA regulations limit total dose from the repository to 15 mrem/yr, and limit dose from drinking water to 4 mrem/yr for the first 10,000 years. Predictions of that dose rate depend on an enormous variety of factors, most important of which is the primary pathway for release. In the YMR primary pathway of radionuclides from an accidental release will be from cracking aged canisters. Subsequently, transport of the radionuclides to the water table requires that the radionuclides come in contact with water and travel through the rock to the water table. This results in contamination of drinking water downstream.

Source term is a measure of the quantity of a radionuclide released into the environment whereas radiotoxicity is a measure of the hazardous effect of that particular radionuclide upon human ingestion or inhalation. In particular, radiotoxicity is measured in terms of the volume of water dilution required to make it safe to ingest. Studies of source term and radiotoxicity therefore make probabilistic assessments of radionuclide release, transport, and human exposure.

Importantly, due to the long time scale and intrinsic uncertainties required in such probabilistic assessments it is in general not advisable to base any maximum repository capacity estimates on source term. This is due to the fact that in order to give informative values for the risk associated with transport of particular radionuclides, for example, it is necessary to make highly uncertain predictions concerning waste form degradation, water flow, and other parameters during the long repository evolution time scale. However, source term remains a pertinent metric for the comparison of alternative separations and fuel cycle scenarios as it is a fundamental factor in the calculation of risk.

Arriving at a generalized metric of probabilistic risk is fairly difficult. For example, the Peak Environmental Impact (PEI) metric from Berkeley (ref. [14]) is a multifaceted function of spent fuel composition, waste conditioning, vitrification method, and radionuclide transport through the repository walls and rock. Also, it makes the assumption that the waste canisters have been breached at  $t = 0$ . Furthermore, reported in  $m^3$ , PEI is a measure of radiotoxicity in the environment in the event of total breach. While informative, this model on its own does not completely determine a source-term limited maximum repository capacity. Additional waste package failure and a dose pathway model must be incorporated into it.

## **Domestic Research and Development Program**

The DOE-NE Fuel Cycle Technology (FCT) program has three groups of relevance to this effort: these are the Used Fuel Disposition (UFD), the Separations and Waste Forms

(SWF), and Fuel Cycle Options (FCO) (previously Systems Analysis) campaigns. The UFD campaign is conducting the Research Development and Design (RD&D) related to the storage, transportation, and disposal of radioactive wastes generated under both the current and potential advanced fuel cycles. The SWF campaign is conducting RD&D on potential waste forms that could be used to effectively isolate the wastes that would be generated in advanced fuel cycles. The SWF and UFD campaigns are developing the fundamental tools and information base regarding the performance of waste forms and geologic disposal systems. The FCO campaign is developing the overall fuel cycle simulation tools and interfaces with the other FCT campaigns, including UFD.

This effort has interfaced with those campaigns to develop the higher level dominant physics representations for use in fuel cycle system analysis tools. Specifically, this work has leveraged conceptual framework development and primary data collection underway within the Used Fuel Disposition Campaign as well as work by Radel, Wilson, Bauer et. al. to model repository behavior as a function of the contents of the waste [52]. It then incorporated dominant physics process models into the CYCLUS computational fuel cycle analysis tool [28] based on sensitivity analysis utilizing those detailed tools.

## 1.2 Methodology

In this work, concise dominant physics models suitable for system level fuel cycle codes were developed by comparison of analytical models with more detailed repository modeling efforts. The ultimate result of this work is a software library capable of assessing a wide range of combinations of fuel cycle alternatives, potential waste forms, repository design concepts, and geological media.

Current candidate repository concepts have been investigated and reviewed here in order to arrive at a fundamental set of components to model. A preliminary set of combinations of fuel cycles, repository concepts, and geological environments has been chosen that fundamentally captures the domestic option space. Specifically, three candidate geologies and four corresponding repository concepts under consideration by the DOE UFD campaign have been chosen for modeling in this work. These have been implemented to interface with CYCLUS simulations of a canonical set of potential fuel cycles within three broad candidate scenarios put forth by the US DOE.

A review and characterization of the physical mechanisms by which radionuclide and thermal transport take place within the materials and media under consideration was first undertaken. Potential analytical models to represent these phenomena were investigated and categorized within the literature review.

A review and characterization of current detailed computational tools for repository focused analysis was next conducted. Both international and domestic repository modeling efforts were summarized within the literature review. Of these, candidate computational tools with which to perform abstraction and regression analyses were identified. Specifically, a suite of Generic Disposal System Model (GDSM) tools under

development by the DOE UFD campaign has informed radionuclide transport models and a pair of corresponding thermal analysis codes has informed the thermal models.

This suite of subcomponent modules, appropriate for use within the CYCLUS fuel cycle simulator, has included the development of a robust architecture within the repository module that allows for interchangeable loading of system components. Within the system components, dominant physics is modeled based on domain appropriate approximation of analytical models and supported by abstraction with the chosen GDSM tools and thermal tools.

In general, such concise models are a combination of two components: semi-analytic mathematical models that represent a simplified description of the most important physical phenomena, and semi-empirical models that reproduce the results of detailed models. By combining the complexity of the analytic models and regression against numerical experiments, variations can be limited between two models for the same system. Different approaches have been compared in this work, with final modeling choices balancing the accuracy and efficiency of the possible implementations.

Specifically, these models focus on the hydrology and thermal physics that dominate radionuclide transport and heat response in candidate geologies as a function of radionuclide release and heat generation over long time scales. Dominant transport mechanism (advection or diffusion) and disposal site water chemistry (redox state) provide primary differentiation between the different geologic media under consideration. In addition, the concise models are capable of roughly adjusting release pathways according to the characteristics of the natural system (both the host geologic setting and the site in general) and the engineered system (such as package loading arrangements, tunnel spacing, and engineered barriers).

The abstraction process in the development of a geological environment model employs the comparison of semi-analytic thermal and hydrologic models and analytic regression of rich code results from more detailed models as well as existing empirical geologic data. Such results and data will be derived primarily from the UFD campaign GDSMs and data, as well as European efforts such as the RED-IMPACT assessment and Agence Nationale pour la gestion des Déchets RADIOactifs, the French National Agency for Radioactive Waste Management (ANDRA) Dossier efforts [36, 8, 18].

Thereafter, a regression analysis concerning those parameters has been undertaken with available detailed models (e.g. 2D and 3D finite element thermal performance assessment codes) to further characterize the parametric dependence of thermal loading in a specific geologic environment.

Finally, the thermal behavior of a repository model so developed depends on empirical data (e.g. heat transfer coefficients, hydraulic conductivity). Representative values have been made available within the dominant physics models and rely on existing empirical data concerning the specific geologic environment being modeled (i.e. salt, clay/shale, and granite).

A similar process was followed for radionuclide transport models. The abstraction process in the development of waste form, package, and engineered barrier system

models will be analogous to the abstraction process of repository environment models. Concise models have resulted from employing the comparison of semi-analytic models of those systems with regression analysis of rich code in combination with existing empirical material data.

Coupling effects between components were considered carefully. In particular, given the important role of temperature in the system, thermal coupling between the models for the engineered system and the geologic system were considered. Thermal dependence of radionuclide release and transport as well as package degradation were analyzed to determine the magnitude of coupling effects in the system.

The full abstraction process was iterated to achieve a balance between calculation speed and simulation detail. Model improvements during this stage sought a level of detail appropriate for informative comparison of subcomponents, but with sufficient speed to enable systems analysis.

By varying input parameters and comparing with corresponding results from detailed tools, each model's behavior on its full parameter domain was validated.

## 1.3 Outline

A literature review, Chapter 2, presents background material that organizes and reports upon previous relevant work. First it summarizes the state of the art of repository modeling integration within current systems analysis tools. It then describes current domestic and international disposal system concepts and geologies. Next, the literature review focuses upon current analytical and computational modeling of radionuclide and heat transport through various waste forms, engineered barrier systems, and geologies of interest. It also addresses previous efforts in generic geologic environment repository modeling in order to categorize and characterize detailed computational models of radionuclide and heat transport available for regression analysis.

Chapter 3 details the computational paradigm of the CYCLUS systems analysis platform and Cyder repository model which constitute this work. It describes the CYCLUS fuel cycle simulation context which drives fundamental Cyder design decisions.

Chapter 4 describes the radionuclide and heat transport models that were implemented. Models representing waste form, waste package, buffer, backfill, and engineered barrier components are defined by their interfaces and their relationships as interconnected modules, distinctly defined, but coupled. This modular paradigm allows exchange of technological options (i.e. borosilicate glass and concrete waste forms) for comparison but also exchange of models for the same technological option with varying levels of detail.

Chapter 5 describes demonstration cases conducted to demonstrate radionuclide transport and thermal capacity analysis in Cyder. It also describes verification and validation procedures which benchmarked Cyder behavior against more detailed models.

Finally, in Chapter ??, contributions to the field and suggested future work are summarized.

Chapter ?? will

## 2 LITERATURE REVIEW

---

The following literature review addresses areas of current research integral to the work at hand. The contribution of computational nuclear fuel cycle simulation tools to sensitivity analyses of repository performance metrics is first summarized. A discussion of the disposal system concepts and geologies under consideration domestically and internationally are then also summarized. A review of analytical models of radionuclide transport and a review of analytical models of heat transport follow. An overview of current detailed computational models, available data and algorithms characterizing radionuclide transport are addressed next, including both standalone and those incorporated into nuclear fuel cycle simulation tools. Finally, a review of current computational models of heat transport in the waste disposal system context is given. Special focus is paid to the availability of supporting data and algorithms informing geochemical and hydrological transport on long time scales and in various geologies.

### 2.1 Repository Capabilities within Systems Analysis Tools

Current top-level simulators largely disregard the waste disposal phase of fuel cycle analysis. Choosing instead to report metrics such as mass or volumes of accumulated spent nuclear fuel, current tools fail to address the impact of those waste streams on the performance of the geologic disposal system [62]. To fully inform the decision making process, metrics that depend on the performance of the geologic disposal system will be necessary within the tool proposed here.

A model for repository capacity was developed for the the Verifiable Fuel Cycle Simulation Model (VISION) fuel cycle simulator and recent efforts on the Nuclear Waste Assessment System for Technical Evaluation (NUWASTE) simulator have made some progress in addressing this deficiency, but despite a proliferation of sophisticated fuel cycle simulators, similar efforts are lacking in this regard [64, 51, 2].

#### NUWASTE

NUWASTE is a Nuclear Waste Technical Review Board code under development that determines many metrics about the fuel cycle according to various parameters and for various fuel cycles [2]. Its use is limited to the Nuclear Waste Technical Review Board (NWTRB) and access is further restricted by its utilization of commercial Microsoft Access and Visual Basic database and functional capabilities.

NUWASTE tracks 65 isotopes within material objects, discretely models individual shipping casks and incorporates cooling time in both dry and wet intermediate storage facilities. Though it tracks the number of assemblies through a simulation and their

isotopic composition, NUWASTE lacks radionuclide transport and heat based capacity calculations.

## VISION

VISION, a fuel cycle simulator created at Idaho National Laboratory (INL) is built on the commercial systems analysis platform, PowerSim. The code therefore has both commercial and governmental license restrictions and is sensitive to laboratory export control requiring explicit developer approval [63, 60]. VISION is capable of modeling an array of fuel cycle options. It tracks and conducts decay calculations for upwards of 80 isotopes of interest [64, 62].

While its repository model calculates YMR specific information about waste package heat production and heat based repository capacity, continuous masses are modeled rather than discrete waste packages, and no radionuclide transport calculations are conducted [51, 13].

## DANESS

The Dynamic Analysis of Nuclear Energy System Strategies (DANESS) tool is developed at Argonne National Laboratory and discretely models reactors within regional reactor parks for a flexible array of fuel cycles. Material movement is based on a fuel ordering paradigm and is written in a combination of FortranIV and C, but is limited to a 10 reactor simulation. Repository capabilities are also limited to mass accounting and perform no radionuclide or heat transport calculations.

Input and output are in Microsoft Excel format and DANESS relies on the proprietary IThink simulation platform. The code therefore has both commercial and governmental license restrictions and is sensitive to export control requiring explicit developer approval [63, 60].

## COSI

Commelini-Sicard (COSI) is a code from the Commissariat à l'Energie Atomique et aux Energies Alternatives (CEA) of France and is implemented in the Java programming language. It is capable of performing a large range of full fuel cycle scenarios in great detail. COSI6 utilizes fully detailed physics analysis packages and is capable of making assessments of repository capacity as well as radiotoxicity and decay heat calculations of waste packages [13]. Radionuclide transport through the repository post-emplacement is, however, not calculated and the distribution license is very restrictive.

## NFCSim

The Nuclear Fuel Cycle Simulator (NFCSim) code was implemented in the Java programming language by Erich Schneider and Los Alamos National Lab. Primarily a mass tracking code, the repository model was limited to a heat analysis. Uniquely, in NFCSim the transportation of each waste package was modeled discretely [54].

## CAFCA

Code for Advanced Fuel Cycles Assessment (CAFCA) is a fuel cycle code from the Massachusetts Institute of Technology (MIT) based on the VENISIM system dynamics platform. While CAFCA is capable of tracking processed fuel assemblies and isotopics, it does not calculate capacity metrics or conduct detailed radionuclide or heat transport. Its license, held by MIT, is of a less restrictive academic nature, but the source is not in wide distribution and the dependence on VENISIM necessitates that potential developers acquire a proprietary license for that software.

## ORION

This code is a proprietary code developed at the United Kingdom's National Nuclear Laboratory. While there is no heat-limited capacity model or calculation of radionuclide transport, the material destined for the repository can be described with a number of mass indexed metrics such as activity [ $Bq$ ], radiotoxicity [ $Sv$ ], toxic potential [ $m^3$ ], spontaneous neutron emission [ $s^{-1}$ ], and heat production [ $W$ ]. None of these metrics, however, incorporate a dose pathway or calculate radionuclide transport.

## OCRWM Yucca Mountain Total System Model

The Total System Model (TSM) code, developed at Office of Civilian Radioactive Waste Management (OCRWM) is a very detailed model of the Yucca Mountain disposal system. It includes transportation issues and detailed emplacement timing and strategy models, but considers only the fuel cycle associated with the current U.S. reactor fleet. Casks are modeled discretely and radionuclide and heat transport are modeled in great detail. This level of detail results in a dramatically extended run time making this model inappropriate for top level fuel cycle systems analysis. The TSM model can only be run by its development team and runs a typical simulation, processing 70,000 MTHM, in 12-15 hours [58].

The TSM framework is based on the commercial SimCAD platform. The simulation steps through times in 8 hour time steps during the waste cask transportation, processing and emplacement. This event based simulator is primarily focused on the operation stage of the Yucca Mountain repository, but is equipped with a thermal management model that informs waste package emplacement.



## Repository Focused Fuel Cycle Analyses

While top level fuel cycle system analyses fail to incorporate repository models, some repository focused fuel cycle sensitivity analyses have been conducted. Some repository focused analyses emphasizing used fuel disposition and waste management in the Yucca Mountain Repository (YMR) have been conducted by Ahn, Li, Piet, Wigeland, Wilson, and others . With a focus on YMR capacity benefit, repository performance metrics of interest for these analyses were heat, source term, and more global environmental impact metrics. Sensitivity analyses for other geologic environments were conducted concerning repository concepts relevant to other nations as well.

## 2.2 Conceptual Discussion of Disposal Environments

A suite of three geologic media and four disposal concepts of interest were chosen to capture the primary geologies and concepts found in the following review of international and domestic efforts. Granite, clay, and salt geologic environments will be modeled with flexible layouts and an array of available canonical engineered subcomponent models. The detailed Generic Performance Assessment Model (GPAM) effort and associated GDSM tools were chosen to support the for this work will support abstraction for these concepts and further comparison with ANDRA and RED-IMPACT results will provide further benchmarks for validation.

The concepts that have been investigated internationally and will be investigated in this work are dominated by saturated, closed concepts. Saturated concepts are those located below the water table such that, in contrast to YMR, the porosity within the rock matrix as well as fractures and other open spaces is suffused with water. A closed concept is one that neither relies on ventilation shafts nor an extended open period after waste emplacement.

Enclosed modes are appropriate for low permeability rock formations (clay/shale, granite, salt). Low permeability does not permit oxygen entry, so these are chemically reducing environments. Chemically reducing environments are reducing insofar as they induce redox reactions to proceed in the reduction direction. This attribute has the primary effect of slowing corrosion, dissolution, and alteration rates in materials that are subject to degradation. A reducing disposal environment also lowers solubility limits and increases sorption of many actinide species. The dominant dose contributors in reducing environments are therefore the soluble, long lived fission and activation products such as  $^{129}\text{I}$  and  $^{79}\text{Se}$  [45, 36]. Furthermore, rather than being primarily kinetically limited, as in an oxidizing environment, sorption behavior is primarily thermodynamically limited [43, 55]. The models created here will be designed such that these distinctions between reducing and oxidizing environments may be parsed in the event that an extension model simulates an oxidizing environment.

Since heat is carried away less effectively once closure has occurred, heat limits are

lower in closed repository concepts than in open ones, such as YMR, where drift tunnels are ventilated for a number of years after emplacement before closure.

A number of waste form options will be modeled as a part of this effort. To sufficiently model the fuel cycles of interest, it will be necessary to model a borosilicate glass high level waste form as well as an oxide ceramic waste form. These together will provide a sufficient but not comprehensive option space for modeling candidate domestic disposal systems. They will also provide enough diversity to demonstrate the validity of the abstraction methodology here applied. Additional waste forms of interest are listed in Table 2.6. Waste forms will be distinguished by their alteration, corrosion, and other degradation behaviors.

Various engineered barrier system components will also be modeled as a part of this effort. Sufficient waste package, buffer, backfill, and other sealing components will be modeled in order to cover the option space demonstrated by both domestic and international repository concept research. Fundamentally, concrete, salt, and bentonite buffer and backfill options will be modeled and copper, carbon steel, and stainless steel waste package concepts will be modeled.

Distinctions between the four repository concepts that will be considered here include varying coefficients of hydraulic conductivity, thermal conductivity, sorption, solubility, etc.

## Clay Disposal Environments

Clays, including a range of claystones, shales, and argillites, have been investigated in Belgium, France, Japan, and Switzerland as well as the US [36, 18]. Attractive qualities of clay for repository investigations include its ease of excavation as well as the tendency, particularly for some very plastic clays under consideration, to coalesce over time around waste packages within the zone disturbed by excavation. A less attractive quality of clay is a low thermal limit around  $100^{\circ}\text{C}$  temperature limit to prevent alteration [25]. Some characteristics of clay disposal concepts are given in Table 2.1.

Clay Repository Features			
Hydrology	Geochemistry	Design Concepts	Thermal Behavior
Very low conductivity High porosity (up to 0.5) Low effective porosity Slow water velocity diffusion dominated	Reducing Saline Saturated	no/bentonite/concrete backfill $\sim 500\text{m}$ deep closed horizontal or vertical emplacement	alteration limited $100^{\circ}\text{C}$ limit

Table 2.1: Clay geological repository concept demonstrates certain dominant physical phenomena.

## Disposal System Components

The French ANDRA analysis modeled borosilicate glass as well as ceramic oxide waste forms within carbon steel waste packages in combination with a bentonite buffer material and a crushed clay or shale backfill [8]. The Belgian reference concept focused on a highly plastic Boom Clay, which eventually completely seals around stainless steel, nickel, or titanium waste packages [46]. The Swiss concept modeled glass waste forms in stainless steel waste packages with a bentonite buffer and a bentonite and sand backfill [32]. Each of these analyses considered horizontal emplacement in multiple-package emplacement drifts.

## Hydrology

In the clay disposal environment, an exceptionally low interconnected porosity, diffusion dominated water movement and very little fracturing result in a very low overall hydraulic conductivity. Hydrology in the far field is typically assumed to be diffusion dominated.

## Geochemistry

This environment is very reducing in both the near and far field. The salinity of this environment increases with depth and it is expected that the pH will be near neutral in this environment. However, for some concepts incorporating cementitious backfill materials for protection of steel, the pH can become significantly alkaline, resulting in expedited alteration of glass wasteforms, bentonite buffers, and the clay matrix [8].

Highly mobile radionuclides which dominate dose from clay repository concepts for most fuel cycles include  $^{129}\text{I}$ ,  $^{79}\text{Se}$ , and  $^{36}\text{Cl}$  [57].

## Thermal Behavior

Heat limits in clay are based on the domain of known behavior in clay and the tendency for bentonite fill material to lose its isolating properties with high temperatures [8, 50]. Limits in clay are fairly low as the thermal conductivity of clay is typically lower than  $2[\text{W}/\text{m} \cdot ^\circ\text{K}]^1$ .

The alteration of high smectite bentonite to non-expandable clays is a primary limitation for heat tolerance in the clay concept. The isolation characteristics of bentonite buffer materials are reduced after this alteration. The time integral of this phenomenon determines total bentonite alteration. While short bursts of heat might be allowable, because the bentonite will not alter immediately, the kinetic alteration into smectite clays is hastened by temperatures above approximately  $100^\circ\text{C}$  [50]. The Belgian program

---

<sup>1</sup> Belgium (ref. [46]) used values between 1.25 and  $1.7[\text{W}/\text{m} \cdot ^\circ\text{K}]$ .  
 France (ref. [8]) used values between 1.9 and  $2.7[\text{W}/\text{m} \cdot ^\circ\text{K}]$ .  
 Switzerland (ref. [? ]) used  $1.8[\text{W}/\text{m} \cdot ^\circ\text{K}]$ .

has considered increasing the thermal limit of the clay in the buffer region by adding graphite. Conversely, well understood behavior for argillaceous clay and bentonite buffer backfill is conservatively assumed by the ANDRA assessment to occur only under  $90^{\circ}\text{C}$ , which is effectively a limit at the waste package interface with the bentonite buffer material[8] . The National Cooperative for the Disposal of Radioactive Waste (NAGRA) Opalinus Clay assessment less conservatively uses a maximum heat limit in the bentonite buffer of  $125^{\circ}\text{C}$  [31] .

## Granite Disposal Environments

Granite disposal concepts have been considered in Finland, Japan, Sweden, China, Spain, the Czech Republic, South Korea and Switzerland as well as the US [25, 9, 36].

Attributes of granite that make it an attractive candidate geology for nuclear waste disposal include its very low porosity and permeability and high thermal conductivity. Fracturation in granite, however, has a negative effect on the isolation properties of the rock. Some characteristics of granite disposal concepts are given in Table 2.2.

Granite Repository Features			
Hydrology	Geochemistry	Design Concepts	Thermal Behavior
Low porosity ( $\sim 0.01$ ) High Fracturation Low permeability High Water Velocity	Reducing in Near Field Slightly Oxidizing in Far Field Increasing saline with depth [36] Cement causes alkalinity [9] Saturated or Unsaturated	Single WP tunnels Carbon-Steel [9]or Copper overpack Bentonite buffer Crushed granite backfill [36] $\sim 500\text{m}$ deep	Closed Bentonite Limit $100^{\circ}\text{C}$

Table 2.2: Granite repository concepts demonstrate certain dominant physical phenomena.

## Disposal System Components

The Swedish KBS-3 concept includes ceramic oxide spent fuel waste forms within a steel shell and copper waste package buffered by bentonite clay and backfilled with clay and sand and emplaced vertically in horizontal drifts [1]. A similar Czech Republic repository concept consists of borosilicate glass waste forms within a stainless steel Universal Canister waste package, vertically emplaced in horizontal drifts and with a bentonite buffer and backfilled with a clay and sand mixture. The Spanish concept is almost exactly similar to these, except emplacement is horizontal within the horizontal repository drifts [36].

This work will model borosilicate glass and ceramic oxide waste forms, carbon steel and copper waste packages, and bentonite and concrete buffer options. A flexible repository layout model will support approximated modeling of each of these designs.

## Hydrology

In the granite disposal environment, with a low porosity combined with higher expected water velocity (relative to other repository concepts in this work) and significant fracturing, the overall granite hydraulic conductivity is low, typically [55, 25]. Within this environment, the water behavior in the far field must be modeled as both diffusive and advective.

## Geochemistry

This environment is very reducing in the near field and less reducing in the near surface far field. Far field fracturing in the granite near the surface of the site exposes the medium to the atmosphere, resulting in a slightly oxidizing condition in the near surface far field, most importantly resulting in higher actinide solubilities in that region. Salinity in the granite environment increases monotonically with depth. At a typical concept depth of 500m, the repository is therefore expected to be in a location of high salinity, an indicator of historically low fluid flow but resulting in increased corrosion rates and for some radionuclides, changed solubilities [9]. It is expected that the pH will be near neutral in this environment except with the introduction of concretes, due to which the pH becomes significantly alkaline, resulting in more rapid alteration of bentonite buffers.

The relatively fast advective pathway provided by granite fracturing has the effect of increasing the importance of  $^{234}\text{U}$  in the initial waste stream. While  $^{234}\text{U}$  and its decay daughter  $^{230}\text{Th}$  are not very mobile in a reducing environment, their subsequent decay daughter  $^{226}\text{Ra}$  is highly mobile. In clay, the 1601 year half life of  $^{226}\text{Ra}$  is too short for a significant quantity to traverse the diffusive pathway. In granite, however,  $^{226}\text{Ra}$  is a dominant dose contributor [57].

## Thermal Behavior

Granite repository concepts are limited by the bentonite buffer in a manner similar to that of clay. However, in the absence of the bentonite limitation, a thermal limit within the granite itself is greater than  $200^{\circ}\text{C}$ , limited by the increased risk of micro-cracking. This relatively high resistance to heat induced mechanical failure is due to the high thermal conductivity of granite, which is typically <sup>2</sup> found to be between 2.4 and 4  $[\text{W}/\text{m} \cdot ^{\circ}\text{K}]$ .

The effective thermal limit for granite disposal concepts, however, is usually related to the bentonite limit, which is conservatively assumed by the ANDRA assessment to occur under  $90^{\circ}\text{C}$  at the waste package interface with the buffer material. Mechanical

---

<sup>2</sup> Sweden (ref. [1]) used 3.4 - 4  $[\text{W}/\text{m} \cdot ^{\circ}\text{K}]$  and 2.45 - 2.9  $[\text{W}/\text{m} \cdot ^{\circ}\text{K}]$ .  
 France (ref. [8]) used 2.4 - 3.8  $[\text{W}/\text{m} \cdot ^{\circ}\text{K}]$ .  
 Finland (ref. [49]) used 2.3 - 3.2  $[\text{W}/\text{m} \cdot ^{\circ}\text{K}]$ .

stresses and strains in the matrix due to heating at this level were analyzed by ANDRA and shown to have a negligible effect of flow behavior in granite. Similarly, thermo-hydraulic effects due to thermally induced fluid density changes are expected to be slight [9]. Similarly, for reasons of buffer isolation integrity, the Czech and Spanish granite disposal concepts both maintained a thermal limit at the waste package interface with the buffer of  $100^{\circ}\text{C}$ . [36]

## Salt Disposal Environments

The salt disposal concept has been investigated in Germany and demonstrated for non-heat-generating waste at the Waste Isolation Pilot Plant (WIPP) facility in the US. Salt demonstrates many attractive properties including ease of mining, creep behavior over time, which is expedited by heat, low permeability, and a high thermal conductivity, which affords a high temperature limit near  $200^{\circ}\text{C}$  [25]. Some characteristics of salt disposal concepts are given in Table 2.3.

Salt Repository Features			
Hydrology	Geochemistry	Design Concepts	Thermal Behavior
Dry Waste Package Dry Backfill Saturated Far Field Very low permeability Brine pockets in far field	Reducing in Near Field Far Field Slightly Oxidizing Very saline brines	Alcove Emplacement Crushed Salt Backfill $\sim 500\text{m}$ deep Multiple Packages Breached only from intrusion	$180^{\circ}\text{C}$ limit [36] Heat induced creep sealing Closed limited data

Table 2.3: Salt geological repository concept demonstrates certain dominant physical phenomena.

## Disposal System Components

The German reference concept in a salt dome has hundreds of drifts in which are placed thick steel waste packages and backfilled with crushed salt [36].

The consolidation properties of the backfill and salt are of great isolation importance. The infinitesimally small hydraulic conductivity of consolidated rock salt has the effect of nullifying the possibility of any releases without a disruption scenario. Thus, the accurate characterization of the site for both normal and high temperature will provide the fundamental confidence for repository behavior [16].

## Hydrology

In a rock salt or salt dome disposal environment, a very low porosity combined with negligible water velocity and effectively no fracturing results in a salt hydraulic conductivity that is exceptionally low. Within this environment, extraordinarily slow diffusive speed out of the repository dominates the isolation behavior in a manner similar to the

crystalline basement rock of the deep borehole concept. Candidate salt formations are remarkably uniform and their accessible porosity is near negligible, so almost no water movement is expected to occur except that which is potentially induced by the thermal output of the repository.

### **Geochemistry**

This environment is very reducing in the near field and slightly less so in the far field [18]. The very high salinity in the salt environment expedites corrosive processes, but the engineered barrier system is of limited importance in this concept in which the diffusive rock barrier dominates isolation integrity. It is expected that the pH will be near neutral in this environment [36, 18].

### **Thermal Behavior**

Response of a salt repository to heat has a significant mechanical component. Bulk heating of a salt repository matrix causes coalescing of the salt surrounding the heat source. In the case of a nuclear waste repository, this phenomenon increases isolation capability of the salt. A heat limit, then, is difficult to characterize, but evolution of the heat in a salt environment is of great importance to radionuclide transport modeling.

The German salt repository concept maintains a  $180^{\circ}\text{C}$  temperature limit. The technical basis for this limit has to do with the concern that at temperatures above  $220^{\circ}\text{C}$  the salt formation may release brines capable of facilitating radionuclide transport [36, 16].

A model of temperature dependent salt coalescent behavior is in order. While coalescent phenomena has been observed within the WIPP facility, the emplaced material in WIPP is not high heat generating. Thus, high heat salt coalescent behavior warrants further study [17].

The UFD salt repository concept was based on some experience with construction and maintenance of the horizontal borings at WIPP. The current geometry involves emplacement of waste packages arranged at the corner of an alcove. This alcove is then backfilled with crushed salt. Notably, crushed salt has low conductivity, which increases the sensitivity of rock salt temperature on emplaced package temperature. However, as the crushed salt coalesces with heat over time, its thermal conductivity approaches that of intact salt. Further investigation toward a comprehensive model of the thermal behavior of dry salt has been recommended both domestically and internationally [17].

The behavior of moisture in a salt repository under high heat is also not well characterized. Though it is clear that the salt will creep and coalesce with increased temperature, the potential generation of brines within the salt at high heat is a pertinent issue for salt disposal characterization.

## Deep Borehole Disposal Environments

Deep Borehole disposal system concepts are being evaluated in the UK, Sweden and the United States. Attributes of this concept that are favorable for waste isolation include the stability of the crystalline basement rock in which the borehole emplacement would occur and the elongated diffusion path length for release. The potential technical difficulty of well controlled emplacement at great depth is an unfavorable attribute, however [25]. Some characteristics of deep borehole disposal concepts are given in Table 2.4.

Borehole Repository Features			
Hydrology	Geochemistry	Design Concepts	Thermal Behavior
Crystalline rock	Reducing at depth	$\sim 5km$ deep	cracking unimportant
Low porosity ( $\sim 0.01$ )	Less Reducing at surface	disposal in lower 2km	may affect flow
Limited fracturation at depth	limited solubility	1km bentonite seal	high conductivity
Rock Permeability ( $\sim 10^{-19}$ )	enhanced sorption	bentonite grout	high density
EBS Permeability ( $\sim 10^{-16}$ )	high salinity	bentonite plugs	
Very Limited Upward Flow		400 packages per borehole	
	saturated	closed	

Table 2.4: Borehole geological repository concept demonstrates certain dominant physical phenomena.

## Disposal System Components

In deep borehole concepts many types of waste form and waste package material are equivalently emplaced at great depths, typically between 2 and 5 km<sup>3</sup> in a crystalline rock such as granite basement rock. In each borehole, hundreds of canisters are stacked vertically in the deepest section. In some concepts, dense bentonite plugs are stacked between the packages. Above the packages, swelling bentonite clay, asphalt and concrete provide a seal for the upper few kilometers [18].

## Hydrology

In the deep borehole crystalline rock disposal environment, a low porosity combined with only minor fracturing results in an overall crystalline basement hydraulic conductivity which is very low. Thermally driven, upward water velocity is the primary driver for solute movement upward into the many kilometer diffusive path to the surface where fresh water aquifers may exist [18]. Without the introduction of a fast pathway such as an intersecting fracture or human intrusion, the length of the diffusive pathway has the effect of making the engineered barrier component choices irrelevant since no known engineered barrier choice can be expected to outlast the timescale of the diffusive pathway.

<sup>3</sup>4km in the Swedish concept and 5km in US concept [25, 18]



## Geochemistry

This environment is very reducing in the near field and less in the very far field near the earth's surface. The very high salinity of this environment is due to its depth indicates historically low flow. While this increases corrosion rates of engineered barriers, the isolation worth of this concept does not depend significantly on the engineered barrier components, relying instead on the diffusion path length.

## Thermal Behavior

Since the crystalline basement rock in which deep borehole concepts are envisioned is typically granite, the thermal behavior of the deep borehole environment is exactly similar to the granite case, except the bentonite buffer limitation is no longer applicable. Also, the  $200^{\circ}\text{C}$  limitation in order to avoid microfissures could be shown to be irrelevant in light of the great distance to the surface. That is, even if the damage zone in the vicinity of the emplaced waste packages is enlarged significantly by high heat load, the kilometers of diffusion length to the surface will still dominate the isolation behavior of the repository.

## 2.3 Analytical Models of Radionuclide Transport

A comprehensive model of radiotoxic source term must address radionuclide transport through the full release pathway including waste packages, engineered barrier systems, and geologic media. A model of transport through the repository must incorporate a waste package failure model, a radionuclide release model via waste form dissolution, and advective and diffusive transport through the engineered barrier system and geology. A number of efforts to model radionuclide transport through a geologic repository concept have been made internationally and domestically. These efforts, the geologies they address, and some features of their methodologies will be discussed here and appear in Table 2.5.

Waste package failure depends on near field environmental factors such as pH as well as decay heat and water chemistry due to radiolysis anticipated from the contained waste. In turn, the radionuclide release rate from the waste package depends on the character of the waste form matrix, water flow, radionuclide solubility and the elemental diffusion constant. Similarly, advective transfer through the engineered barrier system and into the geological medium also depends on water flow, radionuclide solubility, and radionuclide diffusion, but must be employed in the context of the hydrology of the rock which sets the boundary condition.

Waste package failure modes vary between models. While some employ detailed computational tools such as GoldSim or EBSFAIL (a part of the EBSPAC module used in the TSPA code), which will be discussed in section 2.5, some analytic models incorporate their own hydrologic approximations of canister degradation or make simpler

Models of Source Term for Various Geologies

Source (Who)	Nation (Where)	Geology (What)	Methodology (How)
Enresa [36]	Spain	Granite	GoldSim Proprietary Framework $^{129}\text{I}$ primary contributor
SCK-CEN [36]	Belgium	Clay	Features, events, processes $^{129}\text{I}$ primary contributor
GRS [36]	Germany	Salt	Systematic Performance Assessment $^{135}\text{Cs}$ , $^{129}\text{I}$ , $^{226}\text{Ra}$ , $^{229}\text{Th}$
Ahn [4, 5]	USA	Yucca Tuff	Solubility Limited Release & Congruent Release
NCSU(Nicholson) [37]	USA	Yucca Tuff	TSPA codes EBSREL and EBSFAIL
NAGRA [31, 32]	Switzerland	Opalinus Clay	TAME code
ANDRA [8]	France	Argile Clay	Very detailed CEA code Mostly homogeneous medium $^{129}\text{I}$ primary contributor
ANDRA [9]	France	Granite	Very detailed CEA code Involves fracturation of medium $^{129}\text{I}$ primary contributor
SKB [1]	Sweden	Forsmark Laxemar	HYDRASTAR solute transport FracMan for fracturation

Table 2.5: Methods by which to evaluate source term dependence of waste package failure, transport through the EBS and hydrogeologic transport. The latter two parts vary significantly among host formations.

assumptions of immediate waste canister failure in order to focus on dissolution and transfer.

Waste form release rate is the rate of mass transfer of a radionuclide from its waste form into surrounding water. The mode of water flowthrough heavily affects radionuclide dissolution rate and is treated differently in various models. While some, inspired by the TSP assessment, assume water moves through the waste packages at a constant volumetric rate ('flowthrough model'), others adopt less conservative assumptions incorporating weather based predictions of hydrologic activity.

Radionuclide transport through the EBS and host rock is dependent upon diffusion as well as advection. Radionuclide transport is retarded by sorption, limited by solubility, and enhanced by colloidal mobility [15].

Dissolution is prerequisite to contribution of a radionuclide to source term [15]. That is, the initial dissolution of a radionuclide from its waste form is a breach of the primary barrier. Dissolution rates depend strongly on pH, Eh, speciation of radionuclides (chemical oxidative state), and radiolysis of the dissolving fluid, but primarily on material properties of the waste form.

Precipitation is the reverse of dissolution and occurs when a solubility limit is reached. In a reducing environment, the approach to chemical equilibrium of dissolution and precipitation is rate dependent and is highly dependent on thermodynamics.

Sorption includes both absorption and adsorption. Absorption is the incorporation of a substance of one state into another of a different state. Adsorption is the interaction of a dissolved species with a surface that removes that species from the dissolving medium models. During sorption, contaminants are removed from the flowthrough water and taken up by the walls of pores or fractures in the rock matrix. Importantly, sorption is a reversible process, the counter process of which is desorption in which the contaminant is returned to the pore or fracture fluid from the matrix [3]. Reversible sorption is typically expressed in terms the mass of a radionuclide sorbed into the rock and the mass left in solution.  $K_d$  values are heavily radionuclide and geochemically dependent.

Finally, a phenomenon called colloidal mobility can enhance radionuclide transport. Mineral colloids, which are suspended molecular solids within a liquid emulsion, are expected in the solution saturating the geological environment. Colloids present in the near field dissolving solution have an effect on the mobility of radionuclides. Studies addressing the subtle differences between resultant behavior of various isotopes indicate that colloidal mobility can be modeled as a correction factor to the sorption coefficient [15].

## **Waste Form Release Models**

Radionuclide release from various possible waste form types will be dominated by an array of degradation, alteration, and dissolution phenomena. These phenomena begin when surrounding waste packages are breached, exposing the waste form to water. Some phenomena dominating the release from canonical waste forms such as Commercial Spent Nuclear Fuel (CSNF), DOE Spent Nuclear Fuel (DSNF), and High Temperature Gas Reactor (HTGR) are listed in Table 2.6.

### **Hedin Model ([26])**

In a saturated fractured rock matrix representative of the KBS-3 granitic Swedish repository concept, copper canister waste packages contain a spent fuel waste matrix, and a bentonite buffer surrounds the canisters within repository drift tunnels. Waste form dissolution within the Hedin model is a rate based model that takes place within the waste package void. Radionuclides are released congruently with the flowthrough water at a fractional degradation rate until the waste form is completely degraded. [26]

### **Ahn Models ([4, 5])**

In an oxidizing, unsaturated environment, waste canisters are modelled as compartments of waste form surrounded by a buffer layer that is in turn surrounded by layers of near field rock and far field rock. Water is introduced to the system at a constant rate, and encounters an array of failed waste packages (at  $t = 0$  in the 2004 model, and at

Waste Form Types			
WF Type	SubTypes	Contents	Release Drivers
Once Through	CSNF Ceramic Oxide CSNF Ceramic Oxide HTGR TRISO Graphite DSNF Metal DSNF Carbides DSNF Ceramic Oxides	Nominal Burnup UOx & MOX High Burnup High Burnup High Burnup N Reactor Fuel Fast Reactor Fuels Research Reactor Fuels	redox reactions redox reactions, heat graphite reactions metal reactions, heat carbide reactions, heat redox reactions, heat
Borosilicate Glass	Current Future	Minor Actinides (MAs) Cs/Sr Mo, no MA no Cs/Sr	heat, glass alteration glass alteration
Glass Ceramic	Glass Bonded Sodalite	Echem processed oxide fuels	ceramic, redox, glass reactions
Metal Alloy	From Echem From Aqueous	Cladding, noble metals transition metals	metal reactions, heat metal reactions, heat
Advance Ceramic		volatized iodine	ceramic reactions, redox
Salt	Cementitious Sodium	separated streams	alkaline reactions, dissolution

Table 2.6: An array of waste forms developed for nuclear wastes will have a corresponding array of dominant release mechanisms [12]

$T_f = 75,000$  years in the 2007 model). The water immediately begins dissolving the waste matrix. Radionuclides with higher solubilities are preferentially dissolved and treated with a “congruent release” advective transport model discussed below. Radionuclides with lower solubilities are transported through the buffer with the alternative “solubility limited” release model. The water flow begins at one waste package and travels through the matrix and buffer space to the next waste package, contacting each waste package consecutively and then flowing on into the near field. In this way, the water is increasingly contaminated as its path through the waste packages proceeds.

### Ahn Congruent Release Model

In the Ahn models, radionuclides with a high solubility coefficient are modeled with the congruent release model. Radionuclides of this type include most of the fission products, but not the actinides. This model states that the release from the waste packages is congruent with the dissolution of the waste matrix and is transported through the rock by advective transfer with the water that flows through the waste packages.

### Ahn Solubility Limited Release Model

In the Ahn models, radionuclides with lower solubility coefficients are modeled with the solubility limited release model. Solubility values are assumed from TSPA for this model, and elements with a solubility of less than  $5 \times 10^{-2} [mol/m^3]$  are taken to be ‘low.’ Elements in this ‘low’ category include Zr, Nb, Sn and some toxic actinides such as Th and Ra for an oxidizing, unsaturated environment similar to YMR. It should be noted that in a reducing environment, the actinides are not as mobile, and the high and low

solubility radionuclides will differ from this model. This model suggests that dissolution of radionuclides into the flowthrough water is dominated by diffusion, which is largely dependent upon the concentration gradient between the waste matrix and the water. The mass balance driving radionuclide release takes the form:

$$\dot{m}_i = 8\epsilon D_e S_i L \sqrt{\frac{U r_0}{\pi D_e}} \quad (2.1)$$

where  $\epsilon$ ,  $U$ ,  $r_0$ , and  $L$  are the geometric and hydrologic factors porosity, water velocity, waste package radius, and waste package length, respectively.  $D_e$  is the effective diffusion coefficient ( $m^2/yr$ ) and  $S_i$  is the solubility ( $kg/m^3$ ) of isotope  $i$ .

### Hedin Solubility Limited Release Model

In the Hedin model of the waste matrix, the amount of solute available within the waste package is solved for, and for radionuclides with low solubility, the mass fraction released from the waste matrix is limited by a simplified description of their solubility. That is,

$$m_{1i}(t) \leq v_{1i}(t) C_{sol} \quad (2.2)$$

where the mass  $m_{1i}$  in  $[kg]$  of a radionuclide  $i$  dissolved into the waste package void volume  $v_1$  in  $[m^3]$ , at a time  $t$ , is limited by the solubility limit, the maximum concentration,  $C_{sol}$  in  $[kg/m^3]$  at which that radionuclide is soluble [26].

### Waste Package Failure Models

Waste package failure can, in general, be represented with an expression of the number of failed waste packages,  $n_F$  failing per unit time. This is a simple product between the initial number of waste packages,  $N$ , and the rate,  $f$ , of failure

$$n_F = N \cdot f(). \quad (2.3)$$

Some current common models addressed in this literature review appear in Table ??.

### Physical Model

When enough data exists, the waste package failure rate  $f$  can be represented more realistically by fractional destruction according to experimentally observed corrosion and dissolution rate functions.

However, this can be complicated to model even if the data exists. In particular, the corrosion rate will depend dramatically on the chosen material as well as hydrologic and

Current Waste Package Failure Models

Model	WP Failure Mode	Waste Form	Details
TSPA	EBSFAIL		300,000 years
Ahn 2003	Instantaneous Failure	Borosilicate Glass	$t = 0$
Ahn 2007		CSNF $UO_2$ matrix	$T_f = 75,000$ years
		Borosilicate Glass	$T_f = 75,000$ years
		Naval $UO_2$ matrix	$T_f = 75,000$ years
Li	EBSFAIL		300,000 years
Hedin 2003	Instantaneous	Copper KBS-3 Concept	$t_{delay} = 300$ years

Table 2.7: The above represent some current methods by which waste package failure rates are modeled.

thermal conditions. Specifically, corrosion rates for the same material are very different under dry oxidizing conditions and wet reducing conditions.

The rate  $f$  of package failure in this case will be a function of time  $t$ , temperature  $T$ , and other physical parameters.

$$f() = N \cdot f(t, T, \dots). \quad (2.4)$$

### Probabilistic

When a probability distribution of waste package failure is available, the discrete waste packages can be modeled to fail according to that distribution. For example, if the expected lifetime of a waste package is some known  $t_F$ , a Gaussian distribution around  $t_F$  would provide a probability density function for waste package failures per time step,  $f(t)$ ,

$$f() = f(t). \quad (2.5)$$

Expressed with a cumulative distribution function  $F(t)$  rather than the probability distribution function, equation (2.4) becomes

$$\sum_{t=0}^{t=t} n_F = N \cdot F(t). \quad (2.6)$$

A particularly appropriate probability distribution for use in the case of failed engineered barriers is the Weibull distribution,

$$f(t, \lambda, k) = \begin{cases} \frac{k}{\lambda} \left(\frac{t}{\lambda}\right)^{k-1} e^{-(t/\lambda)^k} & t \geq 0, \\ 0 & t < 0. \end{cases} \quad (2.7)$$

In this expression,  $k$  is a shape parameter and  $\lambda$  is a scale parameter. The time to failure,  $t$  in the Weibull distribution gives a distribution for which the failure rate is proportional to a power of time [47]. Its complementary cumulative distribution function is

$$f(t, \lambda, k) = 1 - e^{-(t/\lambda)^k}. \quad (2.8)$$

For  $k < 1$ , the rate of failure will decrease over time, while for a value of  $k > 1$ , the rate increases over time, appropriate for the aging process of materials [47].

### Instantaneous

The instantaneous case is a special case of the probabilistic situation. Specifically, the probability density function is clearly just the Dirac delta function, with  $n_F$  being the number of failed waste packages per unit time,  $N$  being the total number of waste packages, and  $t_F$  being the time to failure,

$$f() = \delta(t - t_F). \quad (2.9)$$

The Hedin model of waste package failure is effectively instantaneous, but limited by a release resistance coefficient. The release is assumed to occur through a hole in the waste canister that exists throughout the simulation, and the resistance coefficient limiting flow through the hole represents the magnitude of the canister flaw in combination with the buffer-geosphere interface[26]. Other models also use an instantaneous waste package failure mode for all waste packages simultaneously, in which failure occurs either at the onset of the simulation or at some distinct time during the simulation.

## Radionuclide Transport Through Secondary Engineered Barriers

When the waste package is breached and radionuclides are released from the waste form, radionuclides are transported through the secondary engineered barrier, which includes the buffer, backfill, and tunnel wall. After transport through the secondary EBS, radionuclides reach the geosphere.

### Barrier Dissolution and Failure

The same models of waste package failure (instantaneous, rate based, and probabilistic) can be applied to buffers. While concretes are expected to degrade over time, bentonite buffers are quite stable in a reducing environment and help to keep the environment reducing. Furthermore, if preserved by a low heat environment, plastically deforming bentonite clays tend to swell over time and exhibit increased isolating behavior.

### Transport Through Degraded Barrier Matrix

Diffusive and advective transport occur in the barrier matrix both before and after degradation. Before degradation, transport is primarily diffusive. Thereafter, transport can become advective due to cracking. Cracking can be modeled explicitly or as a continuum model.

### Hydrologic Transport Models

Transport out of the EBS and through the geosphere in clay, shale, granite, and salt can largely be characterized as solute transport in permeable porous media. While clay, shale and salt do not exhibit significant fracturing and can often be modeled as homogeneous, granite is characterized as a fractured permeable porous media. Solute transport in both fractured and homogeneous permeable porous media has both porous and fracture flow paths and involves advection, hydraulic dispersion, and diffusion phenomena.

Advection is transport driven by bulk water velocity, diffusion is the result of Brownian motion across concentration gradients, and hydraulic dispersion is transport resulting from heterogeneities in the water velocity field.

Fundamentally, the effect of these flows on mass transport is captured by the conceptual expression

$$\text{In} - \text{Out} = \text{Change in Storage} \quad (2.10)$$

Rearranging 2.10 and defining incoming and outflowing fluxes in a control volume, solute transport in a permeable medium of homogeneous porosity can be written (as in Schwartz and Zhang [55])

$$\frac{\partial nC}{\partial t} = -\nabla \cdot (F_c + F_{dc} + F_d) + m \quad (2.11)$$

where

$n$  = solute accessible porosity [%]

$C$  = concentration [ $kg \cdot m^{-3}$ ]

$t$  = time [ $s$ ]

$F_c$  = advective flow [ $kg \cdot m^{-2} \cdot s^{-1}$ ]

$= nvC$

$F_{dc}$  = dispersive flow [ $kg \cdot m^{-2} \cdot s^{-1}$ ]

$= \alpha nv \nabla C$

$F_d$  = diffusive flow [ $kg \cdot m^{-2} \cdot s^{-1}$ ]



$$= nD_e \nabla C$$

$$m = \text{solute source } [kg \cdot m^{-3} \cdot s^{-1}].$$

In the expressions above,

$$v = \text{advective velocity } [m \cdot s^{-1}]$$

$$\alpha = \text{dispersivity } [m]$$

$$D_e = \text{effective diffusion coefficient } [m^2 \cdot s^{-1}]$$

and

$$n \cdot v = \text{Darcy flux } [m \cdot s^{-1}]. \quad (2.12)$$

The method by which the dominant solute transport mode (diffusive or advective) is determined for a particular porous medium is by use of the dimensionless Peclet number,

$$Pe = \frac{nvL}{\alpha nv + D_e}, \quad (2.13)$$

$$= \frac{\text{advective rate}}{\text{diffusive rate}}$$

where

$$L = \text{transport distance } [m].$$

For a high  $Pe$  number, advection is the dominant transport mode, while diffusive or dispersive transport dominates for a low  $Pe$  number. If one of these terms can be neglected, the solution is simplified.

Otherwise, the analytical expression in equation (2.11) will be the foundation of simplification by regression analyses for the radionuclide transport interface between components of the repository system model representing permeable porous media.

It is customary to define the combination of molecular diffusion and mechanical mixing as the dispersion tensor,  $D$ ,

$$D = \alpha v + D_e \quad (2.14)$$

such that the mass conservation equation becomes:

$$\nabla (nD \nabla C) - \nabla (nv) = \frac{\partial (nC)}{\partial t} \quad (2.15)$$

Adding sorption, by accounting for a change in mass storage,

$$\nabla (nD\nabla C) - \nabla (nv) = \frac{\partial(nC)}{\partial t} + \frac{\partial(s\rho_b)}{\partial t} \quad (2.16)$$

where

$$\begin{aligned} s &= \text{sorption coefficient} \\ \rho_b &= \text{bulk (dry) density [kg/m}^3\text{]}. \end{aligned}$$

If it is assumed that sorption can be approximated as a linear equilibrium, reversible reaction,

$$\frac{\partial(s\rho_b)}{\partial t} = (R_f - 1) \frac{\partial(nC)}{\partial t} \quad (2.17)$$

equation (2.16) becomes

$$\nabla (nD\nabla C) - \nabla (nv) = R_f \frac{\partial(nC)}{\partial t} \quad (2.18)$$

where

$$R_f = \text{retardation factor} \quad (2.19)$$

$$= 1 + \frac{\rho_b K_d}{n} \quad (2.20)$$

$$\rho_b = \text{bulk density of the rock matrix} \quad (2.21)$$

and

$$K_d = \text{species distribution coefficient.} \quad (2.22)$$

For uniform flow, the dispersion tensor,  $D$ , becomes

$$\begin{aligned} D_x &= D_L \\ &= \alpha_L v_x + \tau D_e \end{aligned} \quad (2.23)$$

$$\begin{aligned} D_y &= D_{TH} \\ &= \alpha_{TH} v_x + \tau D_e \end{aligned} \quad (2.24)$$

$$\begin{aligned} D_z &= D_{TV} \\ &= \alpha_{TV} v_x + \tau D_e \end{aligned} \quad (2.25)$$

where

$$\begin{aligned} D_e &= \text{effective diffusion coefficient}[m^2/s] \\ \alpha_L &= \text{longitudinal dispersivity}[m] \\ \alpha_{TH} &= \text{horizontal dispersivity}[m] \\ \alpha_{TV} &= \text{vertical dispersivity}[m] \end{aligned}$$

and

$$\tau = \text{tortuosity}. \quad (2.26)$$

For unidirectional flow, the unidirectional dispersion tensor gives

$$D_x \frac{\partial^2 C}{\partial x^2} + D_y \frac{\partial^2 C}{\partial y^2} + D_z \frac{\partial^2 C}{\partial z^2} + v_x \frac{\partial C}{\partial x} = R_f \frac{\partial(nC)}{\partial t}. \quad (2.27)$$

A special case of uniform flow, no flow, simplifies to the diffusion equation,

$$D_x \frac{\partial^2 C}{\partial x^2} + D_y \frac{\partial^2 C}{\partial y^2} + D_z \frac{\partial^2 C}{\partial z^2} = R_f \frac{\partial(nC)}{\partial t}. \quad (2.28)$$

Solutions to these equations can be categorized by their boundary conditions. The first, or Dirichlet type boundary conditions define a specified species concentration on some section of the boundary of the representative volume,

$$C(\vec{r}, t) = C_0(\vec{r}, t) \text{ for } \vec{r} \in \Gamma. \quad (2.29)$$

The second type or Neumann type boundary conditions describe a full set of fluxes at the boundary of the domain

$$\frac{\partial C(\vec{r}, t)}{\partial r} = nD\vec{J} \text{ for } \vec{r} \in \Gamma. \quad (2.30)$$

where

$$\begin{aligned} \vec{r} &= \text{position vector} \\ \Gamma &= \text{domain boundary} \\ \vec{J} &= \text{solute mass flux } [kg/m^2 \cdot s]. \end{aligned}$$

The third, Cauchy, type describes a combination of the Dirichlet and Neumann type conditions, defining both a concentration at a boundary and a flux at that boundary,

$$C(\vec{r}, t) = C_0(\vec{r}, t) \text{ for } \vec{r} \in \Gamma \quad (2.31)$$

$$\frac{\partial C(\vec{r}, t)}{\partial r} = nD\vec{J} \text{ for } \vec{r} \in \Gamma. \quad (2.32)$$

### One Dimensional Solution with Constant Concentration

An analytical solution for the one dimensional case with a continuous source of constant concentration is known. For the boundary conditions

$$C(0, t) = C_0 \quad (2.33)$$

and

$$\left. \frac{\partial C}{\partial x} \right|_{x=\infty} = 0 \quad (2.34)$$

as well as the initial condition

$$C(x, 0) = 0 \text{ for } x \in (0, \infty), \quad (2.35)$$

the so called Ogata and Banks solution gives

$$C(x, t) = \frac{C_0}{2} \left[ \operatorname{erfc} \left( \frac{x - \frac{v_x t}{R_f}}{2\sqrt{\frac{D_x t}{R_f}}} \right) + e^{\frac{v_x x}{D_x}} \operatorname{erfc} \left( \frac{x + \frac{v_x t}{R_f}}{2\sqrt{\frac{D_x t}{R_f}}} \right) \right]. \quad (2.36)$$

where

$$\operatorname{erf}(x) = \frac{2}{\sqrt{\pi}} \int_0^x e^{-t^2} dt \quad (2.37)$$

$$\begin{aligned} \operatorname{erfc}(x) &= 1 - \operatorname{erf}(x) \\ &= \frac{2}{\sqrt{\pi}} \int_x^\infty e^{-t^2} dt \end{aligned} \quad (2.38)$$

Equation (2.36) is an appropriate one dimensional solution to the situation in this work where a constant concentration at the internal boundary of each control volume is available at each time step. Abstraction-based approximations based on this solution will be used to advance the concentration values at each time step within each control volume.

### Temperature Dependent Diffusion : Arrhenius

The Arrhenius relationship,

$$D = D_0 e^{-\frac{E_A}{RT}} \quad (2.39)$$

where

$$D = \text{the diffusion coefficient} \quad (2.40)$$

$$D_0 = \text{the maximum diffusion coefficient} \quad (2.41)$$

$$E_A = \text{molar activation energy of diffusion}[J/mol] \quad (2.42)$$

$$R = \text{the ideal gas constant}[J/molK], \quad (2.43)$$

$$T = \text{is the temperature}[^\circ K] \quad (2.44)$$

$$(2.45)$$

gives the diffusion coefficient of solids as a function of temperature and apparent activation energy of the medium.

### Temperature Dependent Diffusion : Stokes Einstein

The Stokes-Einstein relationship,

$$D(T) = \frac{k_B T}{6\pi\eta r} \quad (2.46)$$

gives an equation for the diffusion coefficient in a fluid, as a function of  $T$ , the temperature of the surrounding medium,  $k_B$ , the Boltzmann constant, and  $\eta$ , the viscosity of the medium. The Stokes-Einstein relationship relies on the linearization of the Navier-Stokes equation that preserves only the viscous components [24]. This is most valid for media where diffusion dominates and therefore inherently have a low Reynolds number,

$$Re = \frac{\rho v L}{\mu} \quad (2.47)$$

where

$$\rho = \text{fluid density}[kg/m^3] \quad (2.48)$$

$$v = \text{mean relative velocity of fluid}[m/s] \quad (2.49)$$

$$L = \text{characteristic length of system}[m] \quad (2.50)$$

$$\mu = \text{dynamic fluid viscosity}[kg/m \cdot s]. \quad (2.51)$$

### Continuum Models of Fractured Media

There exist various conceptual models for incorporating fractures into a porous medium model. Some examples are given in Figure 2.1.

The models arrived at via a continuum approximation are appropriate for very fractured or purely porous media. This approximation is not suitable for situations in which the fracture width or frequency varies greatly.

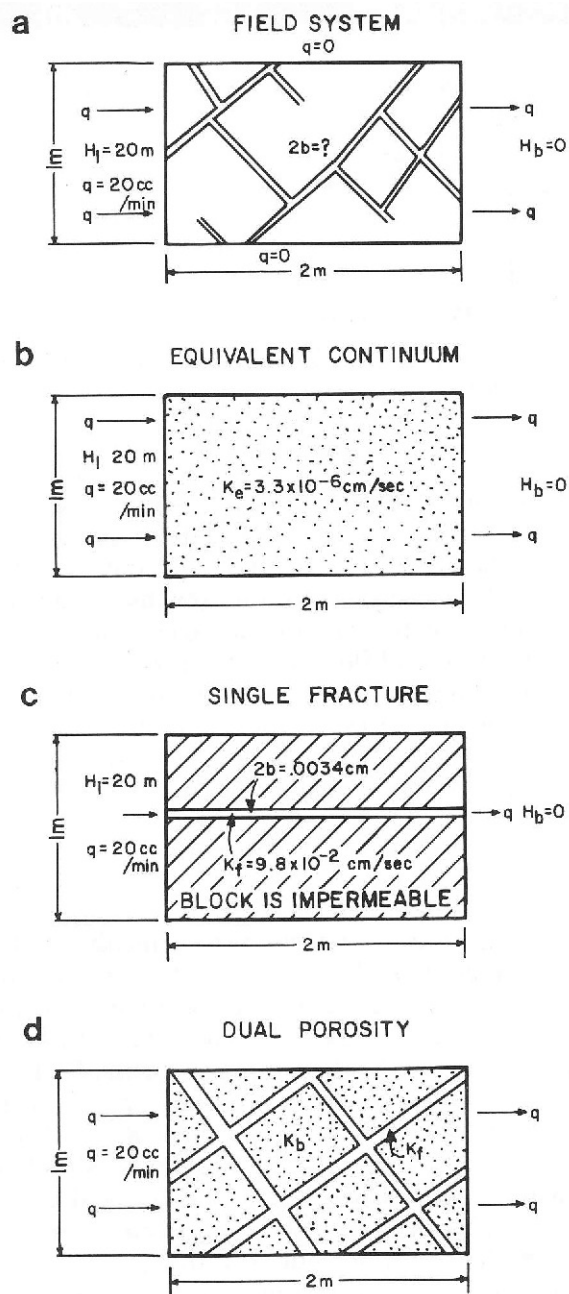


**Fig. 12.6** Conceptual models of a fractured rock system (modified from Gale, 1982).  
 (a) A simplified fracture network of aperture  $2b$  with groundwater flow from left to right.  
 (b) Equivalent porous medium model of (a).  
 (c) Discrete fracture model of (a).  
 (d) Dual porosity medium model of (a).

Equivalent Porous Medium (EPM) models assume that a uniformly fractured medium can be approximated as a fractureless matrix with an effective porosity high enough to account for real fracturing [11, 7].

Dual continuum models are the most widely employed models of fracture flow [19]. Dual Porosity Models make up one type of dual continuum model. This model incorporates advective transport in simplistic, uniform fractures and diffusive sorption and desorption into the stagnant (no advective transfer) water contained in the pores of the rock matrix [59, 27].

Dual Permeability Models are another type. These are similar to dual porosity models, but incorporate advective transfer within the rock matrix and between the rock matrix and the fracture volume [59, 27]. The incorporation of advective transfer in the dual permeability model is more appropriate for modeling granite since it incorporates advective solute transport through the rock matrix as well as diffusion.

### Discrete Fracture Network Models

Discrete fracture network models approximate that water and contaminants move only through the fracture network [7, 55]. Such an approximation is appropriate when flow through fractures is fast relative to porous flow. This modeling formulation is complex and requires detailed knowledge of the candidate geology.

The flow in each fracture can be approximated, as in Schwartz and Zhang, with the flow between two parallel plates having an aperture  $b$ , the mean fracture height [55]. For a fracture perpendicular to gravitational acceleration,  $g$ , the hydraulic conductivity,  $K$ , is described according to the cubic law as

$$K = \frac{\rho_w g b^2}{12\mu} \quad (2.52)$$

where

$$\begin{aligned} \rho_w &= \text{water density } [kg/m^3] \\ g &= \text{gravitational acceleration } [m/s^2] \\ b &= \text{plate aperture } [m] \\ \mu &= \text{dynamic fluid viscosity } [kg/m \cdot s]. \end{aligned}$$

Accordingly, the volumetric flow rate in the single fracture of width,  $w$ , can be described in terms of the hydraulic head gradient,  $\frac{\partial h}{\partial L}$ , as

$$Q = -Kbw \frac{\partial h}{\partial L}. \quad (2.53)$$

Calculation of the volumetric flow rate and corresponding solute transport in a discrete fracture network model for many non-parallel fractures is an intensive numerical computation. However, for uniformly fractured media, a fracture network can be approximated by a set of parallel plates fractures.

If flow is expected in the  $\theta_f$  direction, and the fractures of the set are spaced a distance,  $d$ , apart,

$$\begin{aligned} N &= \text{fracture frequency} \\ &= \frac{\cos(\theta_f)}{d}. \end{aligned} \quad (2.54)$$

The fracture network permeability is then defined as,

$$k_f = \frac{b^3}{12N}. \quad (2.55)$$

The permeability,  $k$ , in an equivalent permeability model is thereby obtained by the permeabilities of the fracture network,  $k_f$ , and the permeability of the host matrix,  $k_m$ . Following the derivation in Schwartz and Zhang, in terms of the cross-sectional contact areas of the matrix and fractures  $A_m$  and  $A_f$ , the equivalent permeability,  $k$ , can be expressed

$$k = \frac{k_m + \frac{A_f}{A_m} k_f}{1 + \frac{A_f}{A_m}}. \quad (2.56)$$

This permeability is then used as the effective permeability of the rock in expressions that utilize it to determine the Darcy velocity, such as Equation (2.11).

## 2.4 Analytical Models of Heat Transport

A comprehensive model of a repository must arrive at an appropriate notion of heat-based waste loading and repository capacity. This requires a model which addresses heat transport through the repository as a function of spatial repository layout, waste stream decay heat, and heat transfer properties of the engineered barrier system and host rock geology. This model must sufficiently solve for peak temperatures at heat limited locations, which are in most cases at the waste package interface with the buffer material and the buffer material interface with the geology. These heat limits were discussed in section 2.2.

Heat transfer in these concepts will be dominated by conductive heat transfer. In a saturated closed system, very few air gaps will exist. For this reason, heat transfer by



radiation is likely to be negligible. Similarly, since water velocities are comparatively low, heat transfer by mass transfer or by convection will be small relative to conduction.

A discussion of analytical models of heat transport follows that quantifies these modes of heat transfer and addresses their applicability to the model at hand.

## Conduction

Conductive heat transfer occurs as a result of a temperature gradient. Heat flows diffusively from the hotter material to the cooler material over time and steadily approaches thermal equilibrium. The general form of the conduction equation can be expressed

$$\nabla^2 T + \frac{q'''}{k} = \frac{1}{\alpha} \frac{\partial T}{\partial t}, \quad (2.57)$$

which with no heat source becomes the transient Fourier equation,

$$\nabla^2 T = \frac{1}{\alpha} \frac{\partial T}{\partial t}, \quad (2.58)$$

or to the Laplace equation in steady state,

$$\nabla^2 T = 0. \quad (2.59)$$

Replacing the source gives the steady state Poisson equation,

$$\nabla^2 T + \frac{q'''}{k} = 0. \quad (2.60)$$

An areal heat flux,  $q''[W/m^2]$  can be derived from an integration of Poisson's equation (2.60) and expressed in terms of the thermal conductivity of the material,  $k[W/m \cdot ^\circ K]$ , and the temperature gradient  $\nabla T[K/m]$  by the expression

$$q'' = -k \nabla T. \quad (2.61)$$

For the one dimensional case, equation 2.61 can be reduced using a finite difference approximation. For a body at  $x_1$  with temperature  $T_1$  and a body with temperature  $T_2$  at position  $x_2$ ,

$$q''_x = -k_x \frac{dT}{dx} \quad (2.62)$$

$$= -k_x \frac{(T_1 - T_2)}{x_1 - x_2}. \quad (2.63)$$

## Convection

Convective heat transfer occurs advectively in accordance with fluid movement. Convection can be expressed as

$$\dot{q} = -hA\Delta T. \quad (2.64)$$

## Radiation

Heat transfer by radiation is the result of the emission of electromagnetic waves. Planck black body radiation is analytically described, using  $\sigma$ , the Stefan-Boltzmann constant as

$$\dot{q} = \sigma A_1 F_{1 \rightarrow 2} (T_1^4 - T_2^4) \quad (2.65)$$

where

$$\sigma = 5.670373 \times 10^8 [W/m^2 K^4]$$

and

$$F_{1 \rightarrow 2} = \begin{cases} \epsilon_1 & \text{for a point source,} \\ \frac{1}{\frac{1}{\epsilon_1} + \frac{1}{\epsilon_2} - 1} & \text{for parallel plates,} \\ \frac{2\pi r_1 L}{\frac{1}{\epsilon_1} + \frac{1}{\epsilon_2} - 1} \frac{r_1}{r_2} & \text{for concentric cylinders} \end{cases} \quad (2.66)$$

where

$$\epsilon_i = \text{emissivity of surface } i \text{ } [-]$$

$$r_i = \text{radius of cylinder } i \text{ } [m]$$

$$L = \text{cylinder length } [m].$$

## Mass Transfer

Heat transfer by mass transfer is straightforward, resulting in the change in temperature in adjacent volumes as a result of matter movement. If the specific heat capacity of the transferred mass can be expressed as  $c_p$ , then the heat transfer is simply,

$$\dot{q} = \dot{m} c_p (T_j - T_i) \quad (2.67)$$

where

$$c_p = \text{specific heat capacity } [J/kg^\circ K].$$

## Lumped Parameter Model

The lumped heat capacitance model makes an analogy to electrical circuit by reducing a thermal system into discrete lumps for an approximate solution of transient heat transfer. Such an approximation is appropriate when it can be assumed that the temperature gradient within each lump is approximately uniform. The appropriateness of this approximation can be quantitatively expressed by comparison of the internal thermal resistance to the external thermal resistance. The Biot number,

$$Bi = \frac{hA}{k} \quad (2.68)$$

indicates the relative speeds with which heat conducts within an object and across the boundary of that object. If the Biot number is low ( $< 0.1$ ), and therefore conduction is faster within the object than at the boundary, the assumption of a uniform internal temperature is appropriate and the lumped parameter model may be expected to give a result within 5% error[29]. This assists in choosing the size of distinct lumps within a conceptual model.

The lumped capacitance model can address multiple media and multiple heat transfer modes. The rate of heat transfer  $\dot{q}$  [ $Wm^{-2}K^{-1}s^{-1}$ ] through a circuit is simply given as the quotient of the temperature difference and the sum of thermal resistances,  $R_i[W \cdot K^{-1}]$ , of the multiple lumps

$$\dot{q} = \frac{\Delta T}{\sum_{i=0}^N R_i}. \quad (2.69)$$

By representing the various modes of heat transport (i.e. conduction, convection, radiation, and mass transfer) with various expressions for resistance, the lumped capacitance model provides a solution to the transient problem described by the energy balance,

$$\begin{aligned} (\text{Energy added to body } j \text{ in } dt) &= (\text{Heat out of adjacent bodies into body } j) \\ c_j \rho_j V_j dT_j(t) &= \sum_{i=0}^{i=N} [q_{i,j}] dt, \end{aligned} \quad (2.70)$$

where  $c_j \rho_j V_j$  is the total lumped thermal capacitance of the body.

For example, in the case of a simple convective circuit between two bodies,  $i$  and  $j$ , the resistance of  $j$  can be described as

$$R_{conv} = 1/hA \quad (2.71)$$

such that

$$c_j \rho_j V_j dT_j(t) = \sum_{i=0}^{i=N} [hA_j(T_i - T_j(t))] dt. \quad (2.72)$$

$$(2.73)$$

A time constant appears under integration that describes the speed with which the body  $i$  changes temperature with respect to the maximum temperature change,

$$\int_{T_j=T_0}^{T_j(t)} \frac{dT_j(t)}{T_i - T_j} = \frac{hA_j}{c_j \rho_j V_j} \int_0^t dt \quad (2.74)$$

$$-\ln \frac{T_i - T_j(t)}{T_i - T_0} = \frac{hA_j}{c_j \rho_j V_j} t \quad (2.75)$$

$$\frac{T_i - T_j(t)}{T_i - T_0} = e^{-(hA_j/c_j \rho_j V_j)t} \quad (2.76)$$

such that

$$\frac{T_j(t) - T_i}{T_i - T_0} = 1 - e^{-t/\tau} \quad (2.77)$$

where

$$\tau = (c_j \rho_j V_j / hA_j). \quad (2.78)$$

The time constant,  $\tau$  is the time it takes for the body to change  $(1 - (1/e))\% \Delta T$  and is equal to the product of the thermal capacitance and thermal resistance of the body,  $CR$ , analogous to an electrical circuit.

[23] This is the case for all resistances,  $R_i$  representing modes of heat transfer. Thus, one can say, in general

$$\tau_j = c_j \rho_j V_j R_j. \quad (2.79)$$

## Impact of Repository Designs

The repository layout has a significant influence on its heat transfer properties. Waste package spacing in drifts, boreholes, or alcoves, tunnel spacing, and multiple gallery level designs all affect available heat loading. For example, in the YMR, a variety of parameters have been shown to affect the potential repository waste loading density.

The YMR statutory limit of once-through, thermal PWR waste is 70,000 tonnes SNF. That is to say, the statutory line load limit is approximately 1.04 tonnes/m for

67km of planned emplacement tunnels (with 81 meters between drifts). The Office of Civilian Radioactive Waste Management Science and Engineering Report gives this basic “statutory limit”, but suggests an inherent design flexibility that could allow for expansion. Multiple efforts have adjusted various repository layout parameters in order to develop expanded capacity models of the YMR. Some of these efforts are detailed in Table 2.8.

Author	Max. Capacity <i>tonnes</i>	Footprint <i>km<sup>2</sup></i>	Details
OCRWM	70,000 97,000 119,000	4.65 6 7	“statutory case” “full inventory case” “additional case”
Yim, M.S.	75,187 76,493 95,970 82,110	4.6 4.6 4.6 4.6	SRTA code STI method 63m drift spacing 75 yrs. cooling
Nicholson, M.	103,600	4.6	drift spacing
EPRI	63,000	6.5	Base Case CSNF
option 1	126,000	13	expanded footprint
option 2	189,000	6.5	multi-level design
option 3	189,000	6.5	grouped drifts
options 2+3	252,000	6.5	hybrid
options 1+(2or3)	378,000	13	hybrid
options 1+2+3	567,000	13	hybrid

Table 2.8: Various analyses based on heat load limited repository designs have resulted in footprint expansion calculations of the YMR.

This inherent flexibility can come from an increase in the areal extent of the repository footprint, the density of drifts, or vertical expansion. The “full inventory” Yucca Mountain design alternative gives a maximum repository capacity of 97,000 tonnes. In addition, the current design for the repository has flexibility for “additional repository capacity” which would give a 119,000 tonne capacity at 1.04 tonnes/m.[20]

In addition to variable drift spacing, other modifications to repository layout have had promising results in terms of heat-limited repository capacity. The Electric Power Research Institute (EPRI) in their Room at the Mountain study found that with redesign of the repository an increased capacity of at least 400% (295 tonnes once-through SNF) and up to 900% (663 tonnes) could be expected to be achieved. Proposed design changes include decreased spacing between drifts, a larger areal footprint, vertical expansion into second and third levels of repository space, and hybrid solutions involving combinations

of these ideas. In particular, EPRI suggests either an expansion of the footprint with redesign of the current line load design plan or a multi-level plan that repeats the footprint and line load design of the current plan[34].

Layout options such as age based fuel mixing also allows for decreases in drift spacing. In aged based fuel mixing, aged (long cool time) SNF is loaded in a mixture with young SNF. This age based fuel mixing has been shown to achieve a 48% increase in the repository capacity as constrained by heat load[42]. This factor uses a fiducial default footprint of  $4.6\text{km}^2$  used in the NRC TSPA. The reported 48% increase in capacity results in total repository capacity of 103,600 tonnes[61].

## Heat Limits in Engineered Components

Various waste form constraints exist that limit fuel loading. These are in general less restrictive than heat limits resulting from geological medium constraints, however in some cases they are more restrictive.

For example, the current constraining heat limit in borosilicate glass reported by the UFD campaign is  $500^\circ\text{C}$ , corresponding to the temperature at which the glass can be expected to begin devitrifying [25, 56]. For ceramic oxide fuel pellet waste forms, zirconium cladding has a heat limit of  $350^\circ\text{C}$  to prevent rupture [56].

## Specific Temperature Integral

Linear mass loading ( $\text{tonnes}/m$ ), linear thermal loading ( $W/m$ ) and areal power density ( $W/m^2$ ) are common metrics for describing the loading of the repository. While these metrics are informative for mass capacity and power capacity respectively, they fail to reflect differences in thermal behavior due to varying SNF compositions. A closer look at the isotopics of the situation has proven much more applicable to thermal performance studies of the repository, and the preferred method in the current literature relies on specific temperature integrals.

Specific temperature integrals model the thermal source as linear along the emplacement paths, similar to the line loading and areal power density metrics. However, a temperate integral takes account of heat transfer behavior in the rock, includes the effects of myriad SNF compositions, and gives the thermal integration over time for any specific location within the rock. Man-Sung Yim calls this the Specific Temperature Increase method[39] though other researchers have other names for this method. Tracy Radel calls her temperature metric at a point in the rock the Specific Temperature Change[51].

In a repository with linear drifts, the heat flux from the drifts can be expressed as the superposition of the linear heat flux contributions of all the radionuclides in the waste. The temperature change, more importantly can be expressed as a superposition of the temperature change contributions due to each radionuclide. Each radionuclide contributes in proportion to its decay heat generation and its weight fraction of the SNF. With information about isotopic composition of the SNF, the Specific Temperature

Increase can determine the maximum thermal capacity of the repository in terms of tonnes/m. The length based accounting in  $\frac{t}{m}$  is converted to  $\frac{t}{Repository}$  by multiplication with the total emplacement tunnel length of the repository. In the case of Yucca Mountain, this was 67 km.

## 2.5 Detailed Computational Models of Radionuclide Transport

Detailed computational models of radionuclide transport seek to quantify the spatial movement of radionuclides within a repository environment due to heat generating waste forms. Such models are detailed with respect to their fine spatial and temporal resolution or with respect to the incorporation and coupling of numerous physical phenomena. Current detailed computational models addressing various repository geologies and geometries will be reviewed here that utilize finite difference and finite element methods in many dimensions, sophisticated numerical solvers, and other high fidelity approaches.

### European RED-IMPACT

The RED-IMPACT assessment compared results from European fuel cycle codes for various specific waste package forms, radioactive and radiotoxic inventories, reprocessing discharges, waste package thermal power, corrosion of matrices, transport of radioisotopes and resulting doses. Granite, clay and salt were analyzed by various countries and codes as listed in table 2.9.

International Repository Concepts				
Geology	Nation	Waste Stream	Metric	Institution
Granite	Spain	HLW	Heat Load	Enresa
Granite	Czech Rep.	HLW	Heat Load	NRI
Clay	Belgium	HLW	Heat Load	SCK·CEN
Salt	Germany	HLW	Heat Load	GRS
Granite	Spain	HLW	Dose	Enresa
Clay	Belgium	HLW	Dose	SCK·CEN
Clay	France	HLW	Dose	CEA
Salt	Germany	HLW	Dose	GRS
Granite	Czech Rep.	ILW	LT Dose	NRI
Granite	Spain	ILW	LT Dose	Enresa
Clay	Belgium	ILW	LT Dose	SCK·CEN
Granite	Spain	HLW/ILW/Iodine	LT Dose	Enresa
Clay	Belgium	HLW/ILW/Iodine	LT Dose	SCK·CEN

Table 2.9: International repository concepts evaluated in the RED Impact Assessment.[36]

## UFD Generic Performance Assessment Model

The UFD campaign is currently conducting an effort to produce a Generic Performance Assessment Model for analysis of GDSMs for various geological environments. Teams from Argonne National Laboratory, Lawrence Berkeley National Laboratory, Los Alamos National Laboratory, and Sandia National Laboratory are developing models of generic clay, granite, and salt disposal environments respectively. Sandia is simultaneously constructing a deep borehole disposal system model in crystalline rock. Each generic disposal system model will perform detailed calculations of radionuclide transport within its respective geology [18]. A 2012 goal of the project includes an overarching generic model that incorporates the various geologically distinct submodels in order to provide a fully generic repository model. This overarching GPAM work will be used in this effort.

The radionuclide transport calculations for the geologically distinct models are performed within the GoldSim simulation platform. GoldSim is a commercial simulation environment [35]. Probabilistic elements of the GoldSim modelling framework enable the models to incorporate Features, Events, and Processes (FEPs) expected to take place probabilistically during the evolution of the repository [18].

Cells within GoldSim represent components of the waste disposal system and are linked by diffusive, advective, precipitated, direct, or otherwise filtered mass transfer links.

Thermal modeling for the GDSMs are conducted independently with associated codes capable of modeling thermal evolution for all geologic environments. For example, one thermal model is being created using the Systems Improved Numerical Differencing Analyzer \ Gaski (SINDA\G) heat transport solver and another is under development at Lawrence Livermore National Laboratory (LLNL) that utilizes a combination of MathCAD and Excel.

### Clay/Shale GDSM

The Clay GDSM is being pursued by the team at Argonne National Laboratory (ANL) and will be the primary model with which this work will conduct parametric regression analyses.

The Clay GDSM models a single waste form, waste package, EBS, Excavation Disturbed Zone (EDZ), and far field zone. This waste unit cell is modeled with boundary conditions such that it may be repeated throughout the extent of a repository configuration.

The waste form and engineered barrier system are modeled as well-mixed volumes and radial transport away from the cylindrical base case unit cell is modeled as one dimensional.

Two radionuclide release pathways are considered. One is the nominal, undisturbed case, while the other is a fast pathway simulating a disturbed case [18].



## Granite GDSM

Los Alamos National Laboratory (LANL) and Sandia National Laboratory (SNL) have created a model of the granite repository concept in a saturated, reducing environment.

Waste form degradation is modeled as a constant, fractional rate to represent dissolution for both canonical borosilicate glass and commercial used fuel waste forms.

Though waste package failure is conservatively assumed to be instantaneous, waste package release into the near field is solubility limited as is the near field to far field interface.

Transport through the buffer is modeled as entirely diffusive coupled with sorption. Advection is neglected.

The far field was represented using a model that includes advection, diffusion and sorption. Specifically, the Finite Element Heat and Mass Transfer (FEHM) code was coupled into GoldSim to represent the far field.

## Salt GDSM

The salt repository concept has an alcove gallery geometry and is located in a bedded salt formation. The formation is located in a reducing, saturated environment. Once waste packages are horizontally placed in a corner of the alcove, the space is backfilled with crushed salt.

Decay heat induced salt consolidation and brine flow are primary focuses of this analysis and inform radionuclide transport calculations.

A constant, temperature independent annual degradation rate model is used to represent waste form dissolution for both canonical borosilicate glass and commercial used fuel waste forms. Waste package failure is conservatively assumed to be instantaneous, and all near field components are modeled as a single mixed cell, the water volume of which is determined by the bulk volumes and degraded porosities of contained materials (e.g. bentonite buffer). A block of rock below the salt provides the pathway interface to an aquifer below. Radionuclide transport into that interface is modeled as diffusive, advective, and solubility limited.

The far field is modeled using an equilibrium sorption model in addition to solubility limited diffusion and advection. In such an equilibrium sorption model, the sorption to precipitation balance is assumed to be at a reaction equilibrium. In this way, the partitioning coefficient  $K_d$  is used to quantify the ratio between dissolved and undissolved reactant. Radionuclide transport in the far field takes place for 5km, and ends in a biosphere model.

Two radionuclide release pathways are considered. One is the nominal, undisturbed case, which the other is a fast pathway simulating a disturbed case [18].

## Deep Borehole GDSM

The deep borehole model concept consists of some 400 waste canisters in a 5km deep hole within a low permeability, high salinity region characteristic of crystalline rock formations at depth. The lower 2km of the hole are filled by waste packages as well as spacing and sealing plugs. A 1km sealing zone extends above the waste disposal region.

As with the salt model, a constant, temperature independent annual degradation rate model is used to represent waste form dissolution for both canonical borosilicate glass and commercial used fuel waste forms. Waste package failure is conservatively assumed to be instantaneous.

Flow in the vicinity of the borehole was modeled using tabulated groundwater flow velocities obtained from simulations run using the FEHM code meshed in three full dimensions with the CUBIT Geometry and Mesh Generation Toolkit (CUBIT) meshing tool [18].

## Li Model[37]

As a function of time, water enters the Engineered Barrier System and corrodes the waste packages. These fail and from the failed waste packages radionuclides are released according to advective transfer. Further transport through the near and far field rock medium is modeled in two modes, one representing the unsaturated zone, and one representing the saturated zone.

Waste package failure and radionuclide release are modeled with two TSPA code modules called EBSFAIL and EBSREL. The waste package failure rate is determined from EBSFAIL, which incorporates waste form chemistry, humidity, oxidation, etc and upon contact from water begins the degradation process. The results of EBSFAIL become the input to EBSREL, which models corresponding radionuclide release from those failed waste packages. Mass balance governing the radionuclide release rate in this model allows advective transfer to dominate and takes the form:

$$\dot{m}_i = w_{li}(t) - w_{ci}t - m_i\lambda_i + m_{i-1}\lambda_{i-1}.$$

In this expression,  $w_{li}(t)$  is the rate  $[mol/yr]$  of isotope  $i$  leached into the water. It is a function of water flow rate, chemistry, and isotope solubility.  $m_i$  describes the mass of isotope  $i$ , and  $\lambda_i [s^{-1}]$  describes its decay constant. Finally,  $w_{ci}(t)$  describes the advective transfer rate  $[mol/yr]$  of the isotope  $i$ . This model defines  $w_{ci}$  as:

$$w_{ci}(t) = C_i(t)q_{out}(t). \quad (2.80)$$

where  $q_{out}$  is the volumetric flow rate of the water  $[m^3/yr]$ , and  $C_i$  is the concentration on isotope  $i$  in the waste package volume  $m_i/V_{wp}$  in  $[mol/m^3]$ . These assumptions fail to take into account any differences in the varying solubilities of the isotopes, but are quite sensitive to the concentration of an isotope  $i$  in the waste package volume.

## ANDRA Dossier 2005

The ANDRA Dossier 2005 studies provided detailed radionuclide transport calculations for both argillaceous clay and granite formations.

### ANDRA Clay Model

In the ANDRA clay model, complicated saturation and resaturation phenomena are neglected and it is assumed that the initial repository condition is fully resaturated. This is a conservative simplification. Another conservative assumption is one in which the evacuation disturbed zone does not heal. Rather, it is modeled in its damaged state immediately after excavation.

This model only tracks 15 radionuclides of importance. These are chosen to be those with half lives over 1000 years and most toxicity or mobility [8]. The behavior of radionuclides in glass vitrification forms can be summarized by categorizing them into mobile, intermediate, and well retained elements.

Some specific codes and the method with which they were used in the ANDRA clay assessment are listed in Table 2.10.

**Detailed Nuclide Transport Models Used in the ANDRA analysis.**

Models	Codes
Hydrogeology and particle tracking in continuous porous media	Connectflow (3D finite element) Geoan (3D finite differences). Porflow (3D finite differences).
Hydrogeology and particle tracking in discrete fracture networks.	Connectflow (3D finite elements). FracMan (discrete fracture networks) and MAFIC (3D finite elements).
Transport in continuous porous media.	PROPER (finite differences), Goldsim (control volumes), and Porflow (control volumes?).
Transport in discrete fracture networks.	PROPER (1D stream tube concept). PathPipe (networks of tubes) and Goldsim (networks of 1D pipes).

Table 2.10: Similar to the Total System Performance Assessment, ANDRA's analyses are a coupled mass of many codes. Table reproduced from Argile Dossier 2005 [8]

Waste form dissolution and package release was assumed to be immediate for some waste forms and corrosion rate based for those where appropriate data were available. Vitrified waste package releases were either modeled with a simple model or a two phase phenomenological model.

Transport through the backfill is modeled as diffusive, with high permeability after degradation. The evacuation disturbed zone has both a fracture zone and a microfissure zone. In the host formation, movement is dominated by diffusion, and advection is modeled, but is negligible.

Tools used in the ALLIANCES software platform include Castem, PorFlow and Trace for hydraulic calculations and radionuclide transport and Prediver and Colonbo for waste package failure.

## 2.6 Detailed Computational Models of Heat Transport

Detailed heat transport models seek to quantify the heat evolution within a repository environment due to heat generating waste forms. Such models are detailed with respect to their detailed spatial and temporal resolution or with respect to the incorporation and coupling of numerous physical phenomena. Such codes typically utilize finite differencing or finite element methods in many dimensions or sophisticated numerical solvers, respectively.

### ANL SINDA\G Model

This model, created at Argonne National Lab uses the SINDA\G lumped capacitance solver. Originally created for optimal waste loading analysis of the YMR, the model is geometrically adjustable in two dimensions, as is demonstrated in Figure 2.2. The tunnel size is a fixed parameter in the model, but the optimal drift spacing for a particular waste stream and package loading is solved for with an optimization loop within this model.

The SINDA\G lumped capacitance solver solves a thermal circuit, for which conducting nodes may be of four types corresponding to the four modes of heat transfer. Nodes are connected by conduction, convection, radiation, and mass flow heat transfer links. As discussed in section 2.4, these are represented by

$$R_{cond} = \frac{L}{kA} \quad (2.81)$$

$$R_{conv} = \frac{1}{hA} \quad (2.82)$$

$$R_{mf} = \frac{1}{\dot{m}c_p} \quad (2.83)$$

$$R_{rad} = \frac{1}{\sigma F_{ij} A [T_i + T_A + T_j + T_A] [(T_i + T_A)^2 + (T_j + T_A)^2]} \quad (2.84)$$

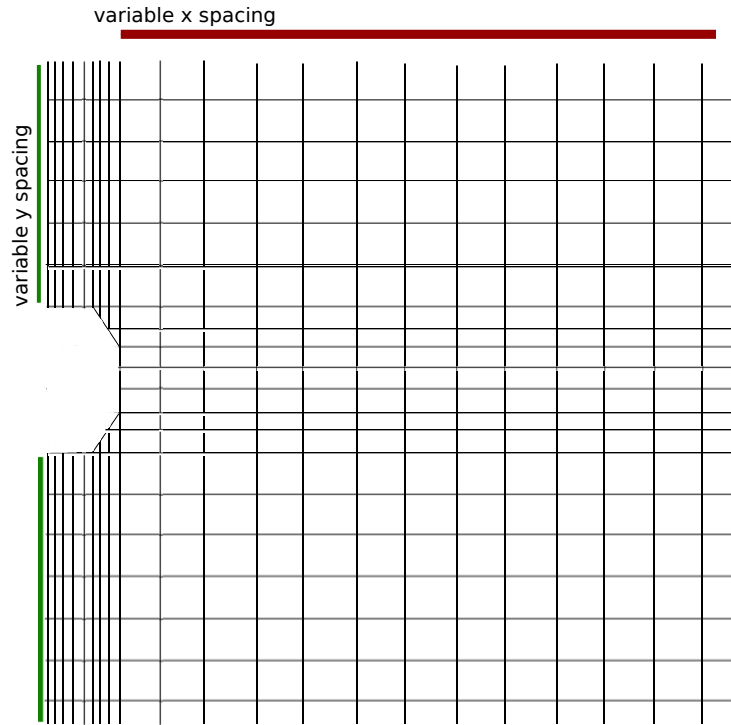


Figure 2.2: The geometry of the thermal model can be adjusted in two dimensions, altering the tunnel spacing and the vertical distance from the aquifer.

where

$$\begin{aligned}
 k &= \text{thermal conductivity}[W \cdot m^{-1} \cdot K^{-1}] \\
 A &= \text{area}[m^2] \\
 c_p &= \text{specific heat capacity}[J \cdot K^{-1}] \\
 h &= \text{heat transfer coefficient}[W \cdot m^{-1} \cdot K^{-1}] \\
 \dot{m} &= \text{mass transfer rate}[kg \cdot s^{-1}] \\
 T_i &= \text{lump temperature}[^{\circ}C] \\
 T_A &= \text{absolute temperature}[^{\circ}C] \\
 F_{ij} &= \text{radiation interchange factor}[-].
 \end{aligned}$$

With these representations of thermal resistance, a lumped parameter model will require an analysis that determines the appropriate length scale for the lumped parameter approximation.

Given one or more heat constraints, the ANL model optimizes spatial waste loading in order to meet those constraints with maximal waste loading. For example, given a

constraint at the edge of the waste package, the model utilizes the SINDA\G lumped capacitance solver to determine the two dimensional heat evolution of the repository as a result of a given waste package composition for various drift spacings and arrives at an ideal drift spacing by iteration.

## LLNL MathCAD Model

This model, created at LLNL for the UFD campaign, is written in a combination of MathCAD and Excel. The model consists of two physical parts, the first is the host rock, and the second models the waste form, package, and buffer as a single EBS unit. Since the thermal mass of the EBS is small in comparison to the thermal mass of the host rock, it may be treated as quasi-steady state. Thus, the transient state of the transient temperature between the host rock and the EBS can be found with a MathCAD solution of the transient homogeneous conduction equation,

$$\nabla^2 T = \frac{1}{\alpha} \frac{\partial T}{\partial t}. \quad (2.85)$$

Superimposed point and line source solutions allow for a notion of the repository layout to be modeled in the host rock. The solution of this equation at the boundary of the EBS and the waste package is then treated as a boundary condition for the heterogeneous steady state equation,

$$\dot{q} = U A_{out} (T_{in} - T_{out}) \quad (2.86)$$

where

$$U = \frac{1}{\sum_i R_i} \quad (2.87)$$

which, for the detailed EBS becomes

$$U = \frac{1}{R_{WF} + R_{WP} + R_{buffer} + \dots} \quad (2.88)$$

which calculates a resulting temperature gradient through the geometry at each point in time for each layer surface, assuming an infinite line source [25].

The process is then iterated with a one year resolution in order to arrive at a heat evolution over the lifetime of the repository. This model seeks to inform heat limited waste capacity calculations for each geology, for many waste package loading densities, and for many fuel cycle options.

## Other Numerical Methods

Codes used by repository modeling efforts investigated in this review include finite difference codes, finite element codes, and specific temperature integrals. Some efforts and their methods are listed in Table 2.11.

**Models of Heat Load for Various Geologies**

Source (Who)	Nation (Where)	Geology (What)	Methodology (How)
Enresa [36]	Spain	Granite	CODE_BRIGHT 3D Finite Element
NRI [36]	Czech Rep.	Granite	Specific Temperature Integral
ANDRA [9]	France	Granite	3D Finite Element CGM code
SKB [1]	Sweden	metagranite	1D-3D Site Descriptive Models
SCK-CEN [36]	Belgium	Clay	Specific Temperature Integral
ANDRA [8]	France	Argile Clay	3D Finite Element CGM code
NAGRA [31, 32]	Switzerland	Opalinus Clay	3D Finite Element CGM code
GRS [36]	Germany	Salt	HEATING (3D finite difference)
NCSU(Li) [38]	USA	Yucca Tuff	Specific Temperature Integral
NCSU(Nicholson) [42]	USA	Yucca Tuff	COSMOL 3D Finite Element
Radel & Wilson [51]	USA	Yucca Tuff	Specific Temperature Change

Table 2.11: Methods by which to calculate heat load are independent of geology. Maximum heat load constraints, however, vary among host formations.

### 3 MODELING PARADIGM

---

The modeling paradigm with which this repository model and simulation platform are implemented are described here. Implications of the simulation platform architecture on the design of the repository model are discussed and the interfaces defining components of the repository model follow.

#### 3.1 CYCLUS Simulator Paradigm

The CYCLUS project at the University of Wisconsin (UW) at Madison is the simulation framework in which this repository model is designed to operate. Modular features within this software architecture provide a great deal of flexibility, both in terms of modifying the underlying modeling algorithms and exchanging components of a fuel cycle system.

The CYCLUS fuel cycle simulator is the result of lessons learned from experience with previous nuclear fuel cycle simulation platforms. The modeling paradigm follows the transaction of discrete quanta of material among discrete facilities, arranged in a geographic and institutional framework, and trading in flexible markets. Key concepts in the design of CYCLUS include open access to the simulation engine, modularity with regard to functionality, and relevance to both scientific and policy analyses. The combination of modular encapsulation within the software architecture and dynamic module loading allows for robust but flexible reconfiguration of the basic building blocks of a simulation without alteration of the simulation framework.

The modeling paradigm adopted by CYCLUS includes a number of fundamental concepts that comprise the foundation on which other, more flexible, design choices have been made.

##### Dynamic Module Loading

The ability to dynamically load independently constructed modules is a heavy focus of CYCLUS development. Dynamically-loadable modules are the primary mechanism for extending CYCLUS' capability. The primary benefit of this approach is encapsulation: the trunk of the code is completely independent of the individual models. Thus, any customization or extension is implemented only in the loadable module. A secondary benefit of this encapsulation is the ability for contributors to choose different distribution and licensing strategies for their contributions. By allowing models to have varied availability, the security concerns of developers can be assuaged (See Figure 3.1).

Finally, this strategy allows individual developers to explore different levels of complexity within their modules, including wrapping other simulation tools as loadable modules within the CYCLUS framework. This last benefit of dynamically-loadable mod-



ules addresses another goal of CYCLUS : ubiquity amongst its potential user base. By engineering CYCLUS to easily handle varying levels of complexity, a single simulation engine can be used by both users keen on big-picture policy questions as well as users interested in more detailed, technical analyses.

## Encapsulation

CYCLUS implements an encapsulated structure that takes advantage of object-oriented software design techniques in order to create an extensible and modular user and developer interface. A primary workhorse for this implementation is the notion of dynamic module loading in combination with well defined module interfaces within a region, institution, and facility hierarchy. In this paradigm, the shared interface of polymorphic objects is abstracted from the logic of their instantiation by the model definition they inherit.

In this way, CYCLUS allows a level of abstraction to exist between the simulation and model instantiation as well as between model instantiation and behavior. An interface defines the set of shared functions of a set of subclasses in an abstract superclass. In CYCLUS main superclasses are Regions, Institutions, Facilities, and Markets while their subclasses are the concrete available model types (e.g. a `RecipeReactorFacility`). See Figure 3.2.

The interface for the `FacilityModel` class is the set of virtual functions declared in the `Facility` class such as `getName`, `getID`, `executeOrder()`, `sendMaterial()`, `receiveMaterial()` etc. Through such an interface, the members of a subclass can be treated as interchangeable (polymorphic) instantiations of their shared superclass.

## Modularity and Extensibility

A modular code must have the traits of encapsulation and abstraction appropriate for a user or developer to flexibly make alterations to the simulation performance with minimal modification to the code. An extensible code should be both robustly suited to the addition of classes and subclasses as well as suited to communication with other codes. In CYCLUS , addition of new models by dynamic loading is possible without any alteration of the software trunk. The modular design of CYCLUS stresses avoidance of rigidity, in which changes to the code are potentially difficult, and fragility, in which changes to the code are potentially damaging.

## Market-based Material Transactions

The foundation of a simulation is a commodity market that collects offers and requests and matches them according to some algorithm. The user is able to select which type of algorithm is used for each market by selecting a `MarketModel` and configure it with a particular set of parameters defined by that `MarketModel`. Changing the parameters of

a market changes its performance and selecting a different MarketModel completely changes its behavior.

The transaction of nuclear materials takes place in markets that act as brokers matching a set of requests for material with a set of offers for that material. A variety of market models will be available to perform this brokerage role. It is important to note that each market is defined for a single commodity and acts independently of other markets. Once the requests and offers have been matched by each market in a simulation, the facilities exchange material objects.

Facilities are deployed to issue offers and requests in these markets. Like markets, the user may select which type of algorithm is used for each facility by selecting a FacilityModel and configure it with a particular set of parameters defined by that FacilityModel. Changing the parameters of a facility changes its performance and selecting a different FacilityModel completely changes its behavior. Unlike markets, multiple independent instances of each facility configuration can be deployed to represent individual facilities.

## Discrete Materials and Facilities

The CYCLUS modeling infrastructure is designed such that every facility in a global nuclear fuel cycle is treated and acts individually. While modeling options exist to allow collective action, this will be as a special case of the individual facility basis. Each facility has two fundamental tasks: the transaction of goods or products with other facilities and the transformation of those goods or products from an input form to an output form. For example, a reactor will receive fresh fuel assemblies from a fuel fabrication facility, transform them to used fuel assemblies using some approximation of the reactor physics, and supply those used fuel assemblies to a storage facility.

A facility configuration is created by selecting a FacilityModel and defining the parameters for that facility configuration. Each FacilityModel will define its own set of parameters that govern its performance. The same FacilityModel may be used for multiple facility configurations in the same region, each with parameter values appropriate for that facility configuration.

The repository model that is the subject of this work is a facility model within the CYCLUS simulation paradigm.

## Materials

Material movement is the primary unit of information in CYCLUS . Materials passed, traded, and modified between and within facilities in the simulation are recorded at every timestep. This material history is stored in the output dataset of CYCLUS . In addition to holding the map of isotopes and their masses, a material object holds a comprehensive history of its own path as it moves through models within the simulation.

## Implications for Repository Model

The above sections outline the fuel cycle simulation platform currently under development at UW in which the repository model at hand is to be implemented. Implemented as a facility within this framework, the repository model interface is defined by the Facility Model interface defined within the CYCLUS paradigm.

That interface requires that a capacity be defined by the repository at every CYCLUS timestep so that the repository may make appropriate requests of disposable material.

Furthermore, the capability for dynamic module loading possible within the CYCLUS paradigm allows the repository system subcomponents to be interchangeably loaded at runtime, enabling comparison of various repository subcomponents, physical models of varying levels of detail.

The repository is both a subclass and a superclass. It is a subclass of the FacilityModel class, and a superclass of its own subcomponents. That is, dynamically loaded subcomponents of the repository inherit data, parameters and behaviors from the repository itself.

## 3.2 Repository Modeling Paradigm

The repository model architecture is intended to modularly permit exchange of disposal system subcomponents, accept arbitrary spent fuel streams, and enable extending modules representing new or different component models.

### Nested Component Concept

The fundamental unit of information in the repository model is the final nuclide release at the boundary of the far field resulting from nuclide release at each stage of containment. The repository model, in this way, is fundamentally a tool to determine the source term at the environmental surface as a result of an arbitrary waste stream. The repository model in this work conducts this calculation by treating each containment component as nested volumes in a release chain.

The capability to allow each component to define the components within it gives this repository the ability to model many types of repository concept while maintaining a simple interface with the simulation.

### Control Volumes

Each component of the repository system (i.e. waste form, waste package, buffer, and geologic medium) is modeled as a discrete control volume. Each control volume performs its own mass balance at each time step and assesses its own internal heat transfer and degradation phenomena separately from the other nested components.

Each control volume will initially be modeled as a mixed cell. That is, for permeable porous media, all contaminants released into the pore and fracture water are assumed to be uniformly distributed.

Thermal energy as well as mass will be conserved within each control volume by demanding continuity of thermal and mass fluxes across the boundaries. Since radionuclide and thermal transport calculations internal to the control volumes may be represented by many models at varying levels of detail, abstraction on the component level against detailed models will be conducted to achieve appropriate detail in each component.

### **Information Passing Between Volumes**

Each component passes some information radially outward to the nested component immediately containing it and some information radially inward to the nested component it contains. A diagram of the fundamental information being passed between components is described in Figure 4.1.

Most component models require external information concerning the water volume that has breached containment, so information concerning incoming water volumes is passed radially inward.

Each component model similarly requires information about the radionuclides released from the component it immediately contains. Thus, nuclide release information is passed radially outward from the waste stream sequentially through each containment layer to the geosphere.

### **Components of the Nested System**

The repository model is a collection of subcomponents which behave collectively to calculate repository metrics of interest. These subcomponents will be models of their own, and within the object oriented paradigm of the software will be a collection of module classes. Each component (i.e. waste form, waste package, buffer, lithology, etc.) will name a component superclass. Each superclass will be inherited by subclass models capable of representing that component in some level of detail specified by the model.

### **Waste Stream**

The waste stream data object contains spent fuel isotopics over the course of the simulation. As radionuclides are gained, lost, and transmuted within the spent fuel object, a history of its isotopic composition is recorded.

For waste streams that vary from each other in composition, the thermal capacity of the repository must be recalculated. One way to model this will be to recalculate the appropriate lengthwise spacing of waste packages when the heat generation rate of a new package is significantly different than other waste packages in the repository.

### **Waste Form**

The waste form model will calculate nuclide release due to dissolution of the waste form. Various heuristics by which nuclide release is modeled in accordance with waste form dissolution as well as the method by which the dissolution is modeled.

Dissolution can be instantaneous, rate based, water dependent, heat dependent, or coupled. Dissolution related release can be modeled as congruent, solubility limited, or both. Some radionuclides are immediately accessible, and some tend to remain in the fuel matrix.

### **Waste Package**

The waste package model calculates nuclide release due to waste package failure. Waste package failure is typically modeled as instantaneous and complete or partial and constant. That is, a delay before full release, or a constantly present hole in the package.

Waste package time to failure is dependent on water contact and heat, but can be modeled as an average, probabilistic, or a rate.

In the case of highly deforming geologic media, such as salt, mechanical failure can be the primary mechanism for release from the waste package.

### **Buffer**

Diffusion is the primary mechanism for nuclide transport through the buffer component of the repository system.

Salt, clay, and borehole repository concepts may not have a buffer material.

### **Backfill**

Similarly, diffusion is the primary mechanism for nuclide transport through the buffer component of the repository system.

Clay concepts and borehole concepts may not have a backfill material.

### **Geological Environment**

The literature review introduced various hydrological models that represent fluid and contaminant travel through permeable porous media and fractured porous media. These assume saturated flow and incorporate diffusive flow, advective flow, hydrodynamic dispersion, and equilibrium sorption. The geological environment control volume component will implement these models appropriately for each geologic environment to provide a mass balance and to communicate concentrations to adjacent components. Dirichlet boundary conditions at the surfaces of the control volume will allow the simulation to step through transport in the rock. Additional boundary condition types maybe implemented as extensions to the base case model.

## Simulation Interface

The interface of the repository model with the CYCLUS fuel cycle simulation interface is intended to be minimally restrictive, requiring only that the simulation supply waste stream information and provide a bookkeeping framework with which to record repository performance metrics. The repository model, in order to participate in the simulation as a facility model, must make requests for spent material up to its capacity. Determination of the repository capacity for various types of spent fuel commodities will comprise the interfacing functionality of the repository model. With the intention of developing the repository model in such a way as to be capable of interfacing with other simulation tools, however, calculation of metrics including expected dose rates and component failures will be the model's primary functionality.

### Waste Stream Input

The repository model must accept arbitrary spent fuel and high level waste streams. Material objects resulting from the simulated fuel cycle arrive at the repository and are emplaced if all repository capacity limits allow it.

Since disposable material in most simulations of interest will be of variable composition and therefore heterogeneous in heat production capability, the repository model will repeatedly need to recalculate its own capacity as new materials are offered.

### Repository Performance Metrics Calculated

Repository performance metrics that may be calculated from the source term and heat data calculated by the model will cover many metrics of interest to sustainability goals. Some metrics support analyses that seek to maximize safe repository capacity under heat and source term limitations. Those include spatial dimensions, spatial dimensions per kWh or equivalent, repository footprint, and number of waste packages generated.

Still other metrics that may be calculated include those being considered by the UFD campaign in a Fuel Cycle Data Package task underway [43]. Additional metrics that will be considered in this context will likely include environmental metrics such as peak dose to the public, radiotoxic fluxes released to the biosphere integrated over time, and the minimum managed lifetime. These metrics are recorded in a database flexibly defined by the repository model.

### Facility Functionality

The repository will behave as a facility within the CYCLUS simulation paradigm. The fundamental facility behavior within CYCLUS involves participating in commodity markets. The repository will participate as a requester of waste commodities. During reactor operation, the repository will make requests to markets dealing in spent fuel streams

according to its available capacity. Possible optional intermediate storage facility model is available for cooling periods.

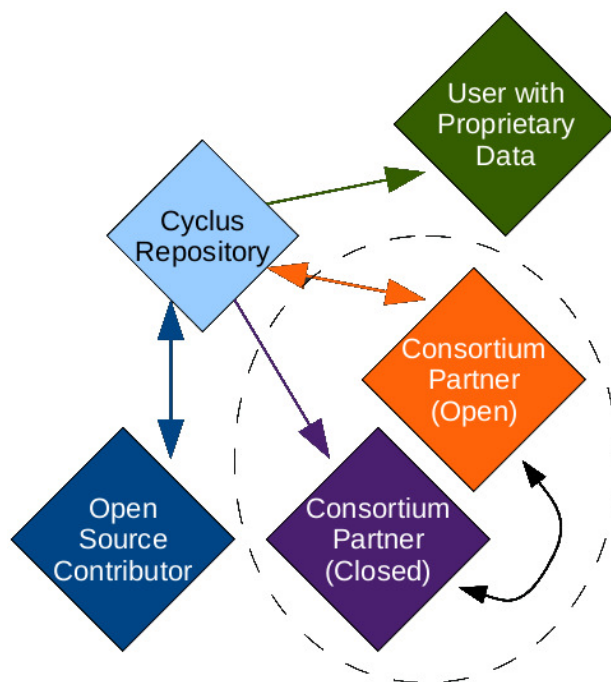


Figure 3.1: The CYCLUS code repository allows for varied accessibility.



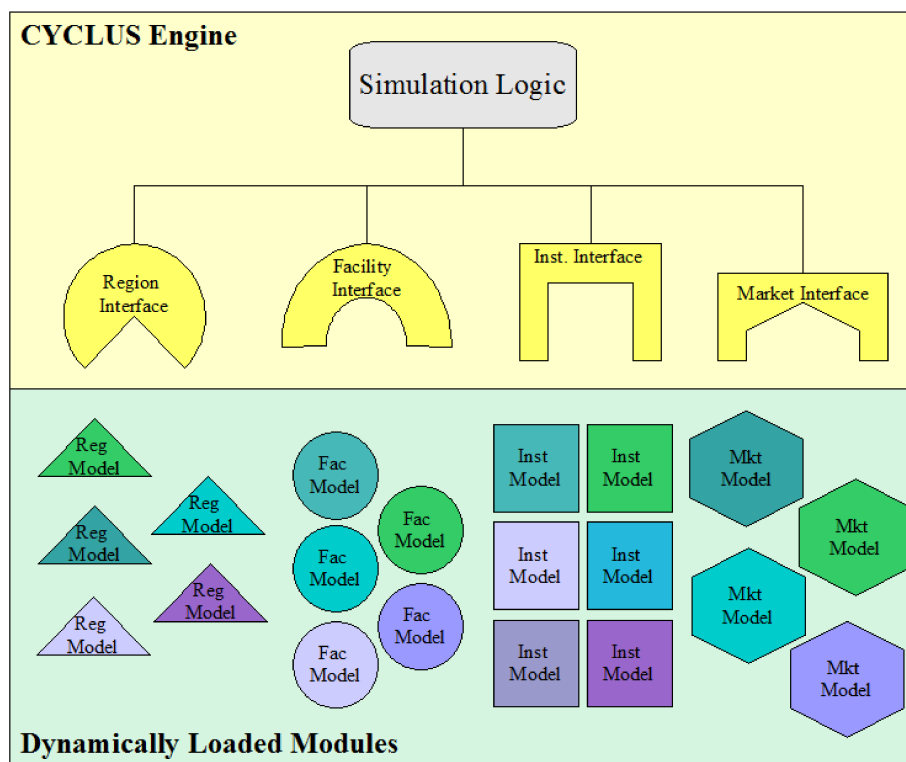


Figure 3.2: Modules are defined solely by their interfaces in a modular paradigm and can be arbitrarily interchanged with modules possessing equivalent interfaces.

### Quantities Calculated Each Timestep

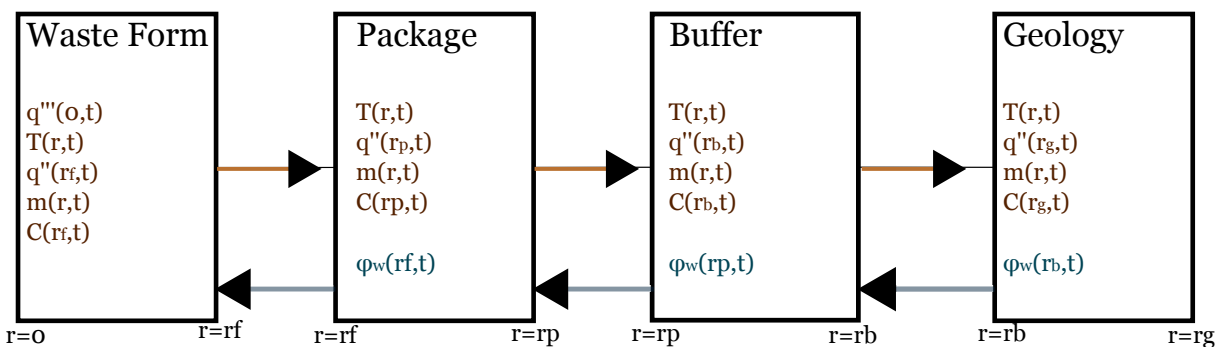


Figure 3.3: The nested components supply thermal flux and concentration information to each other at the boundaries.

## 4 METHODOLOGY

---

### 4.1 Radionuclide Transport In Cyder

Each engineered barrier component within the Generic Repository calculates nuclide transport using a model selected from the four presented in this chapter. In order to be interchangeable within the simulation, these components have identical nuclide transport interfaces.

Radionuclide transport models may rely on a number of boundary condition forms. Each nuclide model interface therefore provides sufficient boundary condition information to support the calculation methods of all other nuclide models. That is, each must provide a superset of the boundary condition forms required by all four models. These include Dirichlet, specified species concentration along the boundary, Neumann, concentration gradients along the boundary, and Cauchy, a combination of the two that provides a concentration flux along the boundary.

#### Interfaces

The interfaces between the models are essential to the understanding of the models themselves. The interfaces define boundary conditions in a number of forms based on information available internally to the component implementation.

In a saturated, reducing environment, contaminants are transported by dispersion and advection. It is customary to define the combination of molecular diffusion and mechanical mixing as the dispersion tensor,  $D$ , such that the mass conservation equation becomes [? ? ? ]:

$$\begin{aligned} J &= J_{dis} + J_{adv} \\ &= -\theta(D_{mdis} + \tau D_m)\nabla C + \theta v C \\ &= -\theta D \nabla C + \theta v C \end{aligned}$$

which, for uniform flow in  $\hat{k}$ , is

$$= \left( -\theta D_{xx} \frac{\partial C}{\partial x} \right) \hat{i} + \left( -\theta D_{yy} \frac{\partial C}{\partial y} \right) \hat{j} + \left( -\theta D_{zz} \frac{\partial C}{\partial z} + \theta v_z C \right) \hat{k}, \quad (4.1)$$

where

$$\begin{aligned}
 J_{dis} &= \text{Total Dispersive Mass Flux } [kg/m^2/s] \\
 J_{adv} &= \text{Advective Mass Flux } [kg/m^2/s] \\
 \tau &= \text{Toruosity } [-] \\
 \theta &= \text{Porosity } [\%] \\
 D_m &= \text{Molecular diffusion coefficient } [m^2/s] \\
 D_{mdis} &= \text{Coefficient of mechanical dispersivity } [m^2/s] \\
 D &= \text{Effective Dispersion Coefficient } [m^2/s] \\
 C &= \text{Concentration } [kg/m^3] \\
 v &= \text{Fluid Velocity in the medium } [m/s].
 \end{aligned}$$

Solutions to this equation can be categorized by their boundary conditions and those boundary conditions serve as the interfaces between components in the Cyder library of nuclide transport models.

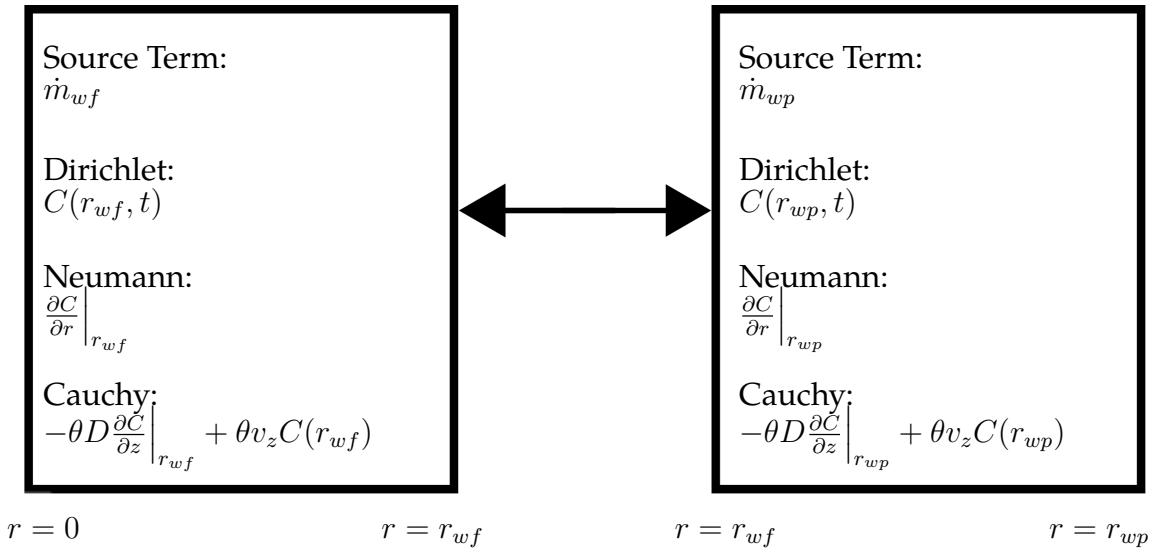


Figure 4.1: The boundaries between components (in this case, waste form (wf) and waste package (wp) components) are robust interfaces defined by Source Term, Dirichlet, Neumann, and Cauchy boundary conditions.

In addition to a specified source term (the zeroth type boundary condition, perhaps), the first, specified-head or Dirichlet type boundary conditions define a specified species concentration on some section of the boundary of the representative volume,

$$C(\vec{r}, t) = C_0(\vec{r}, t) \text{ for } \vec{r} \in \Gamma. \quad (4.2)$$

The second type, specified-flow or Neumann type boundary conditions describe a full set of concentration gradients at the boundary of the domain,

$$\frac{\partial C(\vec{r}, t)}{\partial r} = \theta D \vec{J}(t) \text{ for } \vec{r} \in \Gamma \quad (4.3)$$

where

$\vec{r}$  = position vector

$\Gamma$  = domain boundary

$\vec{J}(t)$  = solute mass flux [ $kg/m^2 \cdot s$ ].

The third, head-dependent mixed boundary condition or Cauchy type, defines a solute flux along a boundary,

$$-D \frac{\partial C}{\partial z} + v_z C = v_z C(\vec{r}, t) \text{ for } \vec{r} \in \Gamma. \quad (4.4)$$

The spatial concentration throughout the volume is sufficient to fully describe implementation of the following nuclide transport models within Cyder. This is supported by the implementation in which vertical advective velocity is uniform throughout the system and in which parameters such as the dispersion coefficient are known for each component. Since this is the case in Cyder, description of the Dirichlet condition is sufficient to fully define calculation of the Neumann and Cauchy type conditions.

## Degradation Rate Radionuclide Transport Model

The degradation rate model, simulating the fractional degradation of the material containment properties, is the simplest of implemented models and is most appropriate for simplistic waste package failure modeling.

The materials that constitute the engineered barriers in a saturated repository environment degrade over time. The implemented model of this nuclide release behavior is based solely on a fractional degradation rate. This model incorporates the source term made available on the inner boundary into its available mass and defines the resulting boundary conditions at the outer boundary as solely a function of the degradation rate of that component.

This results in the following expression for the mass transfer,  $m_{ij}(t)$ , from cell  $i$  to cell  $j$  at time  $t$ :

$$\dot{m}_{ij}(t) = f_i(\dots) m_i(t) \quad (4.5)$$

where

$$\begin{aligned}\dot{m}_{ij} &= \text{the rate of mass transfer from } i \text{ to } j \text{ [kg/s]} \\ f_i &= \text{fractional degradation rate in cell } i \text{ [1/s]} \\ m_i &= \text{mass in cell } i \text{ [kg]} \\ t &= \text{time [s]}.\end{aligned}$$

For a situation as in Cyder and Cyclus, with discrete timesteps, the timesteps are assumed to be small enough to assume a constant rate  $\dot{m}_{ij}$  over the course of the timestep. The mass transferred between discrete times  $t_{n-1}$  and  $t_n$  is thus a simple linear function of the transfer rate in (4.5),

$$\begin{aligned}m_{ij}^n &= \int_{t_{n-1}}^{t_n} \dot{m}_{ij}(t') dt' \\ &= f_i(\dots) m_i^{n-1} (t_n - t_{n-1}).\end{aligned}\tag{4.6}$$

The concentration boundary condition must also be defined at the outer boundary to support parent components that utilize the Dirichlet boundary condition. For the degradation model, which incorporates no diffusion or advection, the concentration,  $C_{ij}$  at the boundary between cells  $i$  and  $j$  is the average concentration in the saturated pore volume,

$$\begin{aligned}C_{ij}^n &= \frac{m_i^n}{V_{vi}} \\ &= \frac{\text{solute mass in cell } i}{\text{void volume in cell } i}.\end{aligned}\tag{4.7}$$

For the case in which all engineered barrier components are represented by degradation rate models, the source term at the outermost edge will be solely a function of the original central source and the degradation rates of the components.

To support parent components that utilize the Cauchy boundary condition, the degradation model assumes that the fluid velocity is constant across the cell as is the concentration. Thus,

$$\begin{aligned}-\theta_i D_{zz} \frac{\partial C}{\partial z} \hat{k} + \theta_i v_z C \hat{k} &= \theta_{i0} v_0 C_0 \hat{k} \\ \theta_i &= \text{porosity in cell } i \text{ [-]} \\ D_{zz} &= \hat{k} \text{ component diffusion tensor component in } \hat{k} \text{ direction [m}^2/\text{s]} \\ C_i &= \text{concentration in cell } i \text{ [kg/m}^3\text{]} \\ v_z &= \text{velocity in } \hat{k} \text{ direction [m/s]}\end{aligned}$$

reduces to

$$\theta_i^n v_z^n C_i^n = \theta_i^{n-1} v_z^{n-1} C_i^{n-1}. \quad (4.8)$$

## Mixed Cell Volume Radionuclide Transport Model

Slightly more complex and suited to representing waste form and buffer components, the mixed cell model incorporates solubility limited, congruent release under the influence of elemental solubility limits, sorption, diffusive behavior, and advective behavior. Abstraction results concerning the transition between primarily diffusive and primarily advective transport regimes were used for benchmarking and to iteratively improve accuracy in the development of this model.

A main nuclide transport component model used in this work is a mixed cell component module incorporating solubility and sorption effects as well as engineered material dissolution.

A graphical representation of the mixed cell model is given in Figures 4.2 and 4.3.

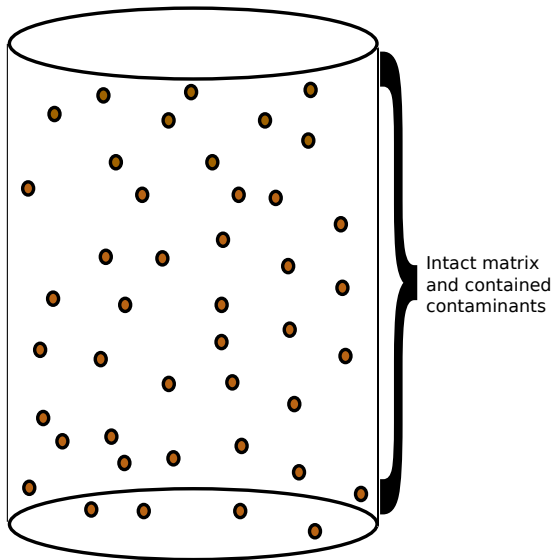


Figure 4.2: The control volume contains an intact material matrix. Contaminants are unavailable to neighboring subcomponents until dissolution has begun.

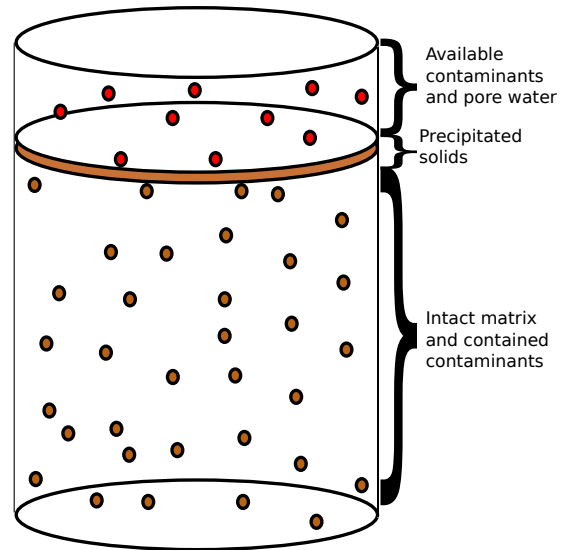


Figure 4.3: Once dissolution begins, the control volume contains a partially dissolved material matrix, contaminated pore water, and degraded and precipitated solids.

After some time degrading, the volume of free fluid can be expressed as

$$V_{ff}(t_n) = \theta V_T \int_{t_0}^{t_n} f(\cdots) dt. \quad (4.9)$$

The volume of the intact matrix can be expressed as

$$V_{im}(t_n) = V_T - V_T \int_{t_0}^{t_n} f(\dots) dt. \quad (4.10)$$

Finally, the volume of the degraded and precipitated solids can be expressed as

$$V_{ps}(t_n) = (1 - \theta) V_T \int_{t_0}^{t_n} f(\dots) dt. \quad (4.11)$$

This model assumes that all net influx to the cell enters the free fluid rather than the intact matrix. The total volumetric contaminant concentration in the intact matrix, can be expressed as

$$C_{im}(t_n) = C_0 \quad (4.12)$$

$$= \frac{m_0}{V_{im}(t_0)} \quad (4.13)$$

where

$$m_0 = \text{total initial mass.}$$

The resulting contaminant mass in the intact matrix at time  $t_n$  is

$$\begin{aligned} m_{im}(t_n) &= C_0 V_{im}(t_n) \\ &= C_0 V_T \left( 1 - \int_{t_0}^{t_n} f(\dots) dt \right). \end{aligned} \quad (4.14)$$

The contaminant mass in the free fluid is just the initial pore water concentration times the free fluid volume plus the time integral of net influx to the cell such that

$$C_{ffT}(t_n) = \left[ C_0 + \frac{\int_{t_0}^{t_n} \dot{m}_i(t') dt'}{V_{ff}(t_n)} \right] \quad (4.15)$$

and

$$\begin{aligned} m_{ffT}(t_n) &= C_{ff}(t_n) V_{ff}(t_n) \\ &= \left[ C_0 + \frac{\int_{t_0}^{t_n} \dot{m}_i(t') dt'}{V_{ff}(t_n)} \right] V_{ff}(t_n) \\ &= C_0 V_{ff}(t_n) + \int_{t_0}^{t_n} \dot{m}_i dt'. \end{aligned} \quad (4.16)$$

It is limited, however, by both solubility limitation and sorption.

## Sorption

The mass in both the free fluid and in the intact matrix exists in both sorbed and non-sorbed phases. The relationship between the sorbed mass concentration in the solid phase (e.g. the pore walls),

$$s = \frac{\text{mass of sorbed contaminant}}{\text{mass of total solid phase}} \quad (4.17)$$

and the dissolved liquid concentration,

$$c = \frac{\text{mass of dissolved contaminant}}{\text{volume of total liquid phase}} \quad (4.18)$$

can be expressed by a number of isotherm models.

In this model, sorption is taken into account throughout the volume. In the intact matrix, the contaminant mass is distributed between the pore walls and the pore fluid by sorption. So too, contaminant mass released from the intact matrix by degradation is distributed between dissolved mass in the free fluid and sorbed mass in the degraded and precipitated solids.

To solve for the boundary conditions in this model, the amount of non-sorbed contaminant mass in the free fluid must be found. This value,  $m_{ffl}$ , can be expressed in terms of the total degraded contaminant mass and the contaminant mass in the degraded and precipitated solid,

$$m_{ffl} = m_{ffT} - m_{psc}. \quad (4.19)$$

The mass of contaminant sorbed into the degraded and precipitated solids can be found using a linear isotherm model [? ], characterized by the relationship

$$s_i = K_{di}c_i \quad (4.20)$$

where

$$\begin{aligned} s_i &= \text{the solid concentration of isotope } i \text{ [kg/kg]} \\ K_{di} &= \text{the distribution coefficient of isotope } i \text{ [m}^3\text{/kg]} \\ c_i &= \text{the liquid concentration of isotope } i \text{ [kg/m}^3\text{]}. \end{aligned}$$

Thus, from (4.17),

$$\begin{aligned} s_{i,ps} &= \frac{\text{contaminant mass in degraded and precipitated solids}}{\text{total mass of degraded and precipitated solids}} \\ &= \frac{m_{psc}}{m_{psT}} \\ &= \frac{m_{psc}}{m_{psm} + m_{psc}} \end{aligned}$$



where

$$\begin{aligned}
 m_{psm} &= \text{noncontaminant mass in degraded and precipitated solids } [kg] \\
 &= \rho_b V_{ps} \\
 m_{psc} &= \text{contaminant mass in degraded and precipitated solids } [kg] \\
 \rho_b &= \text{bulk (dry) density of the medium } [kg/m^3].
 \end{aligned} \tag{4.21}$$

The following expression results, giving contaminant mass in the degraded and precipitated solids in terms of the sorption coefficient,

$$\begin{aligned}
 m_{psc} &= s_{ps} m_{psT} \\
 &= K_d C_{ffl} m_{psT} \\
 &= \frac{K_d m_{ffl} m_{psT}}{V_{ff}} \\
 &= \frac{K_d}{V_{ff}} (m_{ffT} - m_{psc}) m_{psT} \\
 &= \frac{K_d}{V_{ff}} (m_{ffT} - m_{psc}) (m_{psm} + m_{psc}) \\
 &= \frac{K_d}{V_{ff}} (m_{ffT} m_{psm} - m_{psc} m_{psm} + m_{ff} m_{psc} - m_{psc}^2) \\
 &= \frac{K_d}{V_{ff}} (m_{ffT} m_{psm} + (m_{ffT} - m_{psm}) m_{psc} - m_{psc}^2)
 \end{aligned}$$

which, rearranged, becomes

$$0 = m_{psc}^2 + \left( -m_{ffT} + m_{psm} + \frac{V_{ff}}{K_d} \right) m_{psc} - m_{ffT} m_{psm}$$

and is solved using the quadratic formula, such that

$$m_{psc} = \frac{m_{ffT} - m_{psm} - \frac{V_{ff}}{K_d}}{2} \pm \frac{\sqrt{\left( -m_{ffT} + m_{psm} + \frac{V_{ff}}{K_d} \right)^2 - 4m_{ffT} m_{psm}}}{2}$$

which, again rearranged, becomes

$$\begin{aligned}
 &= \frac{1}{2} \left( m_{ffT} - m_{psm} - \frac{V_{ff}}{K_d} \right) \\
 &\pm \frac{1}{2} \sqrt{m_{ffT}^2 + 2m_{ffT} \left( m_{psm} - \frac{V_{ff}}{K_d} \right) + \left( m_{psm} + \frac{V_{ff}}{K_d} \right)^2}.
 \end{aligned} \tag{4.22}$$

Plugging (4.22) into (4.19) results in the following expression for  $m_{ffl}$  in terms of known quantities

$$m_{ffl} = m_{ffT} - \frac{1}{2} \left( m_{ffT} - m_{psm} - \frac{V_{ff}}{K_d} \right) \mp \frac{1}{2} \sqrt{m_{ffT}^2 + 2m_{ffT} \left( m_{psm} - \frac{V_{ff}}{K_d} \right) + \left( m_{psm} + \frac{V_{ff}}{K_d} \right)^2}. \quad (4.23)$$

### Solubility

In addition to engineered barriers, contaminant transport is constrained by the solubility limit [26],

$$m_{s,i} \leq V_w C_{sol,i}, \quad (4.24)$$

where

$m_{s,i}$  = solubility limited mass of isotope i in volume  $V_w$  [kg]

$V_w$  = volume of the solution [ $m^3$ ]

$C_{sol,i}$  = solubility limit, the maximum concentration of i [ $kg/m^3$ ].

The desired boundary conditions can be expressed in terms of  $m_{ffl}$ . First, the Dirichlet boundary condition is

$$C(x, y, z, t) = \frac{m_{ffl}(t)}{V_{ff}(t)} \forall (x, y, z) \in \Gamma. \quad (4.25)$$

From this boundary condition in combination with global advective velocity data, all other boundary conditions can be found.

### Lumped Parameter Radionuclide Transport Model

The response function model implemented interchangeable piston flow, exponential, and dispersion response functions [? ]. For systems in which the flow is sufficiently slow to be assumed constant over a timestep, it is possible to model a system of volumes as a connected lumped parameter models (Figure 4.4).

The method by which each lumped parameter component is modeled is according to a relationship between the incoming concentration,  $C_{in}(t)$ , and the outgoing concentration,  $C_{out}(t)$ ,

$$C_{out}(t) = \int_{-\infty}^t C_{in}(t') g(t - t') e^{-\lambda(t-t')} dt' \quad (4.26)$$

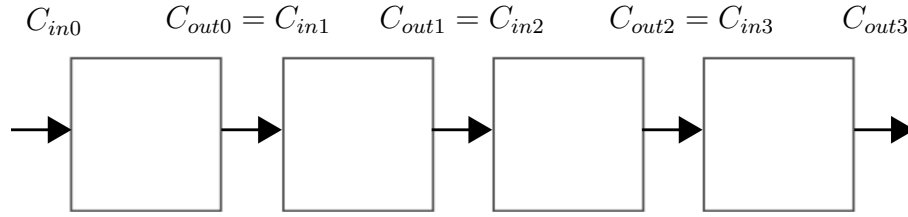


Figure 4.4: A system of volumes can be modeled as lumped parameter models in series.

equivalently

$$C_{out}(t) = \int_0^{\infty} C_{in}(t - t')g(t')e^{-\lambda t'} dt' \quad (4.27)$$

where

$t' =$  time of entry [s]

$t - t' =$  transit time [s]

$g(t - t') =$  response function, a.k.a. transit time distribution[–]

$\lambda =$  radioactive decay constant, 1 to neglect[s<sup>-1</sup>].

Selection of the response function is usually based on experimental tracer results in the medium at hand. However, some functions used commonly in chemical engineering applications [?] include the Piston Flow Model (PFM),

$$g(t') = \delta(t' - t_t) \quad (4.28)$$

the Exponential Model (EM)

$$g(t') = \frac{1}{t_t} e^{-\frac{t'}{t_t}} \quad (4.29)$$

and the Dispersion Model (DM),

$$g(t') = \left( \frac{Pe \, t_t}{4\pi t'} \right)^{\frac{1}{2}} \frac{1}{t'} e^{-\frac{Pe \, t_t \left(1 - \frac{t'}{t_t}\right)^2}{4t'}}, \quad (4.30)$$

where

$$\begin{aligned}
 Pe &= \text{Peclet number for mass diffusion } [-] \\
 t_t &= \text{mean tracer age } [s] \\
 &= t_w \text{ if there are no stagnant areas} \\
 t_w &= \text{mean residence time of water } [s] \\
 &= \frac{V_m}{Q} \\
 &= \frac{z}{v_z} \\
 &= \frac{z\theta_e}{q}
 \end{aligned}$$

in which

$$\begin{aligned}
 V_m &= \text{mobile water volume } [m^3] \\
 Q &= \text{volumetric flow rate } [m^3/s] \\
 z &= \text{average travel distance in flow direction } [m] \\
 v_z &= \text{mean water velocity } [m/s] \\
 q &= \text{Darcy Flux } [m/s] \\
 \theta_e &= \text{effective (connected) porosity } [\%].
 \end{aligned}$$

The latter of these, the Dispersion Model satisfies the one dimensional advection-dispersion equation, and is therefore the most physically relevant for this application. The solutions to these for constant concentration at the source boundary are given in [? ],

$$C(t) = \begin{cases} PFM & C_0 e^{-\lambda t_t} \\ EM & \frac{C_0}{1 + \lambda t_t} \\ DM & C_0 e^{\frac{Pe}{2}} \left( 1 - \sqrt{1 + \frac{4\lambda t_t}{Pe}} \right). \end{cases} \quad (4.31)$$

## One Dimensional Permeable Porous Medium Radionuclide Transport Model

Finally, abstraction results informed modifications to the implementation of an analytic solution to the one dimensional advection-dispersion equation with finite domain and Cauchy and Neumann boundary conditions at the inner and outer boundaries, respectively.

Various solutions to the advection dispersion equation (4.1) have been published for both the first and third types of boundary conditions. The third, Cauchy type, is mass conservative, and will be the primary kind of boundary condition used at the source for this model.

The conceptual model in Figure 4.5 represents solute transport in one dimension with unidirectional flow upward (a conservative assumption) and a semi-infinite boundary condition in the positive flow direction. The solution is given (Leij et. al, [? ]) and described below.

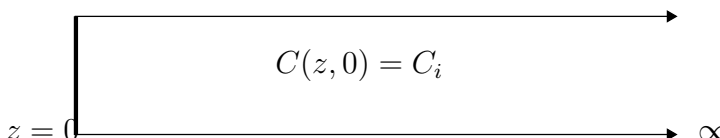
$$-D \frac{\partial C}{\partial z} \Big|_{z=0} + v_z C = \begin{cases} v_z C_0 & t < t_0 \\ 0 & t > t_0 \end{cases} \quad \frac{\partial C}{\partial z} \Big|_{\infty} = 0$$


Figure 4.5: A one dimensional, semi-infinite model, unidirectional flow, solution with Cauchy and Neumann boundary conditions

For the boundary conditions,

$$-D \frac{\partial C}{\partial z} \Big|_{z=0} + v_z c = \begin{cases} v_z C_0 & (0 < t < t_0) \\ 0 & (t > t_0) \end{cases}, \quad (4.32)$$

$$\frac{\partial C}{\partial z} \Big|_{z=\infty} = 0 \quad (4.33)$$

and the initial condition,

$$C(z, 0) = C_i, \quad (4.34)$$

the solution is given as

$$C(z, t) = \frac{C_0}{2} \left[ \operatorname{erfc} \left[ \frac{L - v_z t}{2\sqrt{D_L t}} \right] + \frac{1}{2} \left( \frac{v_z^2 t}{\pi D_L} \right)^{1/2} e^{-\frac{(L - v_z t)^2}{4D_L t}} - \frac{1}{2} \left( 1 + \frac{v_z L}{D_L} + \frac{v_z^2 t}{D_L} \right) e^{\frac{v_z L}{D_L}} \operatorname{erfc} \left[ \frac{L - V_z t}{2\sqrt{D_L t}} \right] \right]. \quad (4.35)$$

## 4.2 Thermal Transport Computational Models

Introduction to the thermal models.

## **Thermal Capacity Approximation Methodology**

### **Lumped Parameter Thermal Transport Computational Model**

## 5 DEMONSTRATION CASES AND BENCHMARKING

---





## **5.1 Nuclide Model Base Cases**

### **No Release**

**Degradation Rate Model**

**Mixed Cell Model**

**Lumped Parameter Model**

**One Dimensional Advective Dispersive Model**

### **Basic Transport**

**Degradation Rate Model**

**Mixed Cell Model**

**Lumped Parameter Model**

**One Dimensional Advective Dispersive Model**

### **Realistic Transport**

**Degradation Rate Model**

**Mixed Cell Model**

**Lumped Parameter Model**

**One Dimensional Advective Dispersive Model**

## **5.2 Nuclide Model Benchmarks**

**Case I : Diffusion Coefficient and Inventory Sensitivity**

**Case II : Vertical Advective Velocity and Diffusion Coefficient Sensitivity**

**Case III : Solubility Sensitivity**

**Case IV : Sorption Sensitivity**

**Case V : Waste Form Degradation Rate and Inventory Sensitivity**

**Case VI : Waste Package Failure Time and Diffusion Coefficient Sensitivity**

## **5.3 Thermal Transport Base Cases**

## **5.4 Thermal Benchmarking**

## 6 CONCLUSIONS AND FUTURE WORK

---

## A RADIONUCLIDE TRANSPORT SENSITIVITY ANALYSIS

---

The four GDSMs developed by the UFD campaign facilitate sensitivity analysis of the long-term post-closure performance of geologic repositories in generic media with respect to various key processes and parameters [18]. Processes and parameters expected to be influential to repository performance include the rate of waste form degradation, timing of waste package failure, and various coupled geochemical and hydrologic characteristics of the natural system including diffusion, solubility, and advection.

The results here provide an overview of the relative importance of processes that affect the repository performance of simplified generic disposal concepts. This work is not intended to give an assessment of the performance of a disposal system. Rather, it is intended to generically identify properties and parameters expected to influence repository performance in each geologic environment.

### A.1 Approach

This analysis utilized four GDSMs developed by the UFD campaign to represent clay, granite, salt, and deep borehole repository concepts. Each GDSM performs detailed calculations of radionuclide transport within its respective geology [18].

The radionuclide transport calculations for the geologically distinct models are performed within the GoldSim simulation platform. GoldSim is a commercial simulation environment [? ?]. Probabilistic elements of the GoldSim modelling framework enable the models to incorporate simple probabilistic FEPs that affect repository performance including waste package failure, waste form dissolution, and an optional vertical advective fast pathway [18].

The GoldSim framework and its contaminant transport module provide a simulation framework and radionuclide transport toolset that the GDSMs have utilized to simulate chemical and physical attenuation processes including radionuclide solubility, dispersion phenomena, and reversible sorption [? ?].

### A.2 Mean of the Peak Annual Dose

In this analysis, repository performance is quantified by radiation dose to a hypothetical receptor. Specifically, this sensitivity analysis focuses on parameters that affect the mean of the peak annual dose. The mean of the peak annual dose,

$$D_{MoP,i} = \frac{\sum_{r=1}^N \max [D_{r,i}(t)|_{\forall t}]}{N} \quad (\text{A.1})$$

where

$$\begin{aligned} D_{MoP,i} &= \text{mean of the peak annual dose due to isotope } i \text{ [mrem/yr]} \\ D_i(t) &= \text{annual dose in realization } r \text{ at time } t \text{ due to isotope } i \text{ [mrem/yr]} \\ N &= \text{Number of realizations,} \end{aligned}$$

is a conservative metric of repository performance. The mean of the peak annual dose should not be confused with the peak of the mean annual dose,

$$\begin{aligned} D_{PoM,i} &= \max \left[ \frac{\sum_{r=1}^N D_{r,i}(t)|_{\forall t}}{N} \right] \\ &= \text{peak of the mean annual dose due to isotope } i \text{ [mrem/yr]}. \end{aligned} \tag{A.2}$$

The mean of the peak annual dose rate given in equation (A.1) captures trends as well as the peak of the mean annual dose rate given in equation (A.2). However, the mean of the peaks metric,  $D_{MoP,i}$ , was chosen in this analysis because it is more conservative since it is able to capture temporally local dose maxima and consistently reports higher dose values than the peak of the means,  $D_{PoM,i}$ .

### A.3 Sampling Scheme

The multiple barrier system modeled in the clay GDSM calls for a multi-faceted sensitivity analysis. The importance of any single component or environmental parameter must be analyzed in the context of the full system of barrier components and environmental parameters. Thus, this analysis has undertaken an analysis strategy to develop a many dimensional overview of the key factors in modeled repository performance.

To address this, both individual and dual parametric studies were performed. Individual parameter studies varied a single parameter of interest in detail over a broad range of values. Dual parameter sensitivity studies were performed for pairs of parameters expected to exhibit some covariance. For each parameter or pair of parameters, forty simulation groups varied the parameter or parameters within the range considered. Example tables of the resulting forty simulation groups for individual and dual parametric study configurations appear in Tables A.1 and A.2 respectively.

For each simulation group, a 100 realization simulation was completed. Each realization held the parameters being analyzed as constant and sampled stochastic values for uncertain parameters not being studied. A sampling scheme developed in previous generic disposal media modeling was implemented in this model in order to ensure that the each 100 realization simulation sampled identical values for uncertain parameters [18? ].

In order to independently analyze the dose contributions from radioisotope groups, four cases,

Individual Parameter Study

<b>P</b>	$P_1$	Group 1
	$P_2$	Group 2
	$P_3$	Group 3
	$\cdot$	$\cdot$
	$\cdot$	$\cdot$
	$\cdot$	$\cdot$
	$P_{40}$	Group 40

Table A.1: For an individual one group of 100 realizations was run for each discrete value,  $P_i$ , within the range considered for  $P$ .

Dual Parameter Study

		<b>Q</b>				
		$Q_1$	$Q_2$	$Q_3$	$Q_4$	$Q_5$
<b>P</b>	$P_1$	Group 1	Group 2	Group 3	Group 4	Group 5
	$P_2$	Group 6	Group 7	Group 8	Group 9	Group 10
	$P_3$	Group 11	Group 12	Group 13	Group 14	Group 15
	$P_4$	Group 16	Group 17	Group 18	Group 19	Group 20
	$P_5$	Group 21	Group 22	Group 23	Group 24	Group 25
	$P_6$	Group 26	Group 27	Group 28	Group 29	Group 30
	$P_7$	Group 31	Group 32	Group 33	Group 34	Group 35
	$P_8$	Group 36	Group 37	Group 38	Group 39	Group 40

Table A.2: The simulation groups for a dual simulation sample each parameter within the range over which it was considered.

- Americium and its daughters,
- Plutonium and its daughters,
- Uranium and its daughters,
- Neptunium, its daughters, and fission products

were run independently. This allowed an evaluation of the importance of daughter production from distinct actinide chains.

## A.4 Clay

These analyses were performed using the Clay GDSM developed by the UFD campaign[18]. The Clay GDSM is built on the GoldSim software and tracks the movement of key radionuclides through the natural system and engineered barriers [? ? ].

The disposal concept modeled by the Clay GDSM includes an EBS which can undergo rate based dissolution and barrier failure. Releases from the EBS enter near field and subsequently far field host rock regions in which diffusive and advective transport take place, attenuated by solubility limits as well as sorption and dispersion phenomena.

The Clay GDSM models a single waste form, a waste package, additional EBSs, an EDZ, and a far field zone using a batch reactor mixing cell framework. This waste unit cell is modeled with boundary conditions such that it may be repeated assuming an infinite repository configuration. The waste form and engineered barrier system are modeled as well-mixed volumes and radial transport away from the cylindrical base case unit cell is modeled as one dimensional. Two radionuclide release pathways are considered. One is the nominal, undisturbed case, while the other is a fast pathway capable of simulating a hypothetical disturbed case [18].

## Vertical Advective Velocity

Transport out of the EBS and through the permeable, porous geosphere involves advection, diffusion, and hydraulic dispersion phenomena. Advection is transport driven by bulk water velocity, while diffusion is the result of Brownian motion across concentration gradients. The method by which the dominant solute transport mode (diffusive or advective) is determined for a particular porous medium is by use of the dimensionless Peclet number,

$$Pe = \frac{nvL}{\alpha nv + D_{eff}}, \quad (A.3)$$

$$= \frac{\text{advective rate}}{\text{diffusive rate}}$$

where

$$\begin{aligned} n &= \text{solute accessible porosity } [\%] \\ v &= \text{advective velocity } [m \cdot s^{-1}] \\ L &= \text{transport distance } [m] \\ \alpha &= \text{dispersivity } [m] \\ D_{eff} &= \text{effective diffusion coefficient } [m^2 \cdot s^{-1}]. \end{aligned}$$

For a high  $Pe$  number, advection is the dominant transport mode, while diffusive or dispersive transport dominates for a low  $Pe$  number [55].

In this analysis, the threshold between primarily diffusive and primarily advective transport was investigated by varying the vertical advective velocity in conjunction with the diffusion coefficient. It was expected that for the low diffusion coefficients and low advective velocities usually found in clay media, the model should behave entirely in the diffusive regime, but as the vertical advective velocity grows, system behavior should increasingly approach the advective regime.

## Parametric Range

The diffusion coefficient was altered as in section A.4 and the vertical advective velocity of the far field was altered as well.

From Table 5.5-1 of the Argile Safety Evaluation by ANDRA, the vertical hydraulic gradient is 0.4, while the hydraulic conductivity is  $5.0 \times 10^{14} [m/s]$ . The resulting vertical advective velocity is then  $2.0 \times 10^{-14} [m/s]$ , which is  $6.31 \times 10^{-7} [m/yr]$  [8].

As in section A.4, in order to isolate the effect of the far field behavior, the waste form degradation rate was set to be very high as were the solubility and advective flow rate through the EBS. This guaranteed that in the first few time steps, the far field was the primary barrier to release.

The forty runs are a combination of the five values of the vertical advective velocity and eight magnitudes of relative diffusivity (see Table A.3).

		Vertical Advective Velocity [m/yr]				
		6.31E-08	6.31E-07	6.31E-06	6.31E-05	6.31E-04
Reference Diffusivity (m <sup>2</sup> /s)		Groupings				
	1.E-08	1	2	3	4	5
	1.E-09	6	7	8	9	10
	1.E-10	11	12	13	14	15
	1.E-11	16	17	18	19	20
	1.E-12	21	22	23	24	25
	1.E-13	26	27	28	29	30
	1.E-14	31	32	33	34	35
	1.E-15	36	37	38	39	40

Table A.3: Vertical advective velocity and diffusion coefficient simulation groupings.

To capture the importance of the vertical advective velocity, a range was chosen to span a number of orders of magnitude between  $6.31 \times 10^{-8}$  and  $6.31 \times 10^{-4} [m/yr]$ . The relative diffusivity was simultaneously varied over the eight magnitudes between  $10^{-8}$  and  $10^{-15} [m^2/s]$ . It is worth noting that both the relative diffusivity and the vertical advective velocity are functions of porosity in the host rock and are therefore expected to vary together.

## Results

For isotopes of interest, higher advective velocity and higher diffusivity lead to higher means of the peak annual dose. However, the relationship between diffusivity and advective velocity adds depth to the notion of a boundary between diffusive and advective regimes.

The highly soluble and non-sorbing elements, *I* and *Cl* were expected to exhibit behavior that is highly sensitive to advection in the system in the advective regime but less sensitive to advection in the diffusive regime.

In Figures A.1, A.2, A.3, and A.4,  $^{129}\text{I}$  and  $^{36}\text{Cl}$  are more sensitive to vertical advective velocity for lower vertical advective velocities. This demonstrates that for vertical advective velocities  $6.31 \times 10^{-6} [\text{m}/\text{yr}]$  and above, lower reference diffusivities are ineffective at attenuating the mean of the peak doses for soluble, non-sorbing elements.

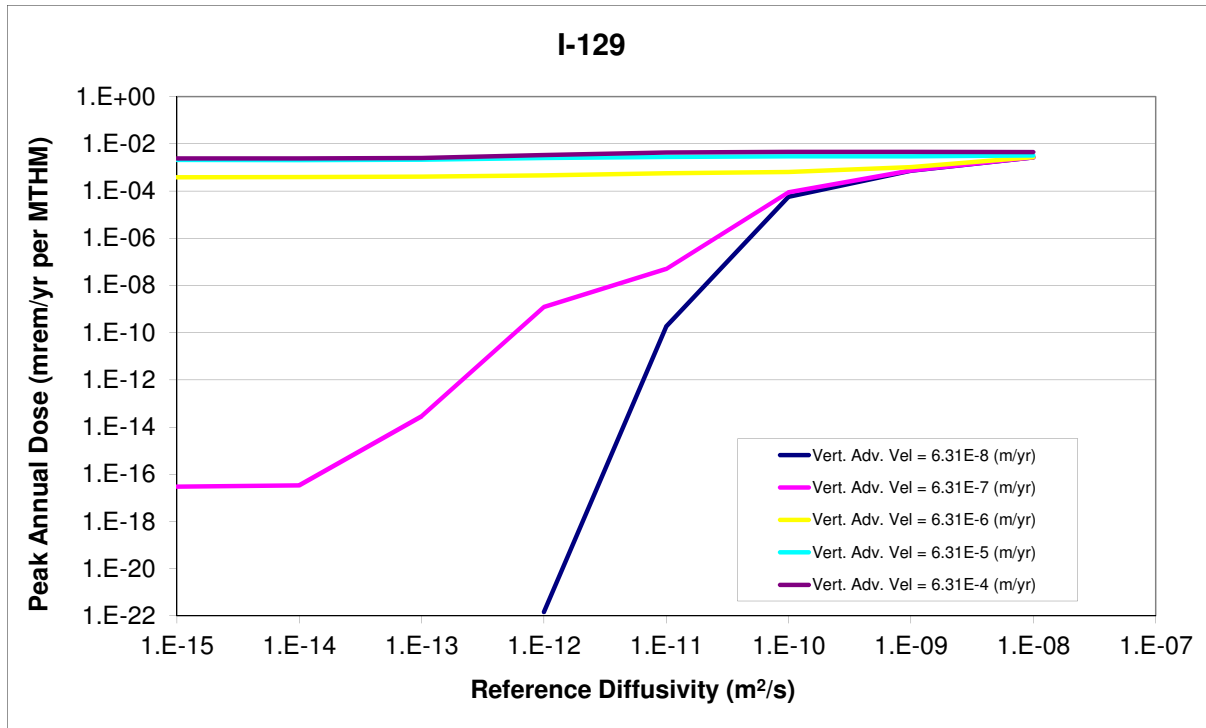


Figure A.1:  $^{129}\text{I}$  reference diffusivity sensitivity.

The solubility limited and sorbing elements,  $Tc$  and  $Np$ , in Figures A.5, A.6, A.7, and A.8 show a very weak influence on peak annual dose rate for low reference diffusivities, but show a direct proportionality between dose and reference diffusivity above a threshold. For  $^{99}\text{Tc}$ , for example, that threshold occurs at  $1 \times 10^{-11} [\text{m}^2/\text{s}]$ .

Dose contribution from  $^{99}\text{Tc}$  has a proportional relationship with vertical advective velocity above a regime threshold at  $6.31 \times 10^{-5} [\text{m}/\text{yr}]$ , above which the system exhibits sensitivity to advection.

The convergence of the effect of the reference diffusivity and vertical advective velocity for the cases above shows the effect of dissolved concentration (solubility) limits and sorption.  $Se$  is non sorbing, but solubility limited. The results from  $^{79}\text{Se}$  in Figure A.9 and A.10 show that for low vertical advective velocity, the system is diffusion dominated. However, for high vertical advective velocity, the diffusivity remains important even in the advective regime as spreading facilitates transport in the presence of solubility limited transport.



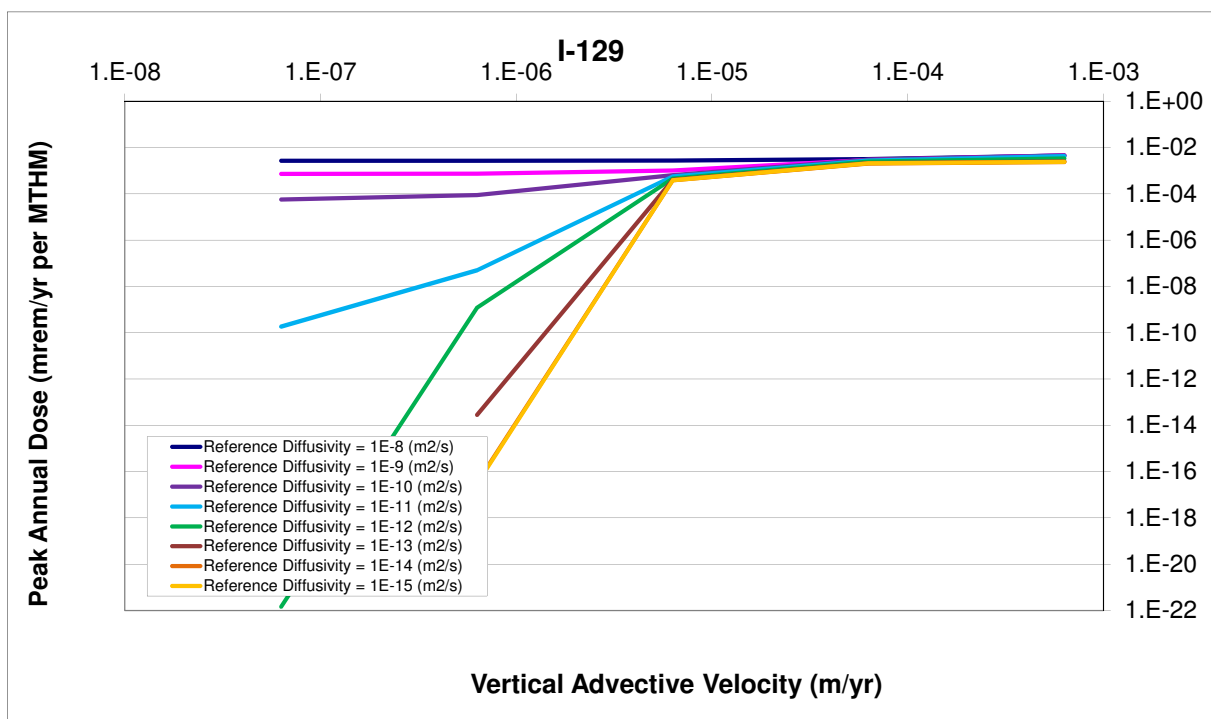


Figure A.2:  $^{129}\text{I}$  vertical advective velocity sensitivity.

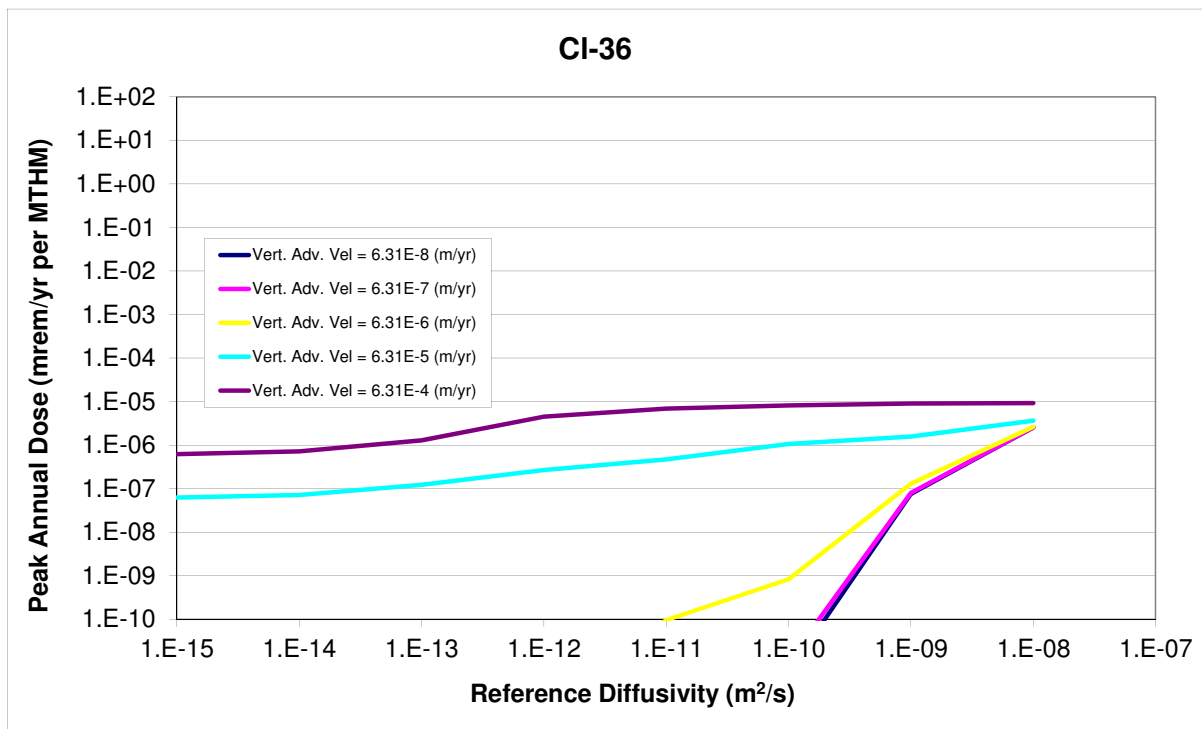


Figure A.3:  $^{36}\text{Cl}$  reference diffusivity sensitivity.

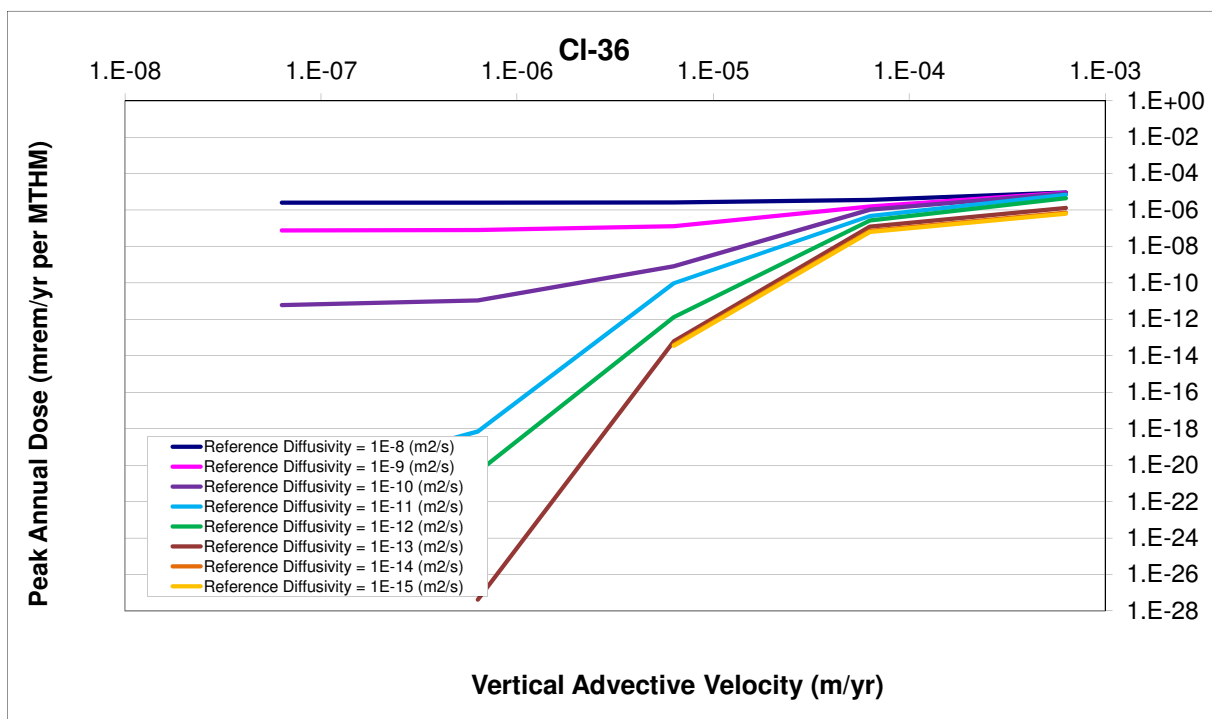


Figure A.4:  $^{36}\text{Cl}$  vertical advective velocity sensitivity.

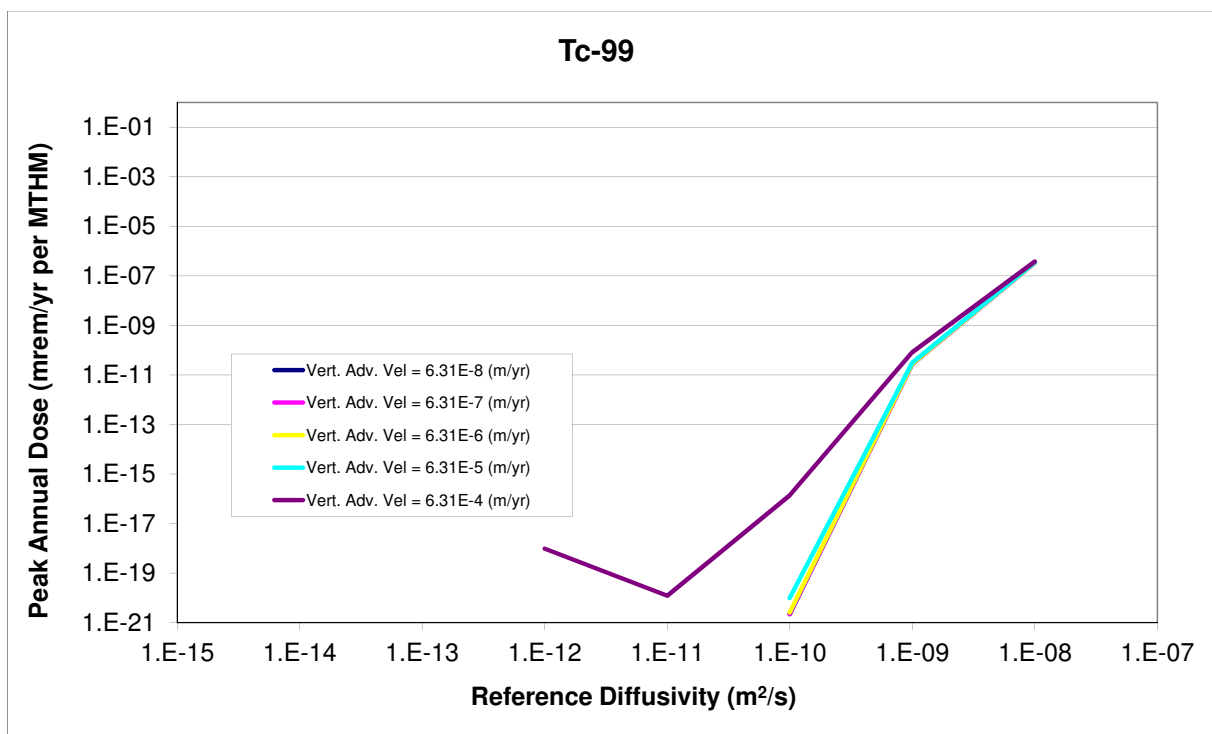
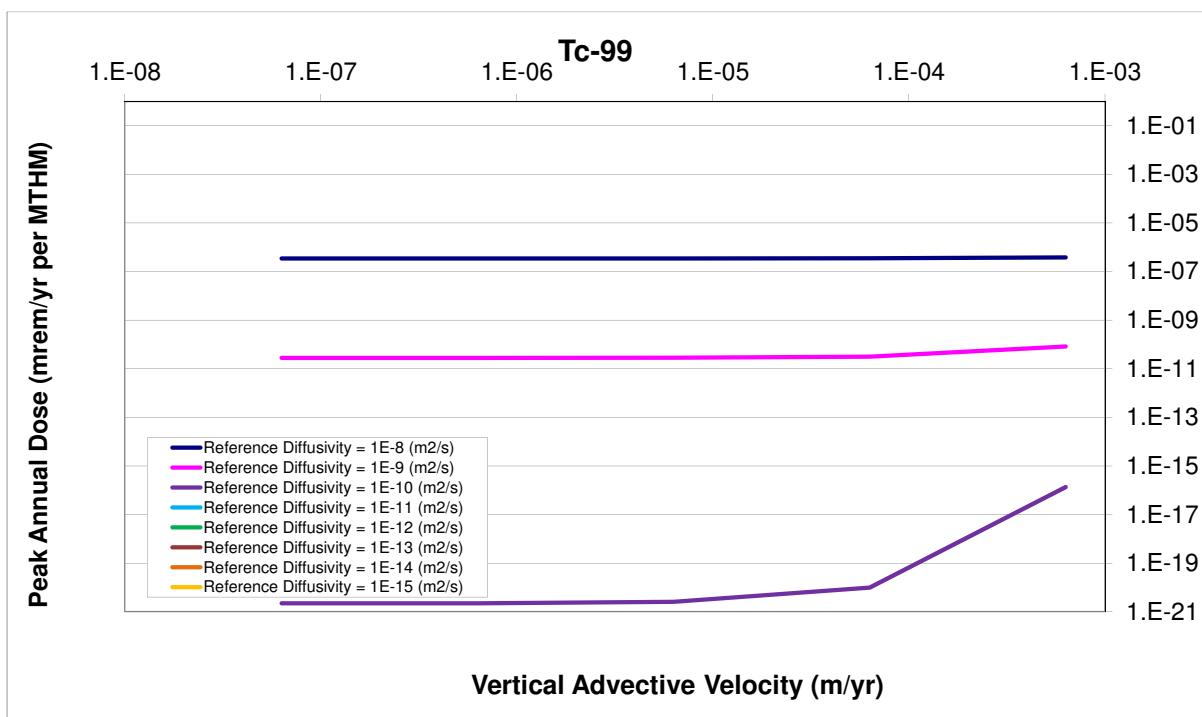
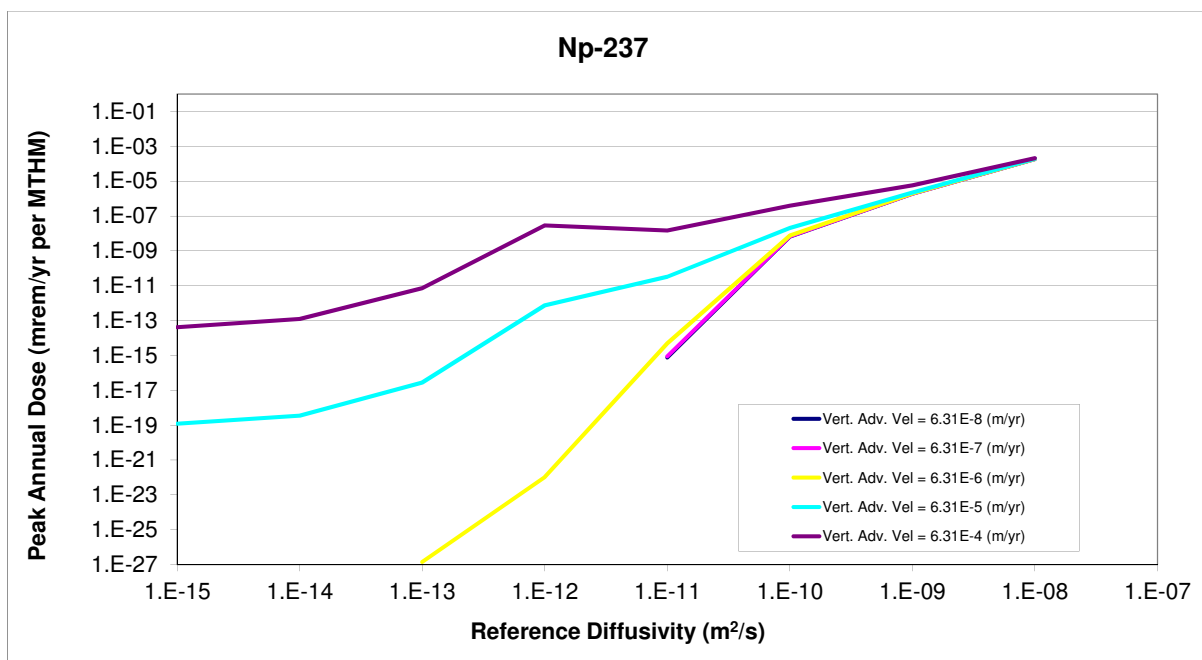


Figure A.5:  $^{99}\text{Tc}$  reference diffusivity sensitivity.

Figure A.6:  $^{99}\text{Tc}$  vertical advective velocity sensitivity.Figure A.7:  $^{237}\text{Np}$  reference diffusivity sensitivity.

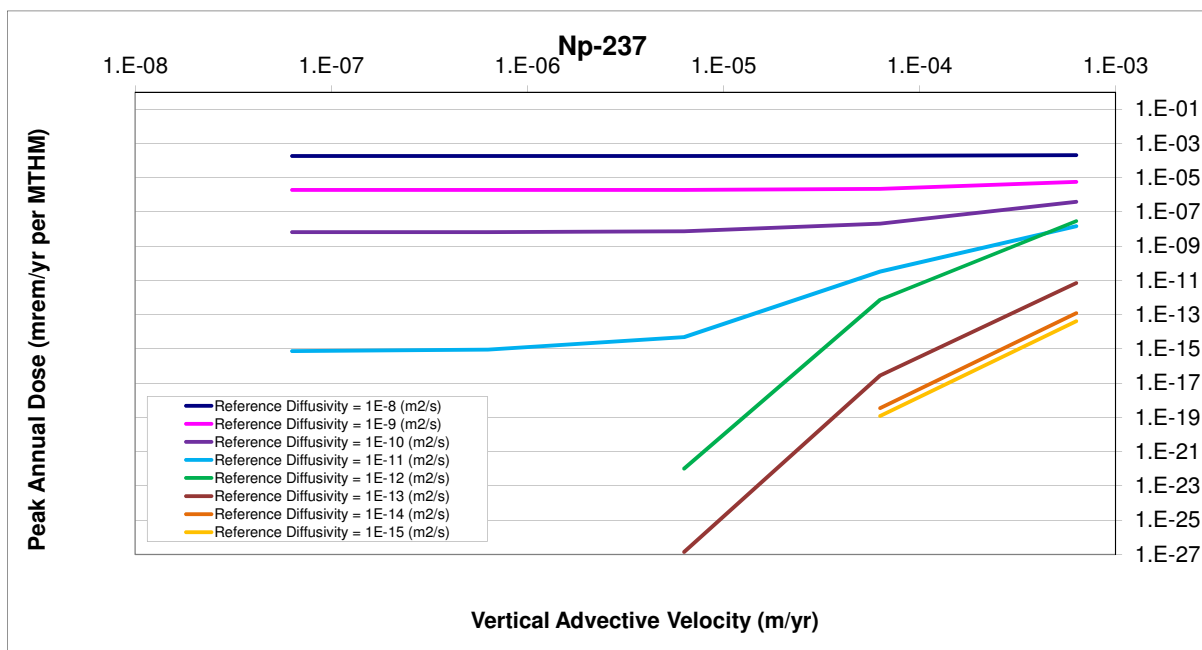


Figure A.8:  $^{237}\text{Np}$  vertical advective velocity sensitivity.

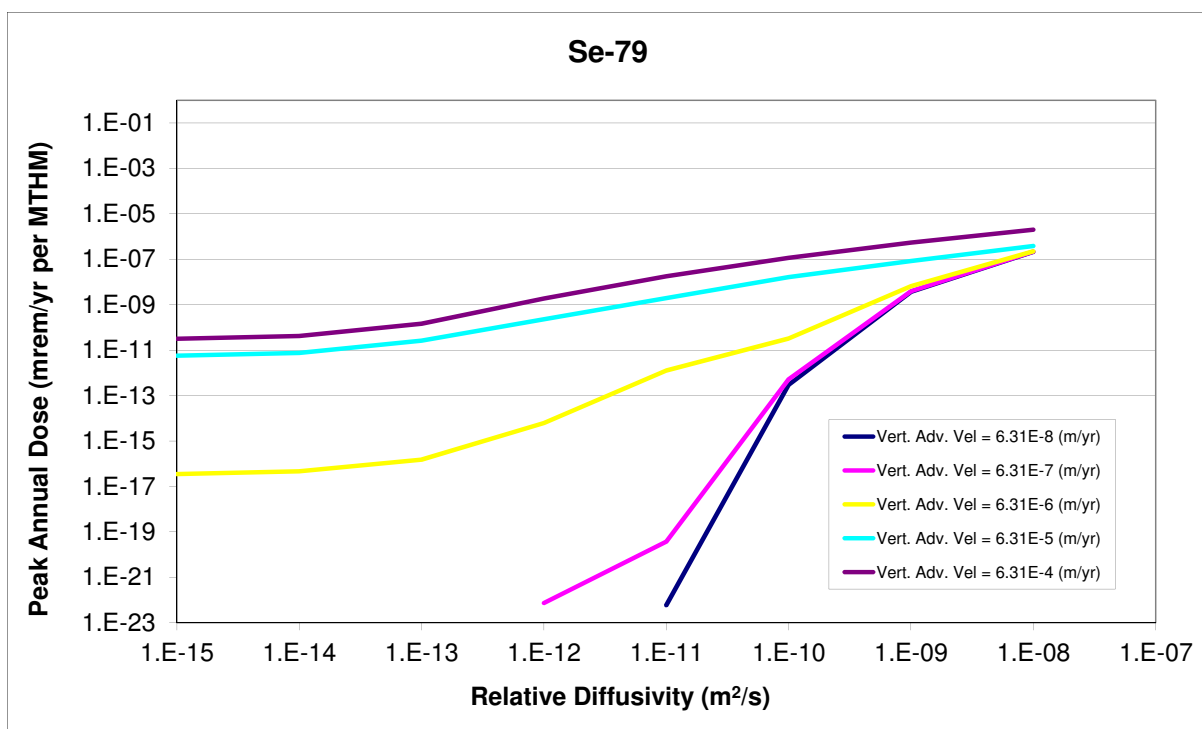


Figure A.9:  $^{79}\text{Se}$  reference diffusivity sensitivity.

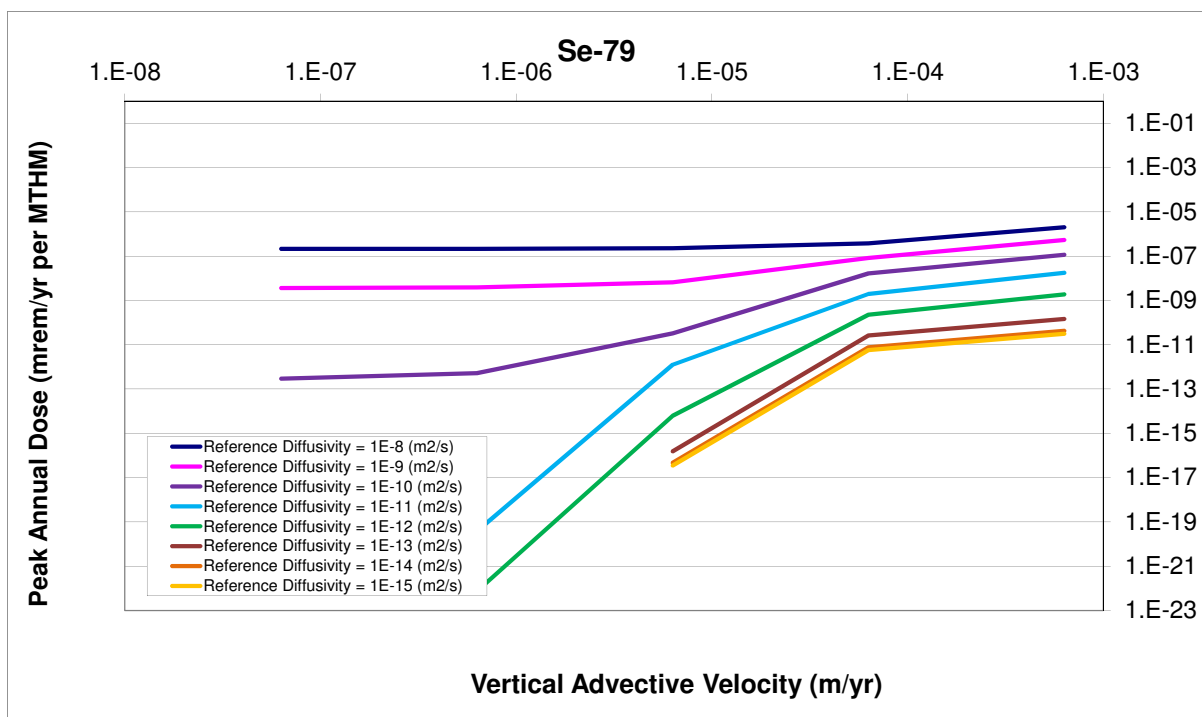


Figure A.10:  $^{79}\text{Se}$  vertical advective velocity sensitivity.

## Diffusion Coefficient of Far Field

In clay media, diffusion dominates far field hydrogeologic transport due to characteristically low hydraulic head gradients and permeability. Thus, the effective diffusion coefficient is a parameter to which repository performance in clay media is expected to be very sensitive.

The sensitivity of the peak dose to the reference diffusivity of the host rock was analyzed. In this model, the reference diffusivity of the medium was the input parameter used to vary the effective diffusivity in a controlled manner. In GoldSim's transport module, the effective diffusion coefficient is defined as

$$D_{eff} = n\tau D_{ref} D_{rel} \quad (A.4)$$

$D_{eff}$  = effective diffusion coefficient [ $m^2/s$ ],

$D_{rel}$  = relative diffusivity for each isotope in water [%],

$D_{ref}$  = reference diffusivity in water [ $m^2/s$ ],

$\tau$  = tortuosity[%],

$n$  = porosity[%].

(A.5)

The reference diffusivity was altered while the porosity and the tortuosity were both set to 1. Thus, the simulation rendered the effective diffusivity equal to the product of the reference diffusivity and the relative diffusivity (set to 1 for all isotopes). This allowed the diffusivity to be controlled directly for all isotopes.

The waste inventory total mass was also altered for each value of the reference diffusivity. That is, the radionuclide inventory in a reference Metric Ton of Heavy Metal (MTHM) of commercial spent nuclear fuel was multiplied by a scalar mass factor. It was expected that changing these two parameters in tandem would capture the importance of diffusivity in the far field to the repository performance as well as a threshold at which the effect of waste inventory dissolution is attenuated by solubility limits.

Finally, in order to isolate the effect of the far field behavior, the waste form degradation rate was set to be very high as were the solubility and advective flow rate through the EBS. This guaranteed that contaminant flowthrough in the near field was unhindered, leaving the far field as the dominant barrier to release.

## Parametric Range

The forty runs corresponded to eight values of relative diffusivity and five values of inventory mass multiplier. That is, the reference diffusivity was varied over the eight magnitudes between  $10^{-8}$  and  $10^{-15}$  [ $m^2/s$ ]. The Mass Factor, the unitless inventory multiplier, was simultaneously varied over the five magnitudes between  $10^{-4}$  and  $10^1$ [-].



That is, the radionuclide inventory was varied between  $10^{-4}$  and  $10^1$  of that in one MTHM of SNF, which is expected to cover the full range of inventories in current wasteforms.

		Mass Factor				
		0.001	0.01	0.1	1	10
		Groupings				
Reference Diffusivity (m <sup>2</sup> /s)	1.E-08	1	2	3	4	5
	1.E-09	6	7	8	9	10
	1.E-10	11	12	13	14	15
	1.E-11	16	17	18	19	20
	1.E-12	21	22	23	24	25
	1.E-13	26	27	28	29	30
	1.E-14	31	32	33	34	35
	1.E-15	36	37	38	39	40

Table A.4: Diffusion coefficient and mass factor simulation groupings.

## Results

The peak doses due to highly soluble, non-sorbing elements such as *I* and *Cl*, are proportional to the radionuclide inventory and largely directly proportional to the relative diffusivity. This can be seen for the cases of  $^{129}\text{I}$  and  $^{36}\text{Cl}$  in Figures A.11, A.12, A.13 and A.14.

Long lived  $^{129}\text{I}$  and  $^{36}\text{Cl}$  are assumed to have near complete solubility, so in Figures A.11 and A.13, the effect of a solubility limited attenuation regime is not seen. Even for very low diffusivities, the diffusion length of the far field is the primary barrier. In Figures A.12 and A.14 it is clear that in the absence of solubility limitation and sorption, the peak dose is directly proportional to mass factor.

Both *Cl* and *I* are soluble and non-sorbing. The amount of  $^{129}\text{I}$  in the SNF inventory is greater than the amount of  $^{36}\text{Cl}$ , so a difference in magnitudes are expected, however, the trends should be the same. Since the halflife of  $^{36}\text{Cl}$ ,  $3 \times 10^5[\text{yr}]$ , is much shorter than the half life of  $^{129}\text{I}$ ,  $1.6 \times 10^7[\text{yr}]$ , a stronger proportional dependence on mass factor is seen for *Cl* due to its higher decay rate.

With the exception of those dose-contributors assumed to be completely soluble, two regimes were visible in the results of this analysis. In low diffusion coefficient regime, the diffusive pathway through the homogeneous permeable porous medium in the far field continues to be a dominant barrier to nuclide release for normal (non-intrusive) repository conditions.

In the second regime, for very high diffusion coefficients, the effects of additional attenuation phenomena in the natural system can be seen. The dependence of peak annual dose on mass factor was consistently directly proportional for all isotopic groups.

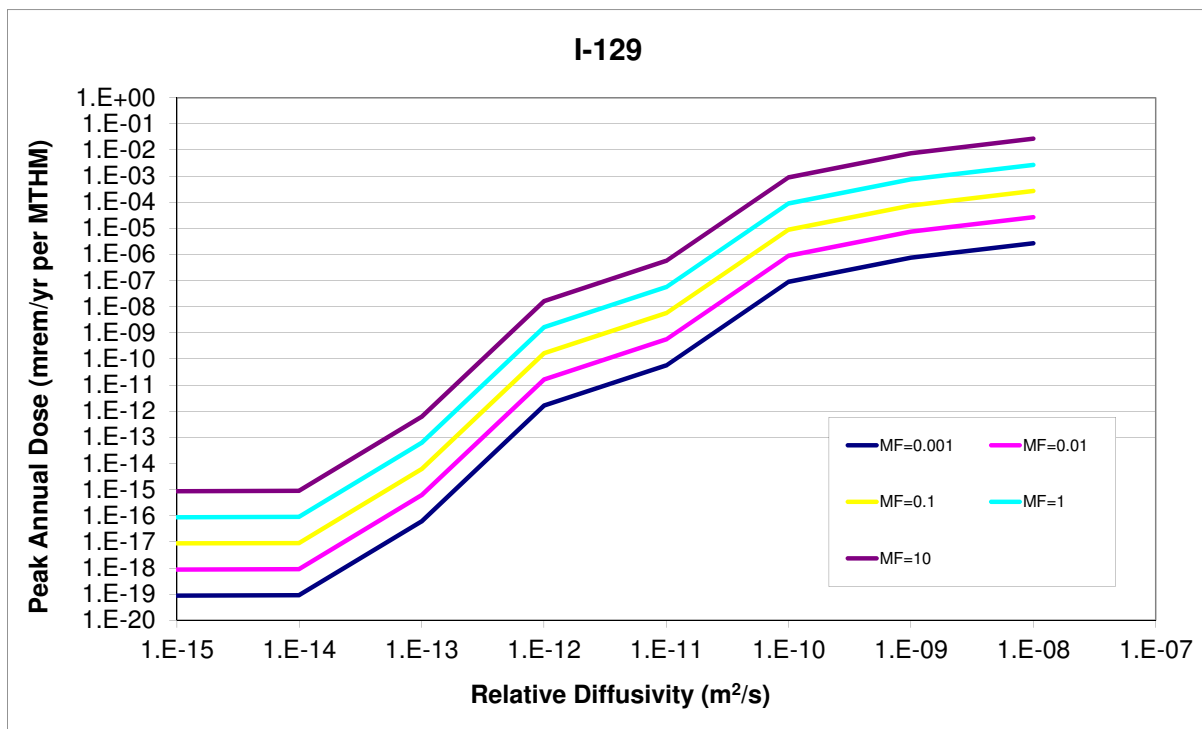


Figure A.11:  $^{129}\text{I}$  relative diffusivity sensitivity.

The peak doses due to solubility limited, sorbing elements such as  $Np$  and  $Tc$  demonstrate two major regimes. In the first regime, for low values of mass factor, the mean of the peak annual dose rates is directly proportional to both reference diffusivity and mass factor. For higher values of mass factor, the sensitivity to reference diffusivity and mass factor are both attenuated at higher values. The attenuation in these regimes is due to natural system attenuation, most notably, sorption.

$^{237}\text{Np}$  and  $^{99}\text{Tc}$  exhibit a strong proportional relationship between diffusivity and dose in Figures A.15 and A.17. This relationship is muted as diffusivity increases. Both are directly proportional to mass factor until they reach the point of attenuation by their solubility limits, as can be seen in Figures A.16 and A.18.

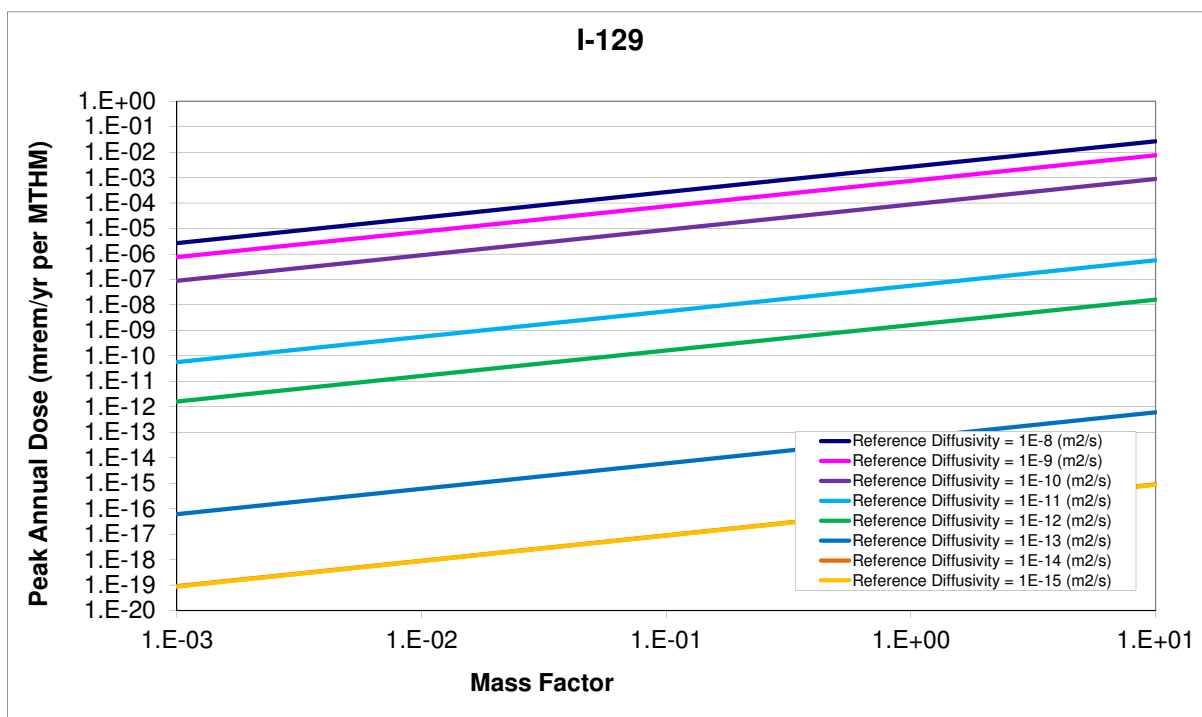


Figure A.12:  $^{129}\text{I}$  mass factor sensitivity.

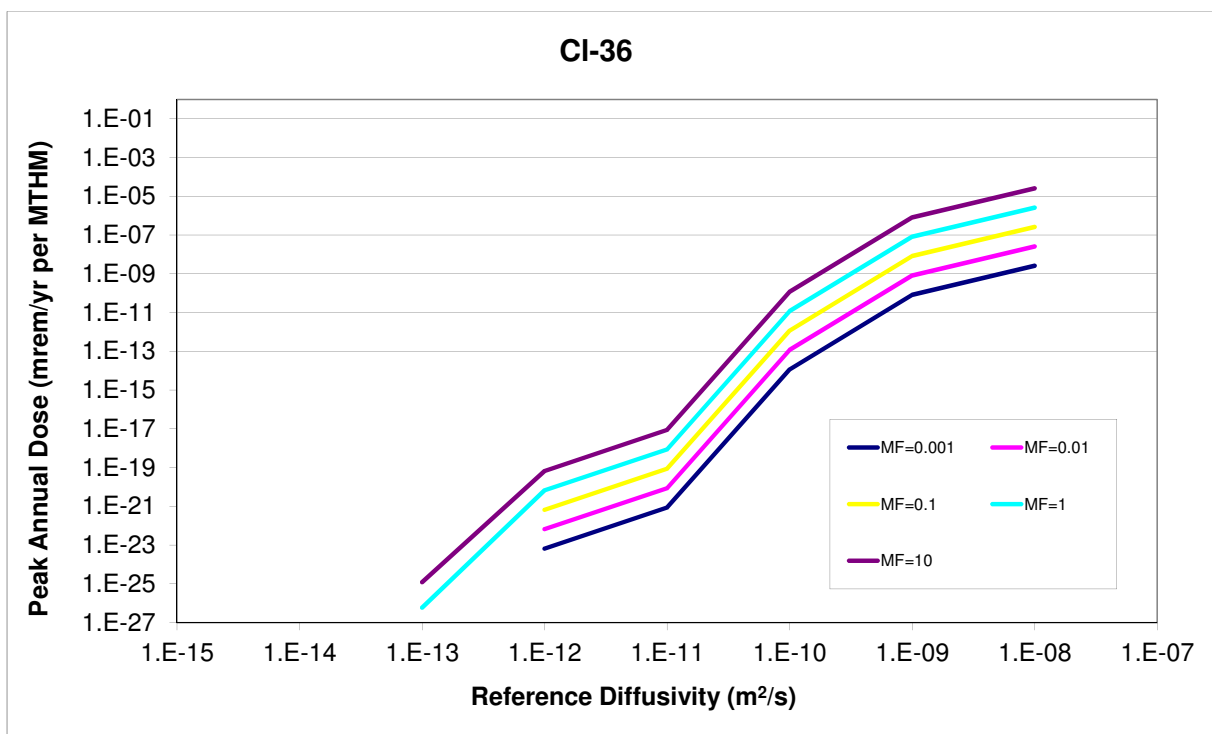


Figure A.13: <sup>36</sup>Cl relative diffusivity sensitivity.

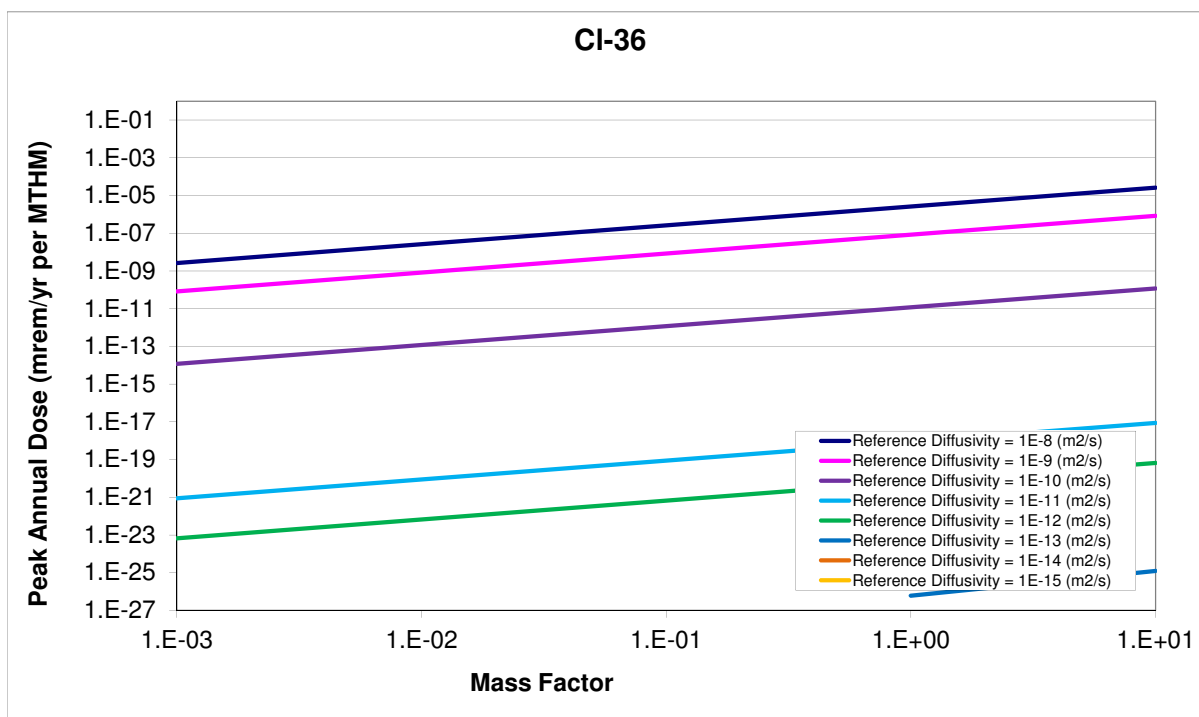


Figure A.14:  $^{36}\text{Cl}$  mass factor sensitivity.

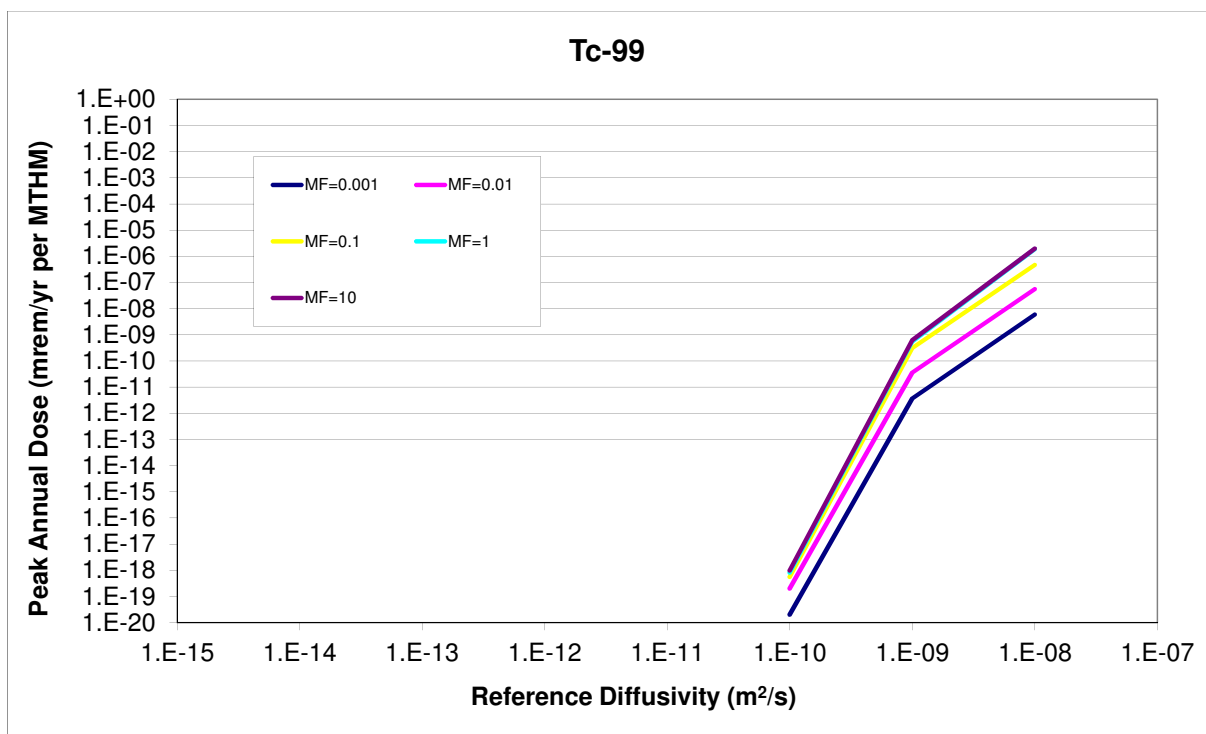


Figure A.15:  $^{99}\text{Tc}$  relative diffusivity sensitivity.

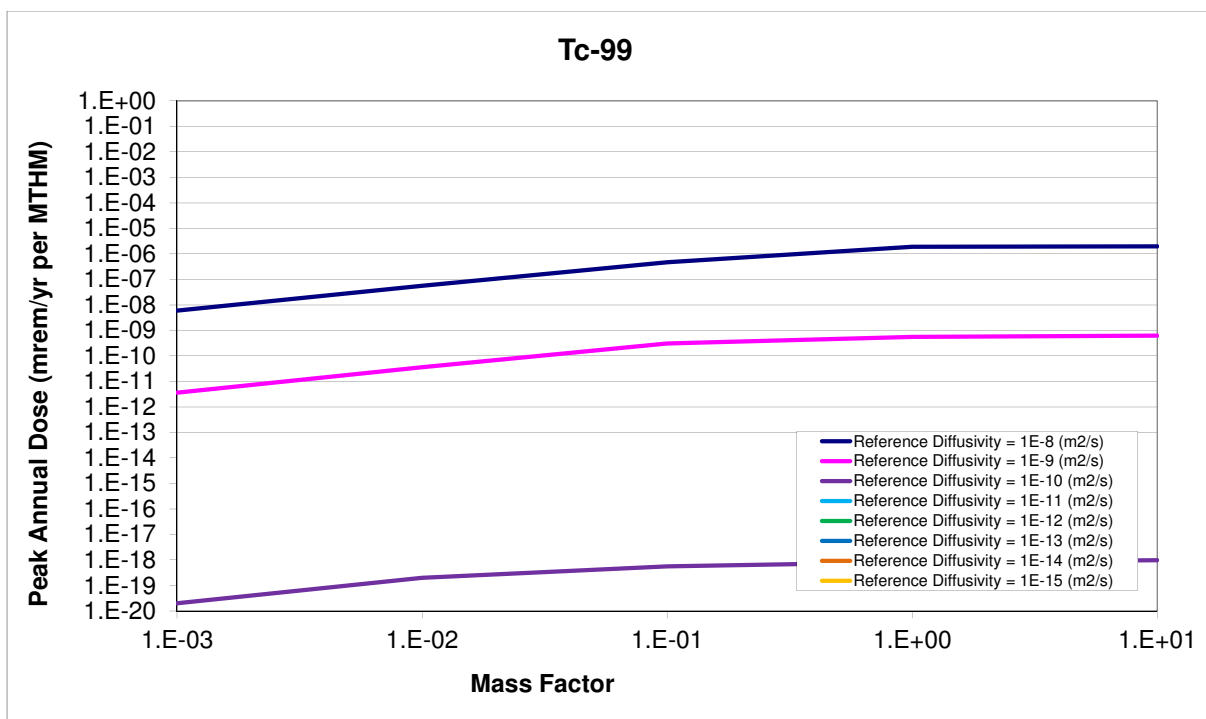


Figure A.16:  $^{99}\text{Tc}$  mass factor sensitivity.

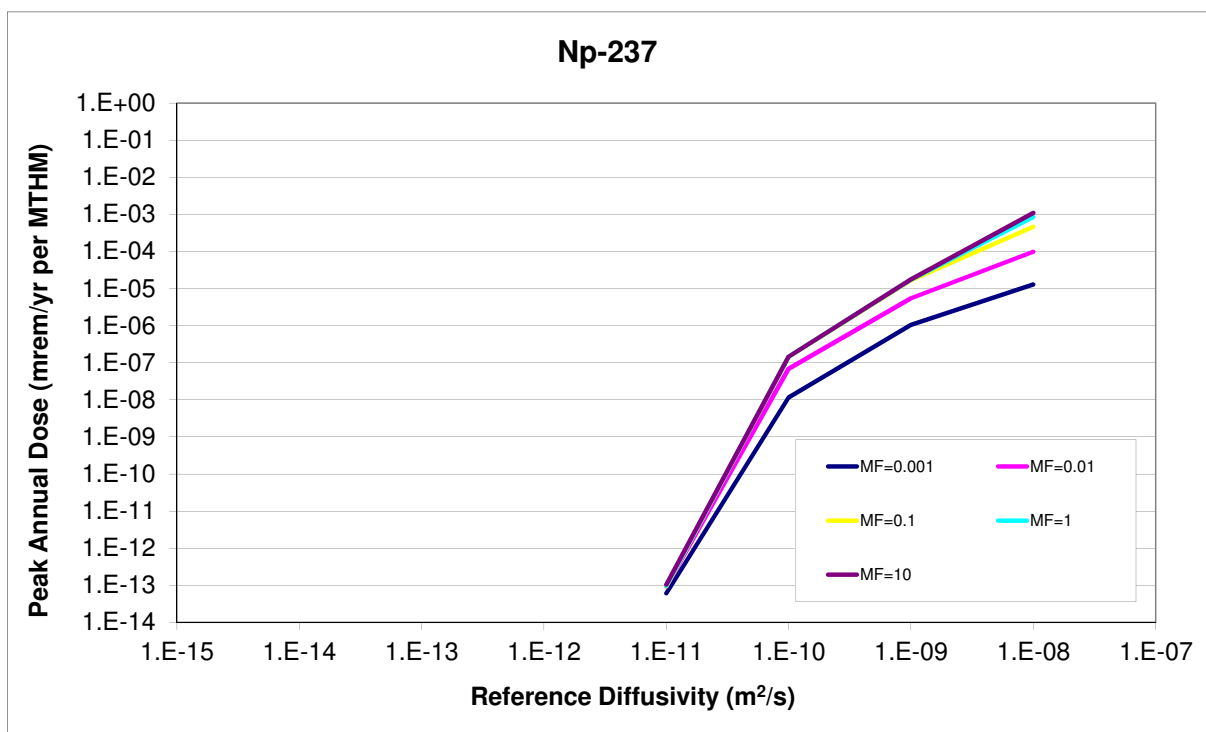


Figure A.17:  $^{237}\text{Np}$  relative diffusivity sensitivity.



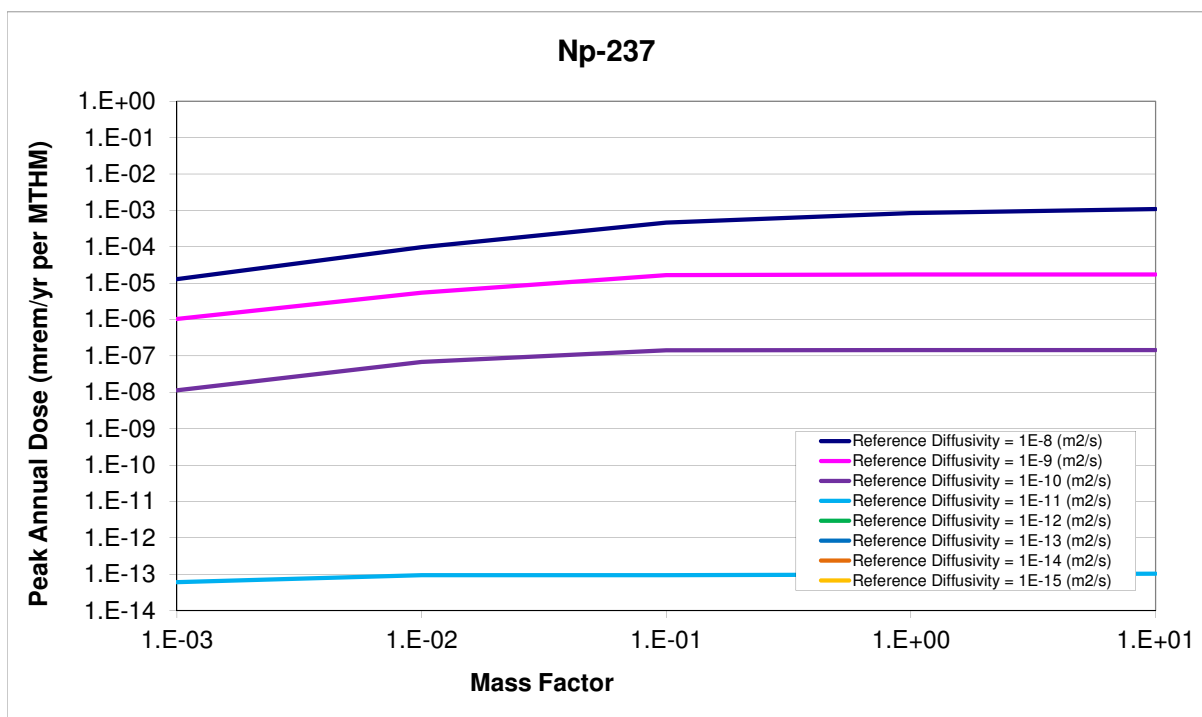


Figure A.18:  $^{237}\text{Np}$  mass factor sensitivity.

## Solubility Coefficients

This study varied the solubility coefficients for each isotope in the simulation to help inform the effect of reprocessing on repository benefit for the clay repository scenario. The importance of the actinide contribution relative to the contribution from  $^{129}\text{I}$ ,  $^{79}\text{Se}$ , and  $^{99}\text{Tc}$  was of particular interest.

The dissolution behavior of a solute in an aqueous solutions is called its solubility. This behavior is limited by the solute's solubility limit, described by an equilibrium constant that depends upon temperature, water chemistry, and the properties of the element. The solubility constant for ordinary solutes,  $K_s$  gives units of concentration,  $[\text{kg}/\text{m}^3]$ , and can be determined algebraically by the law of mass action which gives the partitioning at equilibrium between reactants and products. For a reaction

$$cC + dD = yY + zZ, \quad (\text{A.6})$$

where

$$\begin{aligned} c, d, y, z &= \text{amount of respective constituent } [\text{mol}] \\ C, D &= \text{reactants } [-] \\ Y, Z &= \text{products } [-], \end{aligned}$$

the law of mass action gives

$$K = \frac{(Y)^y (Z)^z}{(C)^c (D)^d} \quad (\text{A.7})$$

where

$$\begin{aligned} (X) &= \text{the equilibrium molal concentration of X } [\text{mol}/\text{m}^3] \\ K &= \text{the equilibrium constant } [-]. \end{aligned}$$

The equilibrium constant for many reactions are known, and can be found in chemical tables. Thereafter, the solubility constraints of a solution at equilibrium can be found algebraically. In cases of salts that dissociate in aqueous solutions, this equilibrium constant is called the salt's solubility product  $K_{sp}$ .

This equilibrium model, however, is only appropriate for dilute situations, and nondilute solutions at partial equilibrium must be treated with an activity model by substituting the activities of the constituents for their molal concentrations,

$$[X] = \gamma_x (X) \quad (\text{A.8})$$

where

$$\begin{aligned} [X] &= \text{activity of X } [-] \\ \gamma_x &= \text{activity coefficient of X } [-] \\ (X) &= \text{molal concentration of X } [\text{mol}/\text{m}^3] \end{aligned}$$

such that

$$IAP = \text{Ion Activity Product } [-].$$

$$= \frac{[Y]^y[Z]^z}{[C]^c[D]^d} \quad (\text{A.9})$$

$$(\text{A.10})$$

The ratio between the IAP and the equilibrium constant ( $IAP/K$ ) quantifies the departure from equilibrium of a solution. This information is useful during the transient stage in which a solute is first introduced to a solution. When  $IAP/K < 1$ , the solution is undersaturated with respect to the products. When, conversely,  $IAP/K > 1$ , the solution is oversaturated and precipitation of solids in the volume will occur.

### Parametric Range

The solubility coefficients were varied in this simulation using a multiplier. The reference solubilities for each element were multiplied by the multiplier for each simulation group. This technique preserved relative solubility among elements. Forty values of solubility coefficient multiplier were used to change the far field solubility. This did not alter any of the solubility in the EDZ, WF, or Fast Path solubilities.

The values of the solubility multiplier were deliberately varied over many magnitudes, from  $1^{-9}$  through  $5 \times 10^{10}$ . This multiplier multiplied the most likely values of solubility for each element, so the relative solubility between elements was preserved.

### Results

The results for varying the solubility coefficient were very straightforward. For solubility limits below a certain threshold, the dose releases were directly proportional to the solubility limit, indicating that the radionuclide concentration saturated the groundwater up to the solubility limit near the waste form. For solubility limits above the threshold, however, further increase to the limit had no effect on the peak dose. This demonstrates the situation in which the solubility limit is so high that even complete dissolution of the waste inventory into the pore water is insufficient to reach the solubility limit.

In Figures A.19 and A.20, it is clear that for solubility constants lower than a threshold, the relationship between peak annual dose and solubility limit is strong.

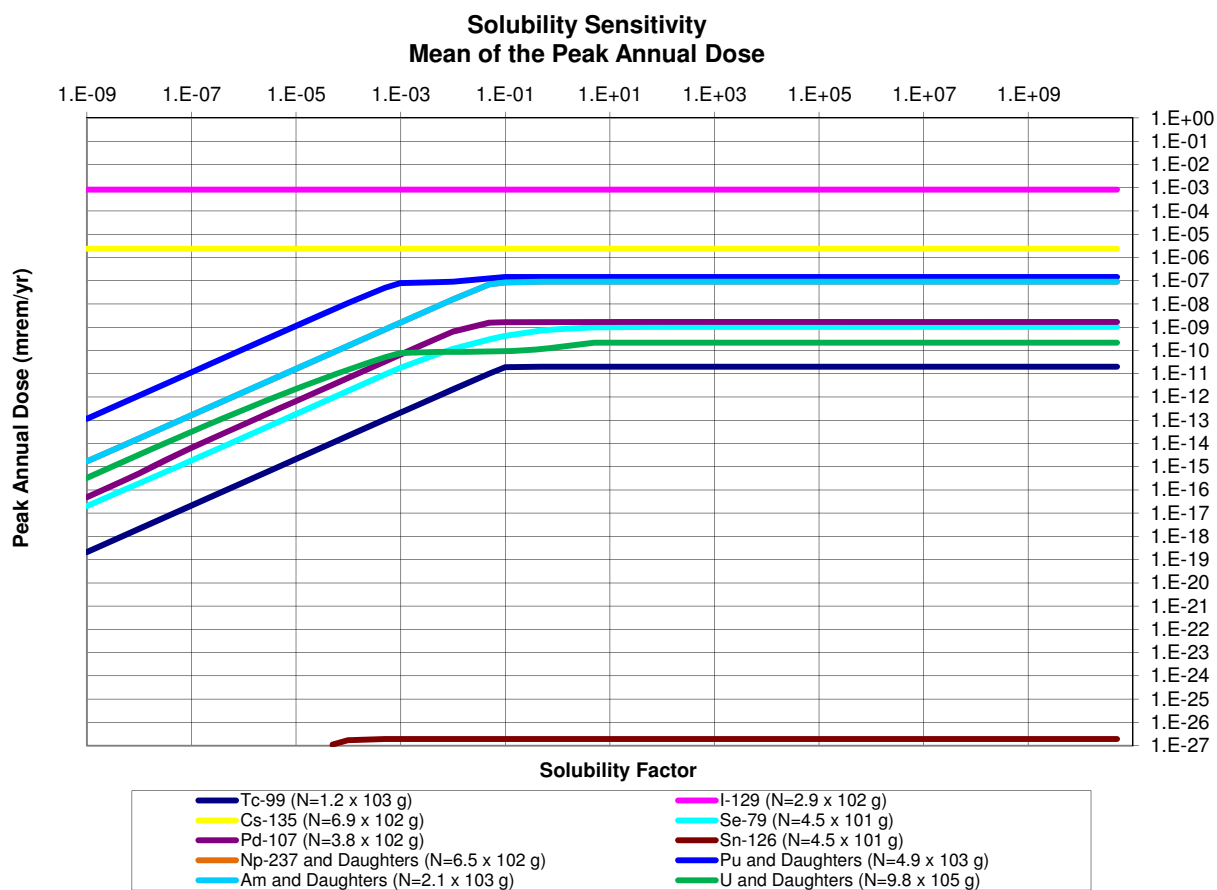


Figure A.19: Solubility factor sensitivity. The peak annual dose due to an inventory,  $N$ , of each isotope.

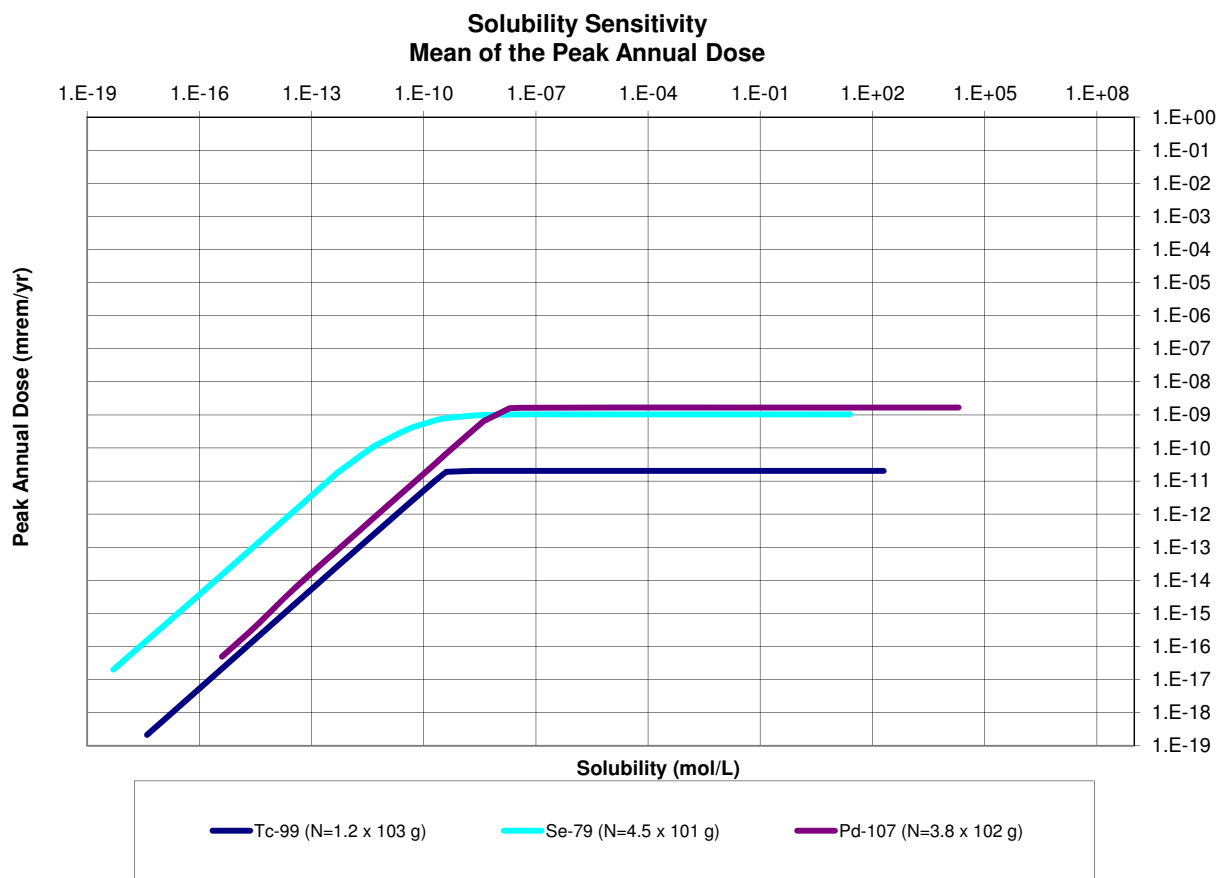


Figure A.20: Solubility limit sensitivity. The peak annual dose due to an inventory,  $N$ , of each isotope.

## The Partition Coefficient

This analysis investigated the peak dose rate contribution from various radionuclides to the partition coefficient of those radionuclides.

The partition or distribution coefficient,  $K_d$ , relates the amount of contaminant adsorbed into the solid phase of the host medium to the amount of contaminant adsorbed into the aqueous phase of the host medium. It is a common empirical coefficient used to capture the effects of a number of retardation mechanisms. The coefficient  $K_d$ , in units of  $[m^3 \cdot kg^{-1}]$ , is the ratio of the mass of contaminant in the solid to the mass of contaminant in the solution.

The retardation factor,  $R_f$ , which is the ratio between velocity of water through a volume and the velocity of a contaminant through that volume, can be expressed in terms of the partition coefficient,

$$R_f = 1 + \frac{\rho_b}{n_e} K_d \quad (A.11)$$

where

$$\rho_b = \text{bulk density} [kg \cdot m^{-3}]$$

and

$$n_e = \text{effective porosity of the medium} [\%].$$

## Parametric Range

The parameters in this model were all set to the default values except a multiplier applied to the partitioning  $K_d$  coefficients.

The multiplier took the forty values  $1 \times 10^{-9}, 5 \times 10^{-8}, \dots, 5 \times 10^{10}$ . Only the far field partition coefficients were altered by this factor. Partition coefficients effecting the EDZ and fast pathway were not changed.

## Results

The expected inverse relationship between the retardation factor and resulting peak annual dose was found for all elements that were not assumed to be effectively infinitely soluble. In the low retardation coefficient cases, a regime is established in which the peak annual dose is entirely unaffected by changes in retardation coefficient. For large values of retardation coefficient, the sensitivity to small changes in the retardation coefficient increases dramatically. In that sensitive regime, the change in peak annual dose is inversely related to the retardation coefficient. Between these two regimes was a transition regime, in which the  $K_d$  factor ranges from  $1 \times 10^{-5}$  to  $5 \times 10^0 [-]$ .

It is clear from Figures A.21 and A.22 that for retardation coefficients greater than a threshold, the relationship between peak annual dose and retardation coefficient is a strong inverse one.

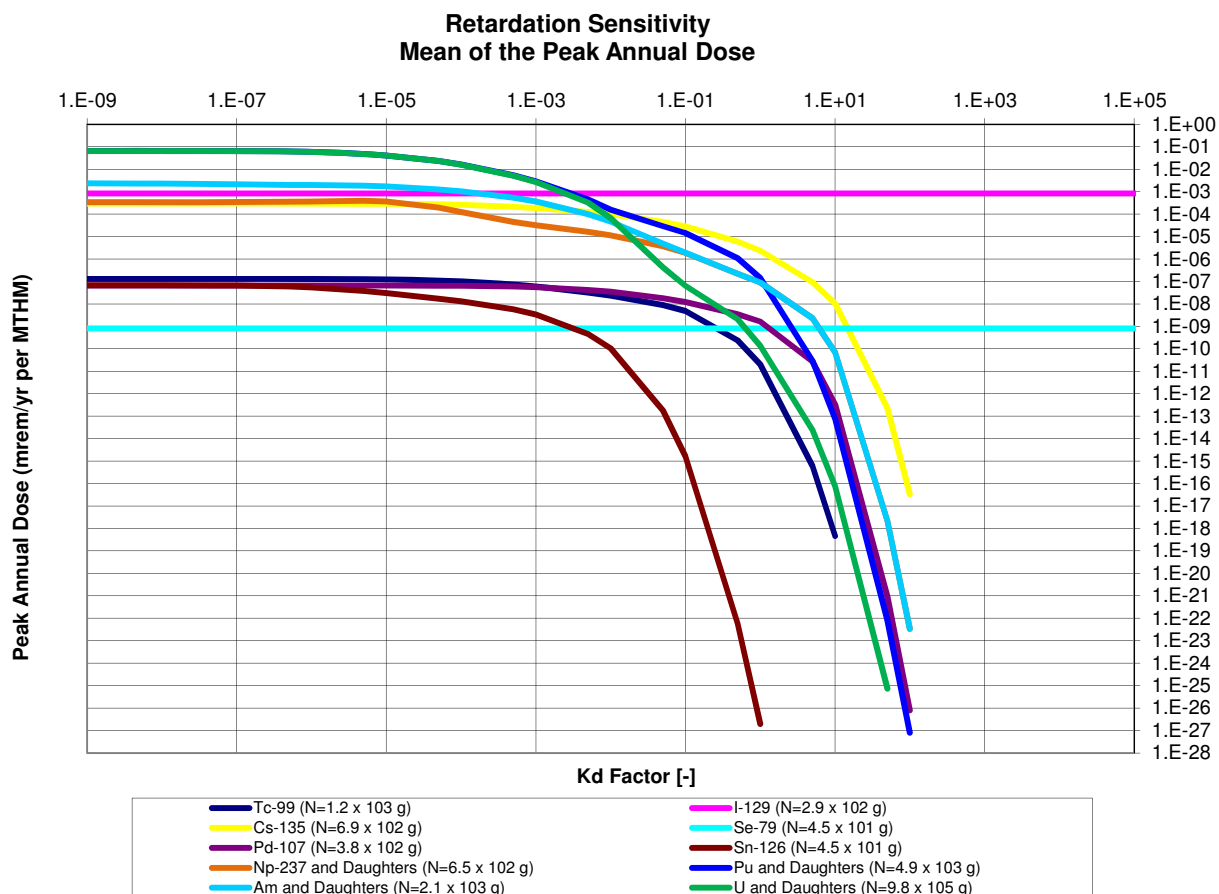


Figure A.21:  $K_d$  factor sensitivity. The peak annual dose due to an inventory,  $N$ , of each isotope.

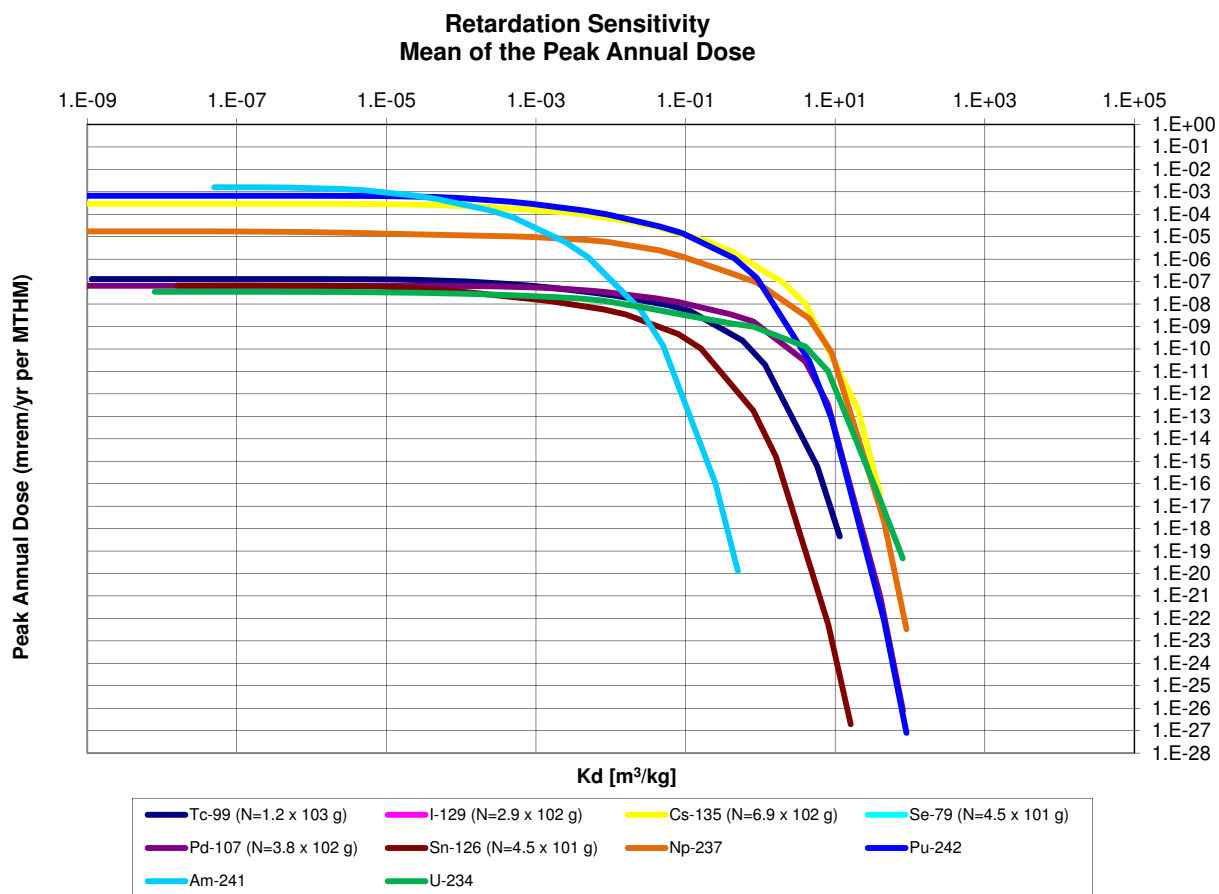


Figure A.22:  $K_d$  sensitivity. The peak annual dose due to an inventory,  $N$ , of each isotope.



## Waste Form Degradation Rate

The sensitivity of peak dose rate to the waste form degradation rate was determined with respect to varying inventories of waste.

The sensitivity of repository performance to waste form degradation rate was expected to vary according to the waste inventory. For cases in which the dominant dose contributing radionuclides have half-lives much shorter than the expected waste form lifetime, the waste form degradation rate is not expected to have an effect. So too, for cases in which the primary barrier to release, the slow diffusive pathway, dominates overall repository performance, the waste form engineered barrier was expected to have a negligible effect on repository performance in comparison.

In the case of a clay repository, the effect of the long time scale of the diffusive release pathway was to dampen the potential effect of high waste form degradation rates.

## Parametric Range

These runs varied the waste form degradation rate and the waste inventory mass factor. There were forty runs corresponding to eight values of the waste form degradation rate and five values of the mass factor.

The waste form degradation rate was varied over the eight magnitudes between  $10^{-9}$  and  $10^{-2}[1/yr]$ . The inventory mass factor was varied over the five magnitudes between 0.001 and 10.0[—].

## Results

These results show two regimes. In the first regime, the mean of the peak annual dose rates is directly proportional to both the mass factor and the fractional waste form degradation rate. For some radionuclides, attenuation occurs for high values of both parameters as the release of radionuclides is limited by dispersion parameters. This phenomenon can be seen in the figures below in which transition between regimes for higher degradation rates happens at lower mass factors than transition between regimes for lower degradation rates.

Safety indicators for post closure repository performance have been developed by the UFD campaign which utilize the inventory multiplier that was varied in this study [? ]. These indicators are normalized by a normalization factor (100 mrem/yr) recommended by the International Atomic Energy Agency (IAEA) as the limit to “relevant critical members of the public” [? ]. The functional form for this safety indicator for a single waste category, high level waste (HLW), is just

$$SI_G = \left( \frac{\sum_{i=1}^N D_{G,i}(I_i, F_d)}{100 \text{ mrem/yr}} \right) [GWe/yr]. \quad (\text{A.12})$$

where

$SI_G$  = Safety indicator for disposal in media type G [ $GWe/yr$ ]

$N$  = Number of key radionuclides considered in this indicator

$D_{G,i}$  = Peak dose rate from isotope i in media type G [ $mrem/yr$ ]

$F_d$  = Fractional waste form degradation rate [ $1/yr$ ].

Tables A.5, A.6, and A.7 report the safety indicators for various independent isotopes and, where applicable, their daughters.

		Inventory Factor				
		0.001	0.01	0.1	1	10
		I-129 ( $N=2.9 \times 10^2$ g)				
Degradation Rate	1.E-09	3.E-11	3.E-10	3.E-09	3.E-08	3.E-07
	1.E-08	3.E-10	3.E-09	3.E-08	3.E-07	3.E-06
	1.E-07	2.E-09	2.E-08	2.E-07	2.E-06	2.E-05
	1.E-06	8.E-09	8.E-08	8.E-07	8.E-06	8.E-05
	1.E-05	1.E-08	1.E-07	1.E-06	1.E-05	1.E-04
	1.E-04	1.E-08	1.E-07	1.E-06	1.E-05	1.E-04
	1.E-03	1.E-08	1.E-07	1.E-06	1.E-05	1.E-04
	1.E-02	1.E-08	1.E-07	1.E-06	1.E-05	1.E-04
		Cl-36 ( $N=1$ g)				
Degradation Rate	1.E-09	1.E-15	1.E-14	1.E-13	1.E-12	1.E-11
	1.E-08	1.E-14	1.E-13	1.E-12	1.E-11	1.E-10
	1.E-07	1.E-13	1.E-12	1.E-11	1.E-10	1.E-09
	1.E-06	9.E-13	9.E-12	9.E-11	9.E-10	9.E-09
	1.E-05	3.E-12	3.E-11	3.E-10	3.E-09	3.E-08
	1.E-04	4.E-12	4.E-11	4.E-10	4.E-09	4.E-08
	1.E-03	4.E-12	4.E-11	4.E-10	4.E-09	4.E-08
	1.E-02	4.E-12	4.E-11	4.E-10	4.E-09	4.E-08

Table A.5: Safety indicators for soluble, non-sorbing nuclides.

		Inventory Factor				
		0.001	0.01	0.1	1	10
Degradation Rate		Pd-107 ( $N=3.8 \times 10^2$ g)				
	1.E-09	2.E-16	2.E-15	2.E-14	2.E-13	2.E-12
	1.E-08	2.E-15	2.E-14	2.E-13	2.E-12	1.E-11
	1.E-07	2.E-14	2.E-13	2.E-12	8.E-12	3.E-11
	1.E-06	5.E-14	5.E-13	3.E-12	2.E-11	3.E-11
	1.E-05	5.E-14	5.E-13	4.E-12	2.E-11	3.E-11
	1.E-04	5.E-14	5.E-13	4.E-12	2.E-11	3.E-11
	1.E-03	5.E-14	5.E-13	4.E-12	2.E-11	3.E-11
Degradation Rate		Sn-126 ( $N=4.5 \times 10^1$ g)				
	1.E-09	0.E+00	0.E+00	0.E+00	0.E+00	0.E+00
	1.E-08	0.E+00	0.E+00	0.E+00	0.E+00	0.E+00
	1.E-07	0.E+00	0.E+00	0.E+00	0.E+00	2.E-29
	1.E-06	0.E+00	0.E+00	0.E+00	2.E-29	5.E-29
	1.E-05	0.E+00	0.E+00	1.E-29	3.E-29	5.E-29
	1.E-04	0.E+00	0.E+00	1.E-29	3.E-29	5.E-29
	1.E-03	0.E+00	0.E+00	1.E-29	3.E-29	5.E-29
Degradation Rate		Zr-93 & Nb-93				
	1.E-09	1.E-17	1.E-16	1.E-15	1.E-14	1.E-13
	1.E-08	1.E-16	1.E-15	1.E-14	1.E-13	7.E-13
	1.E-07	1.E-15	1.E-14	1.E-13	6.E-13	3.E-12
	1.E-06	4.E-15	4.E-14	3.E-13	1.E-12	4.E-12
	1.E-05	6.E-15	6.E-14	4.E-13	2.E-12	4.E-12
	1.E-04	6.E-15	6.E-14	4.E-13	2.E-12	4.E-12
	1.E-03	7.E-15	6.E-14	4.E-13	2.E-12	4.E-12
Degradation Rate		Tc-99 ( $N=1.2 \times 10^3$ g)				
	1.E-09	2.E-18	2.E-17	2.E-16	2.E-15	2.E-14
	1.E-08	2.E-17	2.E-16	2.E-15	2.E-14	1.E-13
	1.E-07	2.E-16	2.E-15	2.E-14	1.E-13	2.E-13
	1.E-06	1.E-15	1.E-14	1.E-13	2.E-13	2.E-13
	1.E-05	5.E-15	5.E-14	1.E-13	2.E-13	2.E-13
	1.E-04	7.E-15	5.E-14	1.E-13	2.E-13	2.E-13
	1.E-03	7.E-15	5.E-14	1.E-13	2.E-13	2.E-13
Degradation Rate		Cs-135 ( $N=6.9 \times 10^2$ g)				
	1.E-09	6.E-14	6.E-13	6.E-12	6.E-11	6.E-10
	1.E-08	6.E-13	6.E-12	6.E-11	6.E-10	6.E-09
	1.E-07	5.E-12	5.E-11	5.E-10	5.E-09	5.E-08
	1.E-06	2.E-11	2.E-10	2.E-09	2.E-08	2.E-07
	1.E-05	3.E-11	3.E-10	3.E-09	3.E-08	3.E-07
	1.E-04	4.E-11	4.E-10	4.E-09	4.E-08	4.E-07
	1.E-03	4.E-11	4.E-10	4.E-09	4.E-08	4.E-07
Degradation Rate		Se-79 ( $N=4.5 \times 10^1$ g)				
	1.E-09	2.E-14	2.E-13	2.E-12	5.E-12	8.E-12
	1.E-08	2.E-13	2.E-12	5.E-12	8.E-12	8.E-12
	1.E-07	2.E-12	5.E-12	8.E-12	8.E-12	8.E-12
	1.E-06	5.E-12	8.E-12	8.E-12	8.E-12	8.E-12
	1.E-05	6.E-12	8.E-12	8.E-12	8.E-12	8.E-12
	1.E-04	6.E-12	8.E-12	8.E-12	8.E-12	8.E-12
	1.E-03	6.E-12	8.E-12	8.E-12	8.E-12	8.E-12
Degradation Rate	1.E-02	6.E-12	8.E-12	8.E-12	8.E-12	8.E-12

Table A.6: Safety indicators for solubility limited and sorbing nuclides.

		Inventory Factor				
		0.001	0.01	0.1	1	10
Degradation Rate	Np-237 and Daughters (N=6.5 × 10 <sup>2</sup> g)					
	1.E-09	3.E-13	3.E-12	3.E-11	3.E-10	9.E-10
	1.E-08	3.E-12	3.E-11	3.E-10	9.E-10	9.E-10
	1.E-07	3.E-11	3.E-10	9.E-10	9.E-10	9.E-10
	1.E-06	1.E-10	8.E-10	9.E-10	9.E-10	9.E-10
	1.E-05	2.E-10	8.E-10	9.E-10	9.E-10	9.E-10
	1.E-04	2.E-10	8.E-10	9.E-10	9.E-10	1.E-09
	1.E-03	2.E-10	8.E-10	9.E-10	9.E-10	1.E-09
	1.E-02	2.E-10	8.E-10	9.E-10	9.E-10	1.E-09
Degradation Rate	Pu and Daughters (N=4.9 × 10 <sup>3</sup> g)					
	1.E-09	4.E-15	4.E-14	4.E-13	3.E-12	2.E-11
	1.E-08	4.E-14	3.E-13	3.E-12	2.E-11	2.E-10
	1.E-07	3.E-13	2.E-12	2.E-11	2.E-10	2.E-09
	1.E-06	2.E-12	2.E-11	2.E-10	1.E-09	9.E-09
	1.E-05	4.E-12	4.E-11	4.E-10	3.E-09	1.E-08
	1.E-04	5.E-12	5.E-11	5.E-10	3.E-09	1.E-08
	1.E-03	5.E-12	5.E-11	5.E-10	3.E-09	1.E-08
	1.E-02	5.E-12	5.E-11	5.E-10	3.E-09	1.E-08
Degradation Rate	Am and Daughters (N=2.1 × 10 <sup>3</sup> g)					
	1.E-09	3.E-13	3.E-12	3.E-11	3.E-10	9.E-10
	1.E-08	3.E-12	3.E-11	3.E-10	9.E-10	9.E-10
	1.E-07	3.E-11	3.E-10	9.E-10	9.E-10	9.E-10
	1.E-06	1.E-10	8.E-10	9.E-10	9.E-10	9.E-10
	1.E-05	2.E-10	8.E-10	9.E-10	9.E-10	9.E-10
	1.E-04	2.E-10	8.E-10	9.E-10	9.E-10	1.E-09
	1.E-03	2.E-10	8.E-10	9.E-10	9.E-10	1.E-09
	1.E-02	2.E-10	8.E-10	9.E-10	9.E-10	1.E-09
Degradation Rate	U and Daughters (N=9.8 × 10 <sup>5</sup> g)					
	1.E-09	2.E-15	2.E-14	1.E-13	5.E-13	6.E-13
	1.E-08	2.E-14	1.E-13	5.E-13	6.E-13	7.E-13
	1.E-07	1.E-13	4.E-13	6.E-13	7.E-13	2.E-12
	1.E-06	3.E-13	6.E-13	7.E-13	1.E-12	7.E-12
	1.E-05	4.E-13	7.E-13	8.E-13	2.E-12	9.E-12
	1.E-04	4.E-13	7.E-13	9.E-13	3.E-12	9.E-12
	1.E-03	4.E-13	7.E-13	9.E-13	3.E-12	9.E-12
	1.E-02	4.E-13	7.E-13	9.E-13	3.E-12	9.E-12

Table A.7: Safety indicators for the actinides and their daughters.

The peaks for highly soluble, non sorbing elements such as  $I$  and  $Cl$  are directly proportional to mass factor for most values of waste form degradation rates. This effect can be seen in Figures A.23, A.24, A.25, and A.26.

Highly soluble and non-sorbing  $^{129}I$  demonstrates a direct proportionality between dose rate and fractional degradation rate until a turnover where other natural system parameters dampen transport. Highly soluble and non-sorbing  $^{129}I$  demonstrates a direct proportionality to the inventory multiplier.

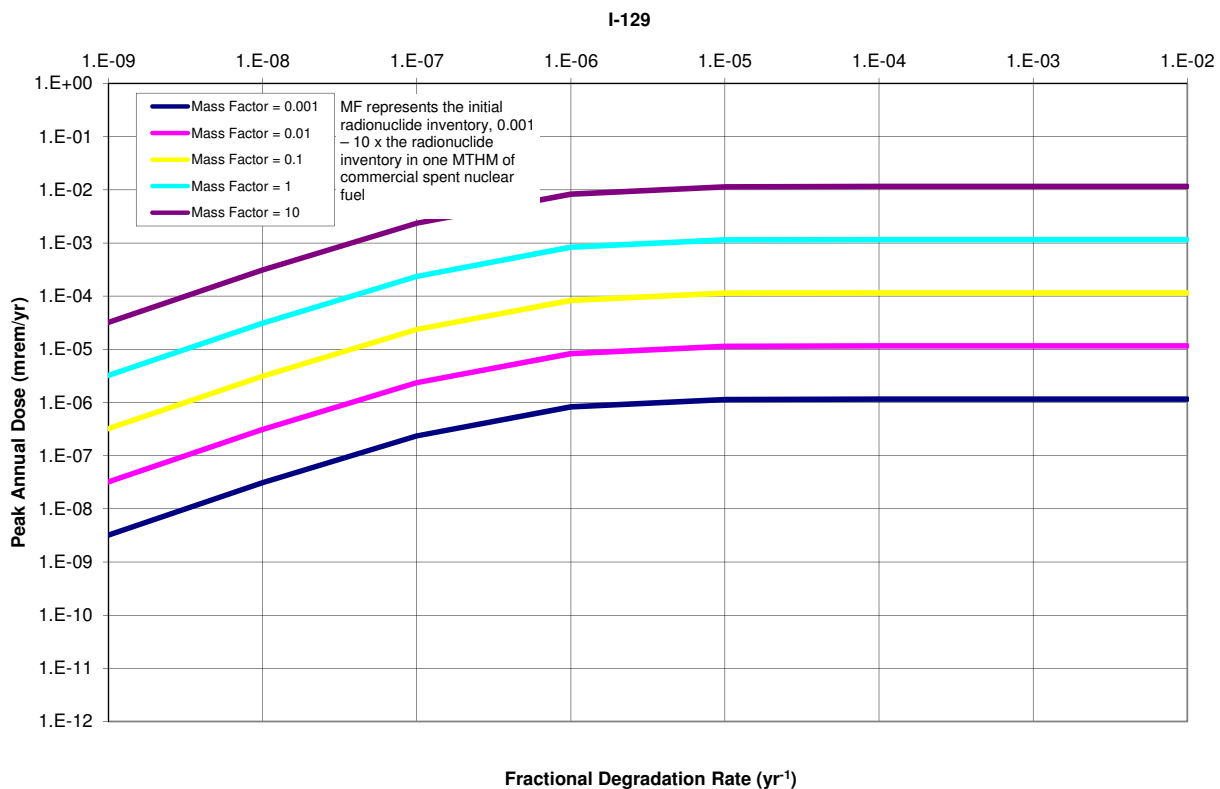


Figure A.23:  $^{129}I$  waste form degradation rate sensitivity.

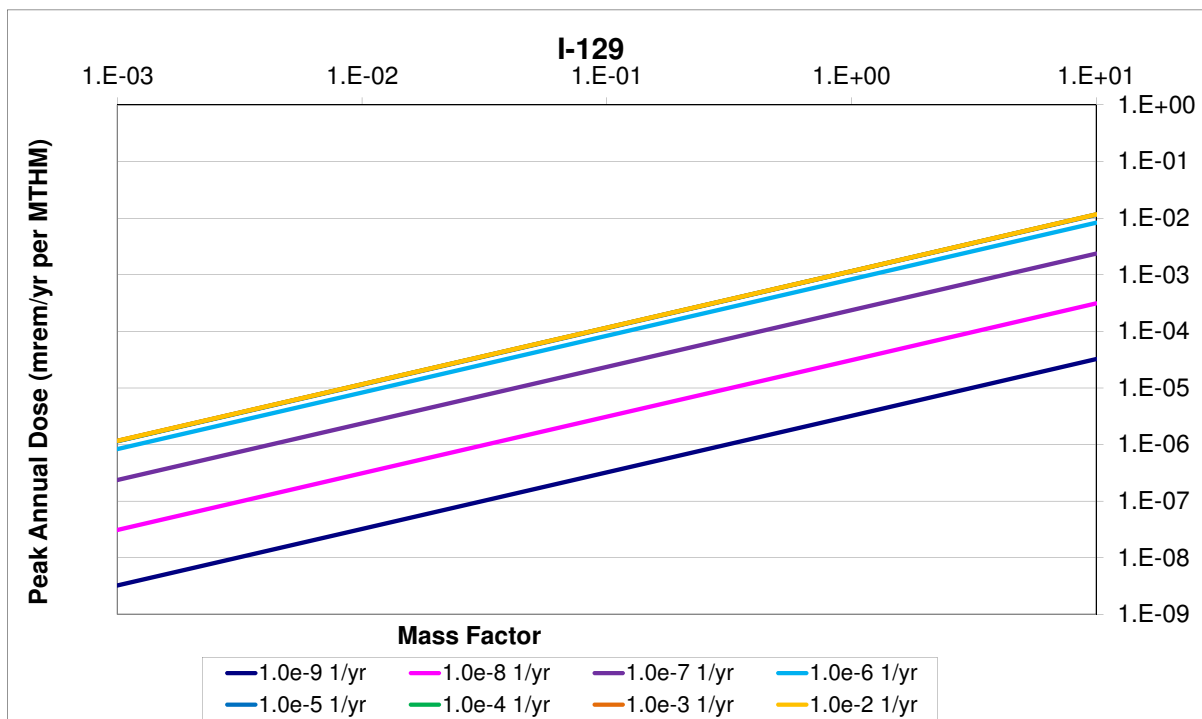


Figure A.24:  $^{129}\text{I}$  inventory multiplier sensitivity.

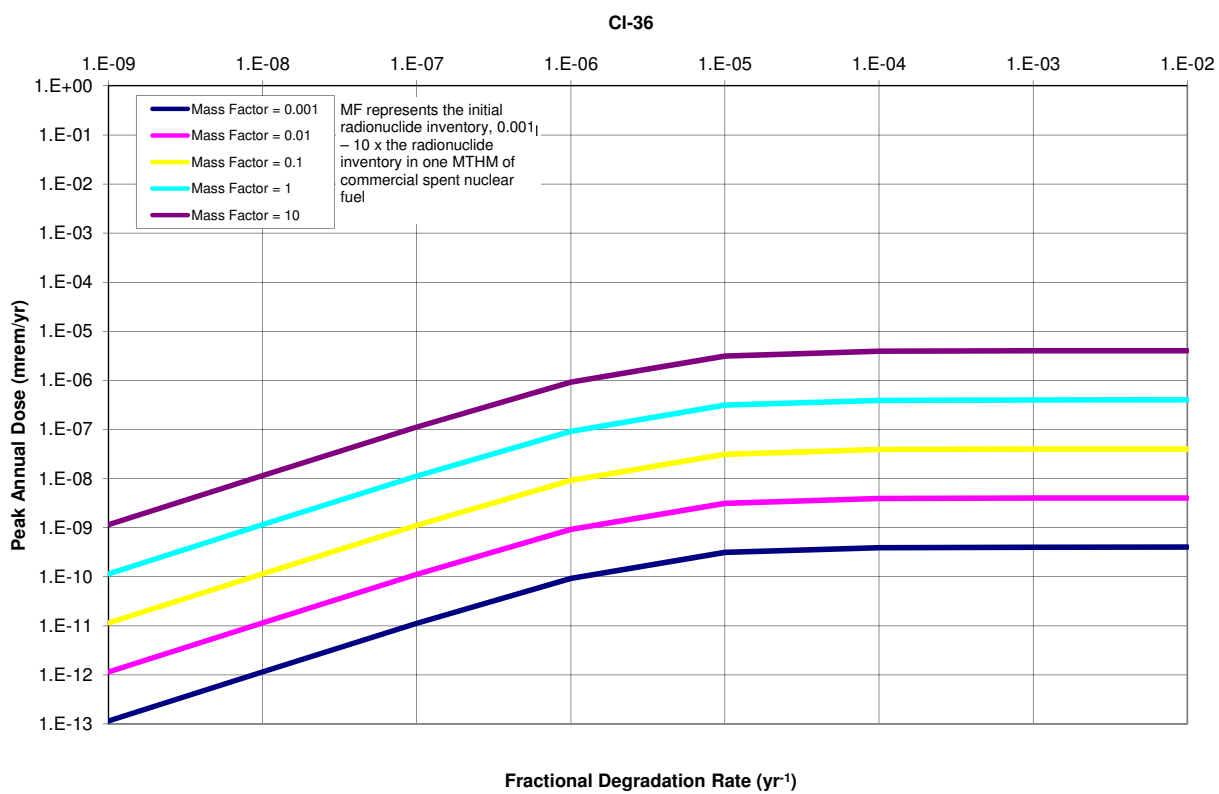


Figure A.25: <sup>36</sup>Cl waste form degradation rate sensitivity.

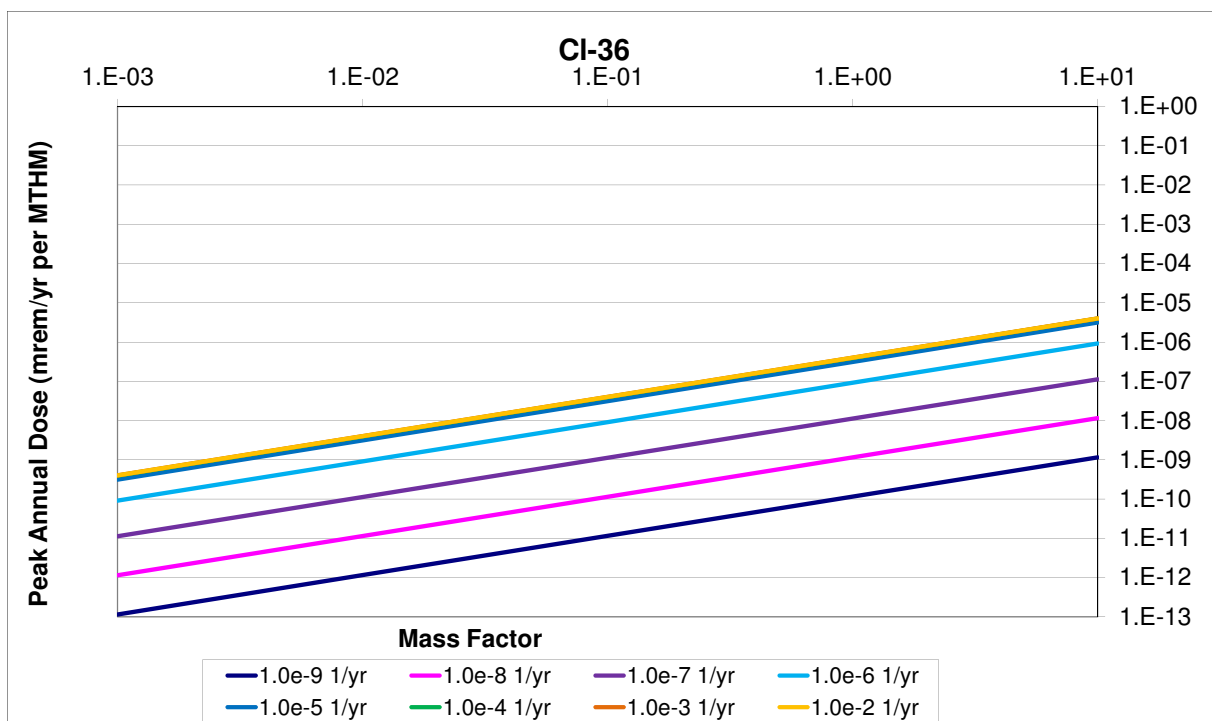


Figure A.26:  $^{36}\text{Cl}$  inventory multiplier sensitivity.



The peaks for solubility limited, sorbing elements such as  $Tc$  and  $Np$ , on the other hand, have a more dramatic turnover. For very high degradation rates, the dependence on mass factor starts to round off due to attenuation by solubility limits, as can be seen in Figures A.29, A.30, A.27, and A.28.

Solubility limited and sorbing  $^{99}Tc$  demonstrates a direct proportionality to fractional degradation rate until attuation by its solubility limit and other natural system parameters.

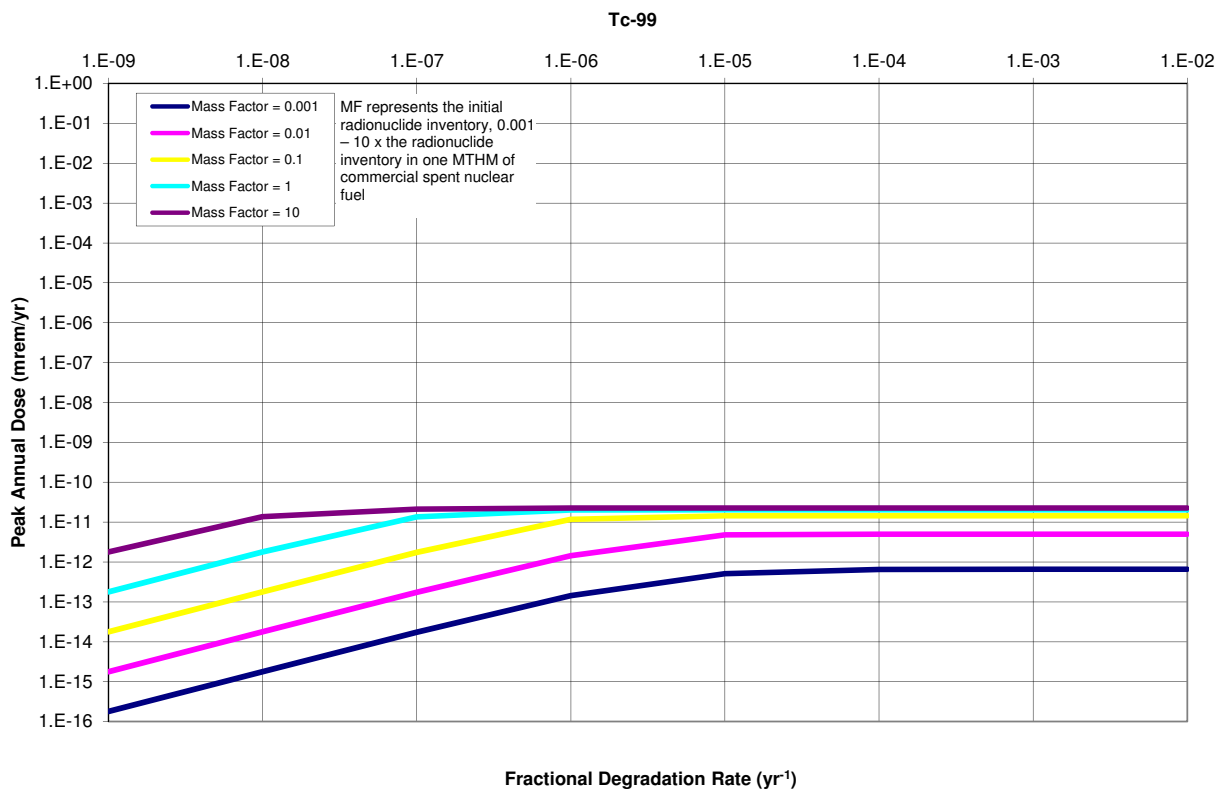


Figure A.27:  $^{99}Tc$  waste form degradation rate sensitivity.

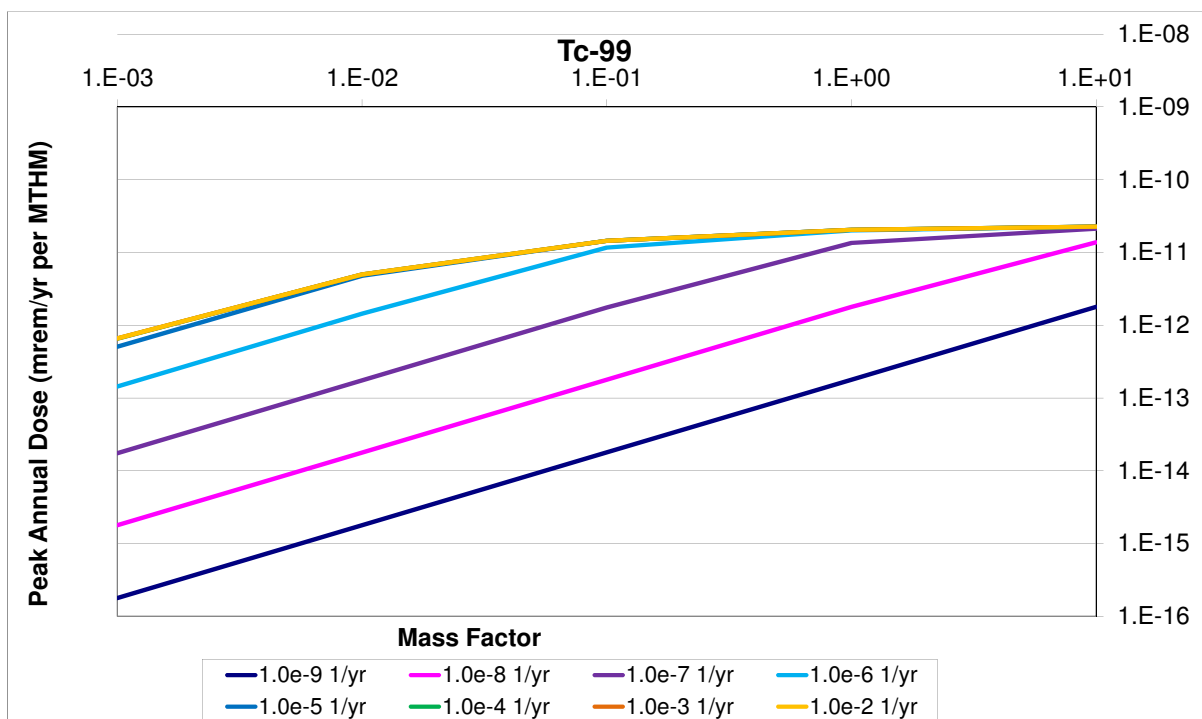


Figure A.28:  $^{99}\text{Tc}$  inventory multiplier sensitivity.

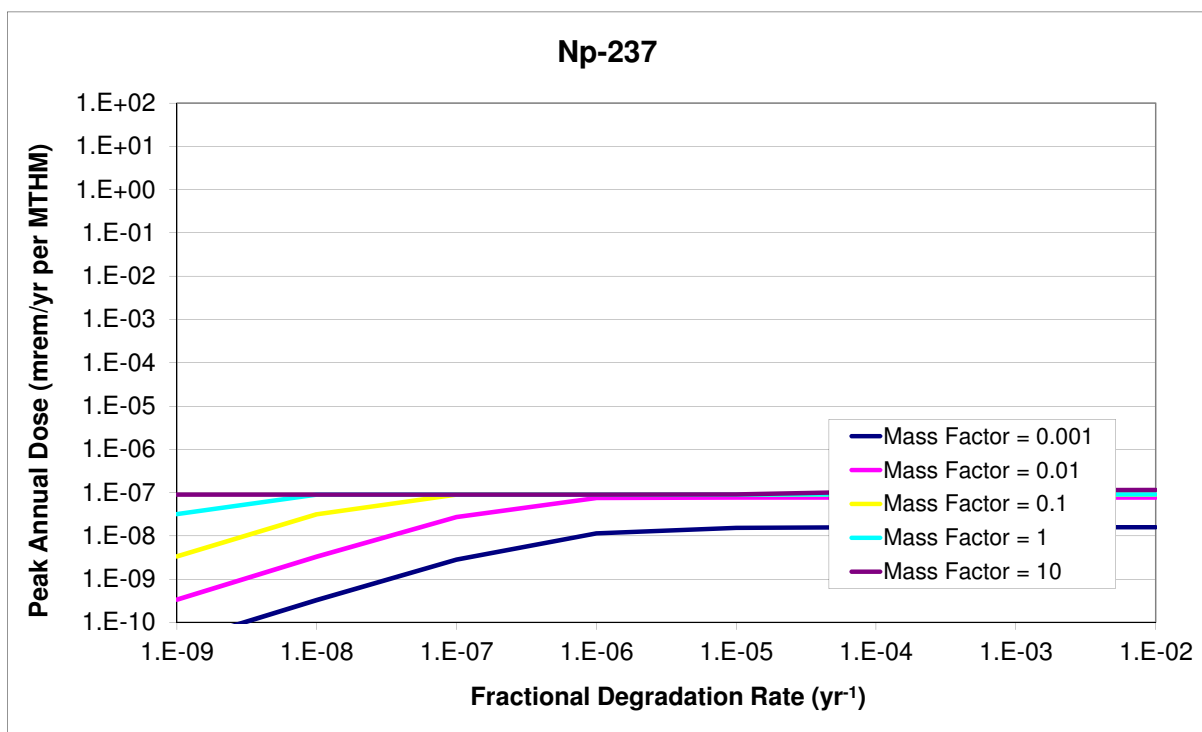


Figure A.29:  $^{237}\text{Np}$  waste form degradation rate sensitivity.

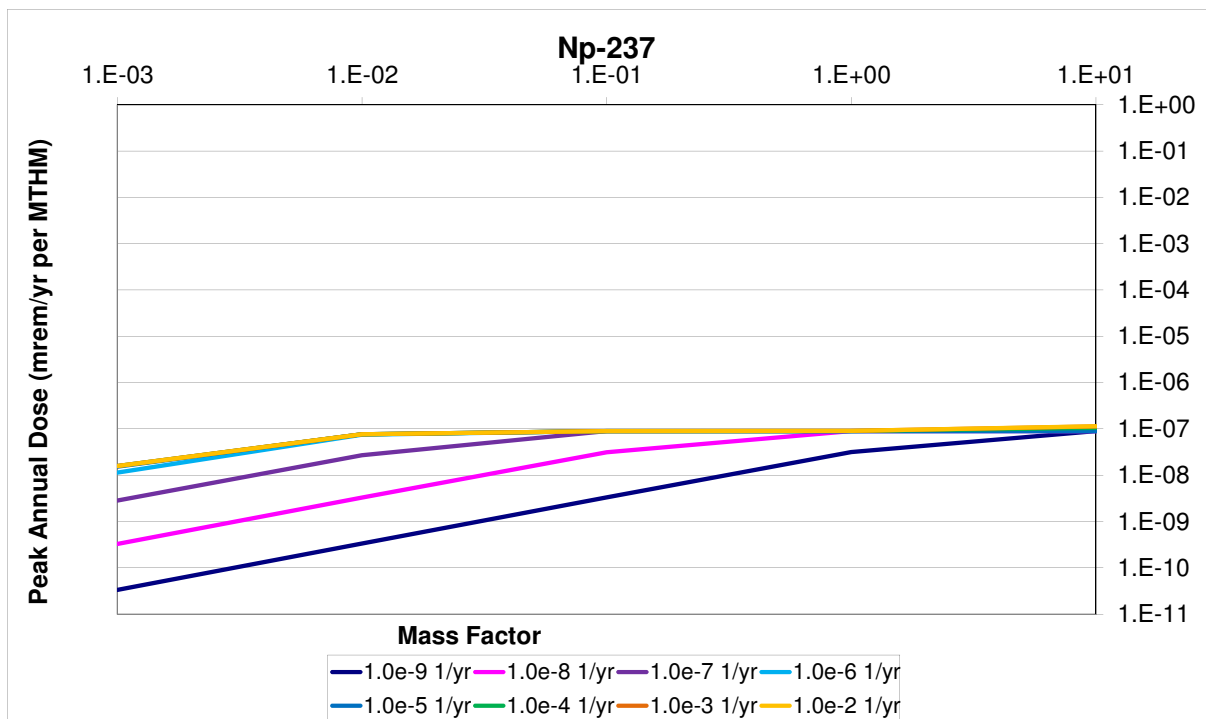


Figure A.30:  $^{237}\text{Np}$  inventory multiplier sensitivity.

## Waste Package Failure Time

The time of waste package failure was not expected to greatly effect the magnitude of the mean of the peak doses except for cases in which waste package failure times exceeded the half lives of dominant dose-contributing nuclides. That is, since the dominant dose-contributing radionuclides for the reference case are quite long lived ( $^{129}\text{I}$ , etc.), all but the longest reasonable waste package containment lifetime is overwhelmed by the half life of the dominant radionuclides. The long time scales of radionuclide release was expected to render the the waste package lifetime irrelevant if it was shorter than a million years.

Though the model contains a unit cell-type model, it is possible to determine, in post processing, the results of a simulation with temporally heterogeneous failures among waste packages. That is, by a weighted sum of the time histories of the no-fail case and the all-fail case, it is possible to mimic a time-varying failure among the many waste packages.

## Parametric Range

To investigate the effect of the waste package failure time, it was varied over five magnitudes from one thousand to ten million years. Simultaneously, the reference diffusivity was varied over the eight magnitudes between  $1 \times 10^{-8}$  and  $1 \times 10^{-15}$  in order to determine the correlation between increased radionuclide mobility and the waste package lifetime.

## Results

For the clay repository, the waste package failure time is entirely irrelevant until waste package failure times reach the million or ten million year time scale.

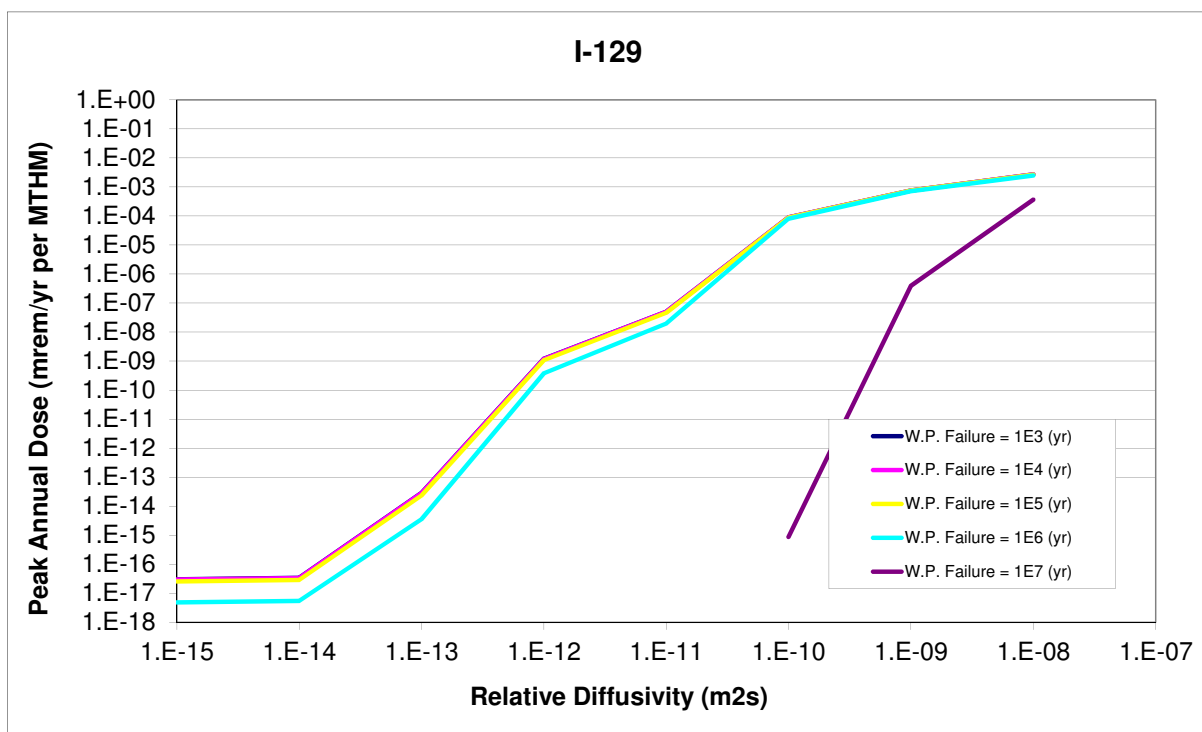


Figure A.31:  $^{129}\text{I}$  waste package failure time sensitivity.

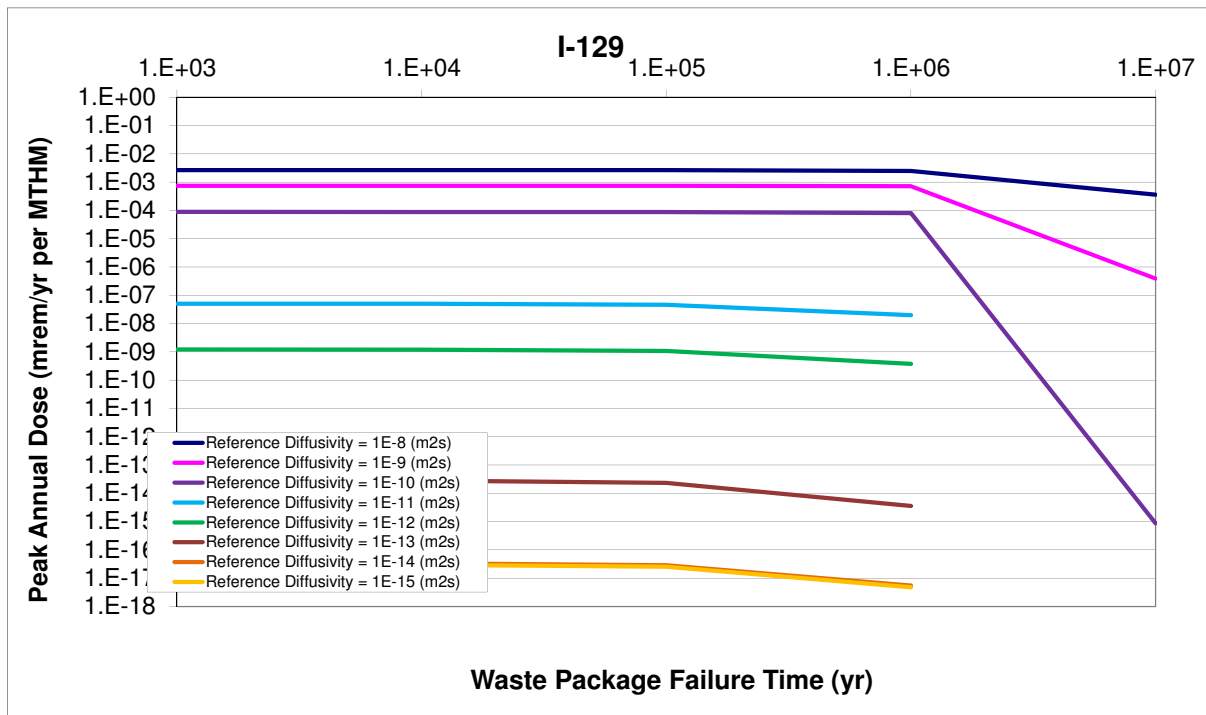


Figure A.32:  $^{129}\text{I}$  waste package failure time sensitivity.

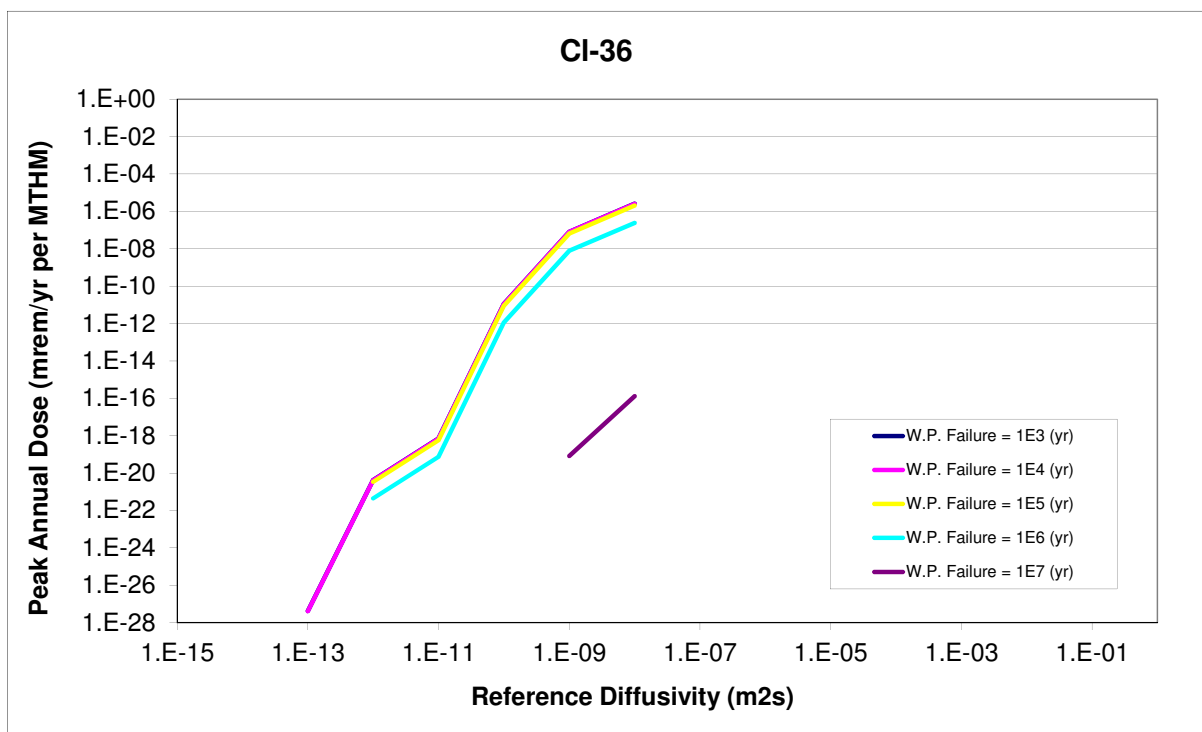


Figure A.33:  $^{36}\text{Cl}$  waste package failure time sensitivity.



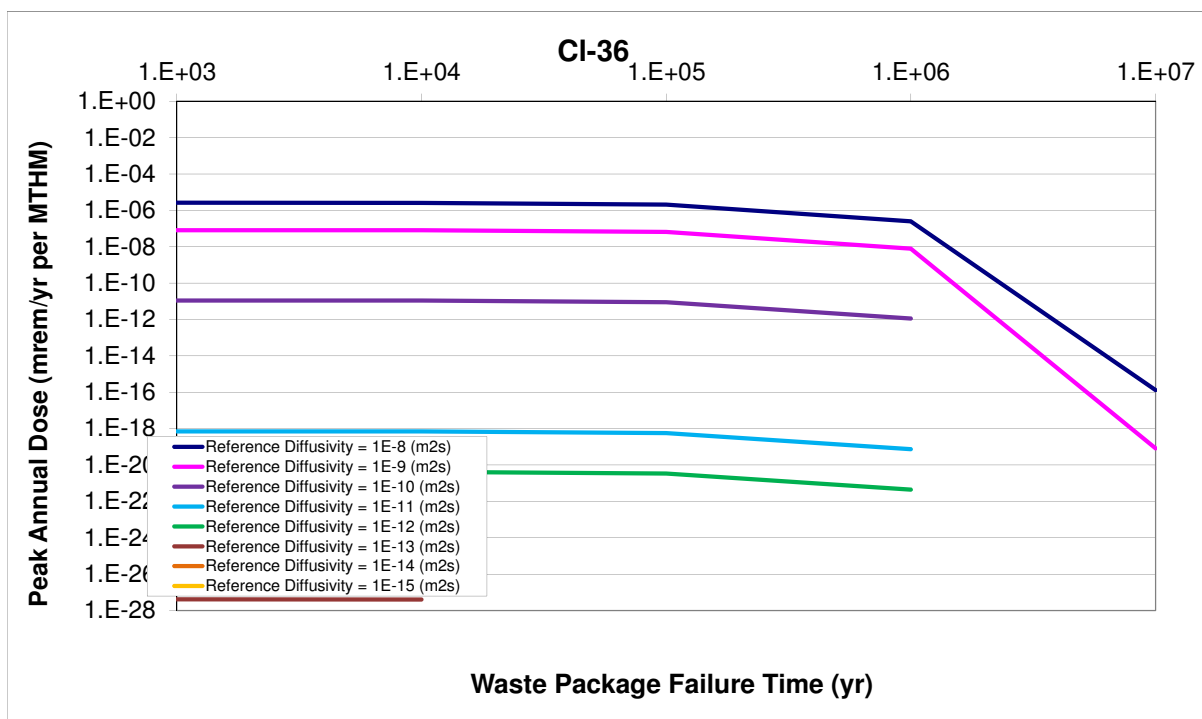


Figure A.34:  $^{36}\text{Cl}$  waste package failure time sensitivity.

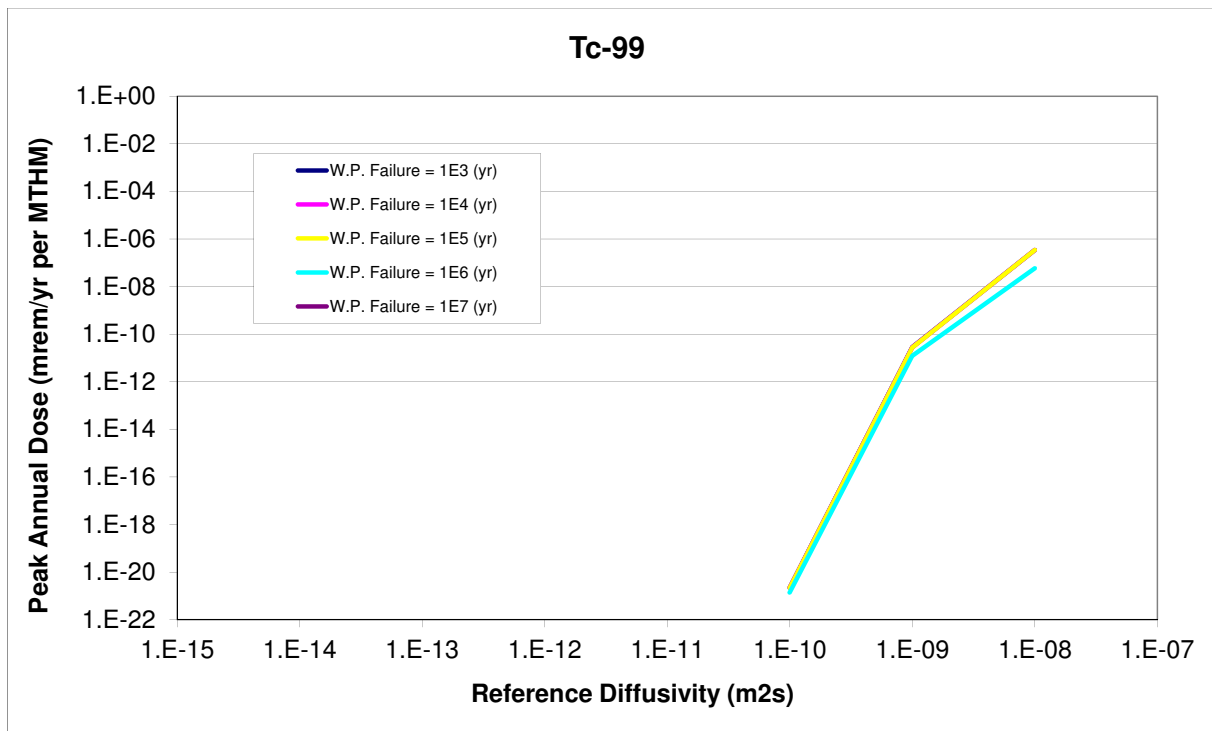


Figure A.35:  $^{99}\text{Tc}$  waste package failure time sensitivity.

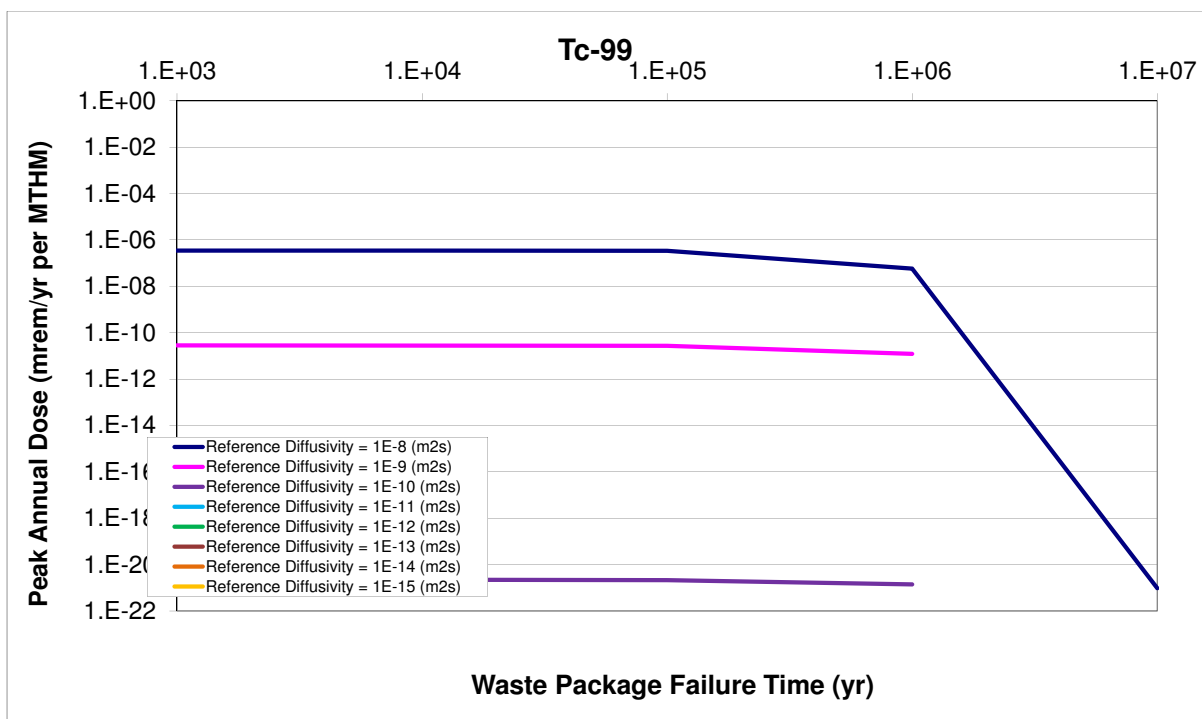


Figure A.36:  $^{99}\text{Tc}$  waste package failure time sensitivity.

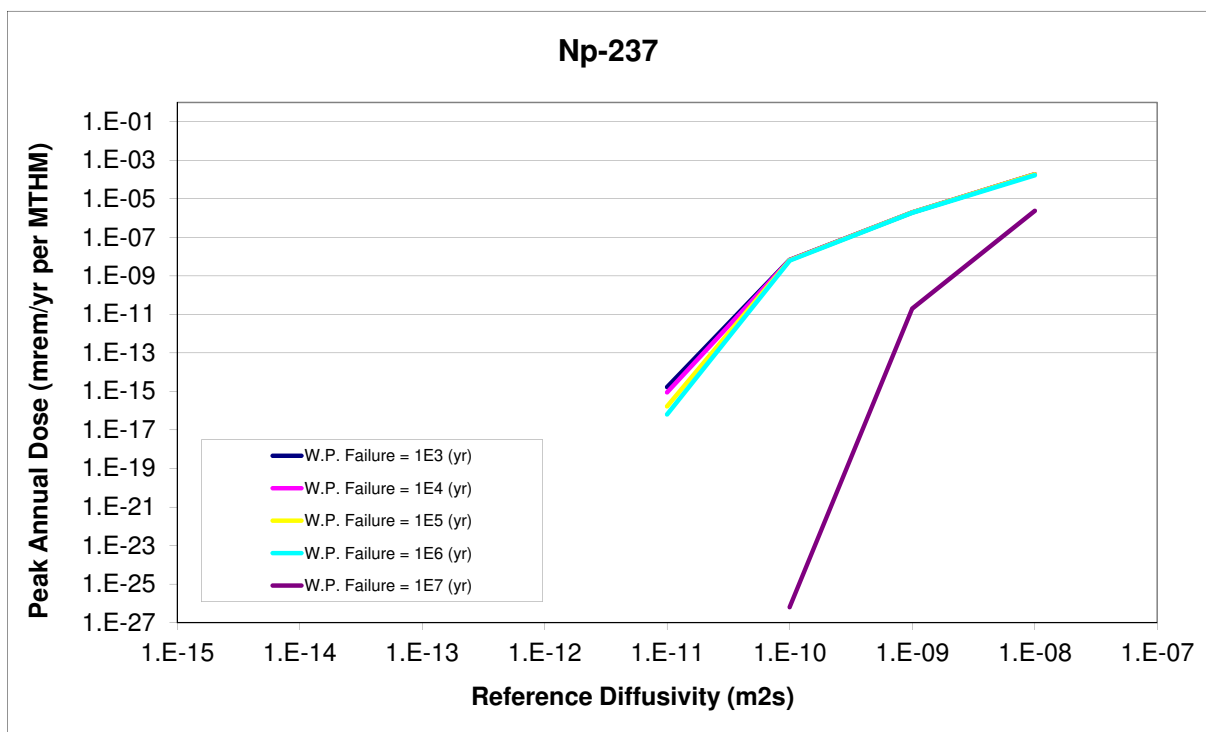


Figure A.37:  $^{237}\text{Np}$  waste package failure time sensitivity.

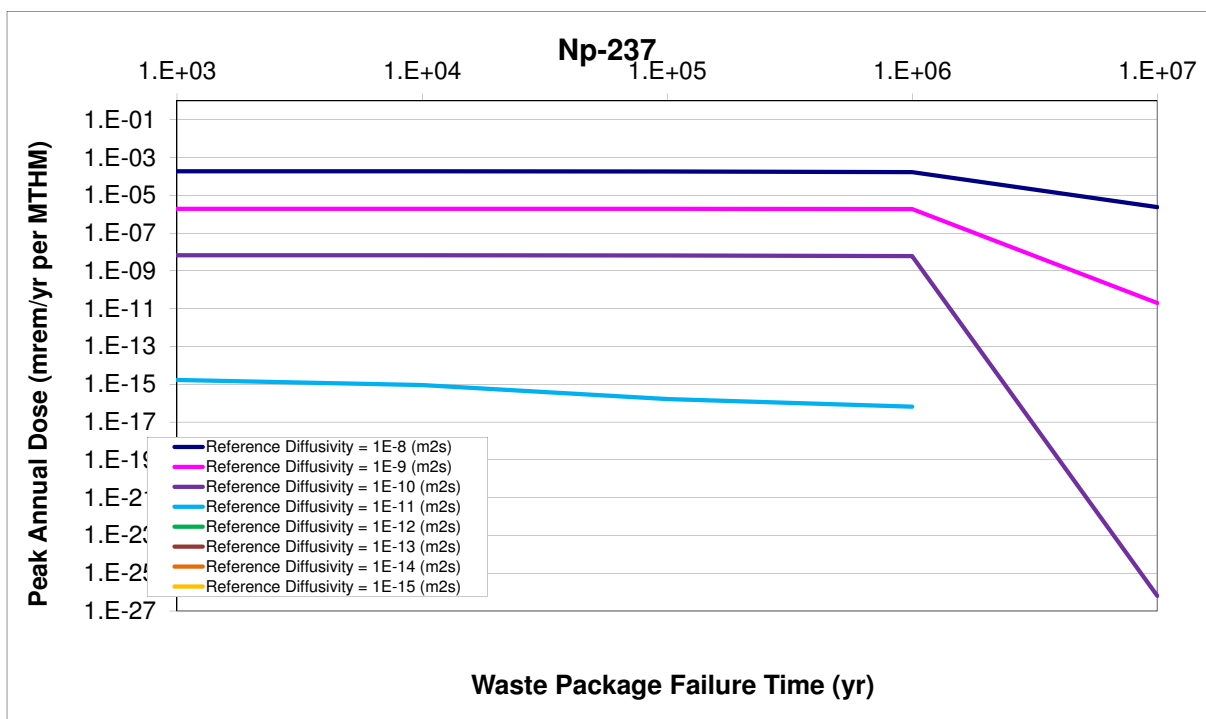


Figure A.38:  $^{237}\text{Np}$  waste package failure time sensitivity.

## **B THERMAL TRANSPORT SENSITIVITY ANALYSIS**

---

### **B.1 Isotopic Thermal Sensitivity Study**

### **B.2 Thermal Conductivity Sensitivity Study**

### **B.3 Diffusivity Thermal Transport Sensitivity Study**

### **B.4 Spacing Thermal Transport Sensitivity Studies**

## REFERENCES

---

- [1] AB, Svensk karnbranslehantering. 2006. *Long-term safety for KBS-3 repositories at forsmark and laxemar-a first evaluation: Main report of the SR-Can project*. SKB.
- [2] Abkowitz, Mark. 2010. Nuclear waste assessment system for technical evaluation - NUWASTE.
- [3] Ahn, J. 1988. Mass transfer and transport of radionuclides in fractured porous rock. Tech. Rep., California Univ., Berkeley, CA.
- [4] Ahn, J. 2004. An environmental impact measure for nuclear fuel cycle evaluation. *Journal of Nuclear Science and Technology* 41(3):296 – 306.
- [5] Ahn, J. 2007. Environmental impact of yucca mountain repository in the case of canister failure. *Nuclear technology* 157(1):87 – 105.
- [6] Ahn, J., D. Kawasaki, and P. L. Chambre. 2002. Relationship among performance of geologic repositories, canister-array configuration, and radionuclide mass in waste. *Nuclear Technology* 140(1).
- [7] Anderson, M. P, and W. W. Woessner. 1992. *Applied groundwater modeling: simulation of flow and advective transport*.
- [8] ANDRA. 2005. Argile: Evaluation de la faisabilite du stockage geologique en formation argileuse. Tech. Rep., Paris.
- [9] ANDRA. 2005. Granite: Evaluation de la faisabilite du stockage geologique en formation granite. Tech. Rep., Paris.
- [10] Bateman, H. 1908. 1910. the solution of a system of differential equations occurring in the theory of radio-active transformations. In *Proc. cambridge philosophical soc*, vol. 15, 423.
- [11] Berkowitz, Brian, Jacob Bear, and Carol Braester. 1988. Continuum models for contaminant transport in fractured porous formations. *Water Resources Research* 24(8):PP. 1225 – 1236.
- [12] Blink, J. A., T. A. Buscheck, W. G. Halsey, and T. Wolery. 2010. Disposal systems evaluations and tool Development-Engineered barrier system evaluation. Tech. Rep., Lawrence Livermore National Laboratory (LLNL), Livermore, CA.
- [13] Boucher, Lionel. 2010. International comparison for transition scenario codes involving COSI, DESAE, EVOLCODE, FAMILY and VISION. CEA France.

- [14] Bouvier, E., J. Ahn, and T. Ikegami. 2007. *Comparison of environmental impacts for PWR-UOsub 2, PWR-MOX and FBR*. LaGrange Park, IL: American Nuclear Society.
- [15] Bracke, G., T. Beuth, K. Fischer-Appelt, J. Larue, and M. Navarro. 2008. Safety functions derived from geochemistry for safety analysis of final disposal of high-level radioactive waste. *Uranium, Mining and Hydrogeology* 771—778.
- [16] Brewitz, Wernt, and Ulrich Noseck. 2002. Long-term performance of spent fuel in geological repositories. *Comptes Rendus Physique* 3(7-8):879–889.
- [17] Carter, Joe. 2011. Disposal of recycling facility waste in a generic salt repository. Predecisional SRNL-RP-2011-00149.
- [18] Clayton, D, G Freeze, E Hardin, W.M. Nutt, J Birkholzer, H.H. Liu, and S Chu. 2011. Generic disposal system modeling - fiscal year 2011 progress report. Tech. Rep. FCRD-USED-2011-000184, U.S. Department of Energy, Sandia, NM.
- [19] Diodato, D. M., and T. Center. 1994. A compendium of fracture flow models—1994. *Work sponsored by US Department of Defense, United States Army, Europe, Combat Maneuver Training Center, Hohenfels, Germany*.
- [20] DOE. 2002. Yucca mountain science and engineering report. *US Department of Energy, Las Vegas, NV DOE/RW-0539-1, Rev 1*.
- [21] DOE. 2008. The report to the president and the congress by the secretary of energy on the need for a second repository | department of energy. Tech. Rep. DOE/RW-0595.
- [22] DOE. 2010. Nuclear energy research & development roadmap: Report to congress.
- [23] El-Wakil, Mohamed Mohamed. 1981. *Nuclear heat transport*. American Nuclear Society.
- [24] Happel, J., and H. Brenner. 1991. *Low reynolds number hydrodynamics: with special applications to particulate media*, vol. 1. Kluwer Academic Print on Demand.
- [25] Hardin, E, J Blink, Harris Greenberg, Mark Sutton, Massimo Fratoni, Joe Carter, Mark Dupont, and Rob Howard. 2011. Generic repository design concepts and thermal analysis - 8.8.2011 draft. Tech. Rep. FCRD-USED-2011-000143, Department of Energy Office of Used Fuel Disposition, Sandia.
- [26] Hedin, A. 2002. Integrated analytic radionuclide transport model for a spent nuclear fuel repository in saturated fractured rock. *Nuclear Technology* 138(2).
- [27] Ho, C. K. 2000. Dual porosity vs. dual permeability models of matrix diffusion in fractured rock. Tech. Rep., Sandia National Laboratories, Albuquerque, NM (US); Sandia National Laboratories, Livermore, CA (US).



- [28] Huff, Kathryn, Paul P. H. Wilson, and Matthew Gidden. 2010. Cyclus: A nuclear fuel cycle code from the university of wisconsin madison. <http://code.google.com/p/cyclus/>.
- [29] Incropera, Frank. 2006. *Fundamentals of heat and mass transfer*. 6th ed. Hoboken N.J.: Wiley.
- [30] Johnson, L., C. Ferry, C. Poinssot, and P. Lovera. 2005. Spent fuel radionuclide source-term model for assessing spent fuel performance in geological disposal. part i: Assessment of the instant release fraction. *Journal of Nuclear Materials* 346(1): 56–65.
- [31] Johnson, L., B. Kunz, C. Frei, Nagra, and Projekt Opalinuston. 2002. *Project opalinus clay: Safety report: Demonstration of disposal feasibility for spent fuel, vitrified high-level waste and long-lived intermediate-level waste (Entsorgungsnachweis)*. Nagra, National cooperative for the Disposal of Radioactive Waste.
- [32] Johnson, L. H., and Nagra. 2002. *Calculations of the temperature evolution of a repository for spent fuel, vitrified high-level waste and intermediate level waste in opalinus clay*. Nagra.
- [33] Kawasaki, D., J. Ahn, P. L. Chambre, and W. G. Halsey. 2004. Congruent release of long-lived radionuclides from multiple canister arrays. *Nuclear technology* 148(2): 181 – 193.
- [34] Kessler, J. H., J. Kemeny, F. King, A. M. Ross, and B. Ross. 2006. Room at the mountain: Estimated maximum amounts of commercial spent nuclear fuel capable of disposal in a yucca mountain repository. Tech. Rep., The ASME Foundation, Inc., New York.
- [35] Kossik, R. F., I. Miller, and S. Knopf. 2006. *GoldSim graphical simulation environment user's guide*. Version.
- [36] von Lensa, W., R. Nabbi, and M. Rossbach. 2008. *RED-IMPACT impact of partitioning, transmutation and waste reduction technologies on the final nuclear waste disposal*. Forschungszentrum Julich.
- [37] Li, J. 2006. A methodology to evaluate nuclear waste transmutation/fuel cycle systems.
- [38] Li, J., M. Nicholson, W. C. Proctor, M. S. Yim, and D. McNelis. 2007. Examining repository loading options to expand yucca mountain repository capacity. In *Proceedings of GLOBAL*, 519 — 525.
- [39] Li, J., M. S. Yim, and D. McNelis. 2008. The specific temperature increase method for repository thermal analysis. *Transactions of the American Nuclear Society* 99:216 — 218.

- [40] Li, J. 2007. A methodology to evaluate nuclear waste transmutation / fuel cycle systems. Ph.D. thesis, North Carolina State University.
- [41] Miron, A., J. Valentine, J. Christenson, M. Hawwari, S. Bhatt, M. L Dunzik-Gougar, and M. Lineberry. 2009. Identification and analysis of critical gaps in nuclear fuel cycle codes required by the SINEMA program. Tech. Rep., University of Cincinnati.
- [42] Nicholson, M. A. 2007. *Thermal loading and uncertainty analysis of high level waste in yucca mountain*. North Carolina State University.
- [43] Nutt, Mark. 2011. Personal communication.
- [44] Nutt, W. M. 2010. Used fuel disposition research and development roadmap-FY10 status. Tech. Rep., Argonne National Laboratory (ANL).
- [45] OECD-NEA. 2006. *Advanced nuclear fuel cycles and radioactive waste management*. OECD Publishing.
- [46] ONDRAF-NIRAS. 2001. Technical overview of the SAFIR 2 report. Tech. Rep. Niron 2001-05 E, Belgium.
- [47] Papoulis, A., and S. U. Pillai. 2002. *Probability, random variables, and stochastic processes*. 4th ed. Series in Electrical and Computer Engineering, McGraw-Hill.
- [48] Piet, S., T. Bjornard, B. Dixon, D. Gombert, C. Laws, and G. Matthern. 2007. Which elements should be recycled for a comprehensive fuel cycle? *Proc. Global 2007* 1595.
- [49] Posiva. 2010. *Interim summary report of the safety case 2009*. POSIVA.
- [50] Pusch, R., L. Borgesson, and M. Erlstrom. 1987. *Alteration of isolating properties of dense smectite clay in repository environment as exemplified by seven pre-quaternary clays*. Swedish Nuclear Fuel and Waste Management Co.
- [51] Radel, T. E. 2007. *Repository modeling for fuel cycle scenario analysis*. University of Wisconsin – Madison.
- [52] Radel, T. E, P. P.H Wilson, R. M. Grady, and T. H. Bauer. 2007. *Effect of separation efficiency on repository loading values in fuel cycle scenario analysis codes*. LaGrange Park, IL: American Nuclear Society.
- [53] Savoye, S., F. Goutelard, C. Beaucaire, Y. Charles, A. Fayette, M. Herbette, Y. Larabi, and D. Coelho. 2011. Effect of temperature on the containment properties of argillaceous rocks: The case study of Callovo-Oxfordian claystones. *Journal of Contaminant Hydrology*.

- [54] Schneider, E., M. Knebel, and W. Schwenk-Ferrero. 2004. NFCSim scenario studies of german and european reactor fleets. Tech. Rep., LA-UR-04-4911, Los Alamos National Laboratory.
- [55] Schwartz, F. W., and H. Zhang. 2004. Fundamentals of ground water. *Environmental Geology* 45:1037–1038.
- [56] Soelberg, N., S. Priebe, D. Gombert, and T. Bauer. 2009. Heat management strategy trade study. *Advanced Fuel Cycle Initiative, AFCI-SYSA-PMO-MI-DV-2009-000169, INL/EXT-09-16708*.
- [57] Swift, Peter, and Mark Nutt. 2010. Applying insights from repository safety assessments. San Francisco, CA.
- [58] Turner, Stephen L. 2010. Discrete modeling: OCRWM total system model DRAFT. DOE FCRD-XXXX-2009-XXXXXX.
- [59] Uleberg, K., and J. Kleppe. 1996. Dual porosity, dual permeability formulation for fractured reservoir simulation. In *Norwegian university of science and technology, trondheim RUTH seminar, stavanger*.
- [60] Van Den Durlpel, L., D. C Wade, and A. Yacout. 2006. DANESS: a system dynamics code for the holistic assessment of nuclear energy system strategies. *Proceedings of the 2006 System Dynamics Conference*.
- [61] Williams, N. H. 2001. Total system performance Assessment—Analyses for disposal of commercial and DOE waste inventories at yucca Mountain—Input to final environmental impact statement and site suitability evaluation REV 00 ICN 02. Tech. Rep.
- [62] Wilson, P. P.H. 2011. Comparing nuclear fuel cycle options. *A report for the Reactor & Fuel Cycle Technology Subcommittee of the Blue Ribbon Commission on America's Nuclear Future*.
- [63] Yacout, A. 2011. DANESS. [www.anl.gov/techtransfer/Software.Shop/Daness/DANESS.html](http://www.anl.gov/techtransfer/Software.Shop/Daness/DANESS.html).
- [64] Yacout, A. M., J. J. Jacobson, G. E. Matthern, S. J. Piet, D. E. Shropshire, and C. Laws. 2006. VISION – verifiable fuel cycle simulation of nuclear fuel cycle dynamics. In *Waste management symposium*.